DEFECT MODEL FOR THE ELECTRONIC CONDUCTION AND BREAKDOWN IN DIELECTRIC THIN FILMS

by

TSAI-KU LIN, B.S., M.S.

A DISSERTATION

IN

PHYSICS

Submitted to the Graduate Faculty
of Texas Tech University in
Partial Fulfillment of
the Requirements for
the Degree of

DOCTOR OF PHILOSOPHY

Approved

December, 1987

801
T3
1987
No. 114
Cop. 2

ACKNOWLEDGMENT

The author wishes to express his sincere appreciation to the chairman of his committee, Dr. V.K. Agarwal, for his continuous guidance, acceptance of the results, and great patient in the preparation of this dissertation. His gratitude is also extended to other committee members, Dr. M.A.K. Lodhi, Dr. L.L. Hatfield, Dr. R. Lichti, and Dr. T. Gibson for their helpful discussions and constructive criticism.

He appreciates the financial assistance provided by Dr. Lichti (Welch grant), Dr. Agarwal (Texas Instrument grant), and the Department of Physics.

The author is deeply indebted to his wife, Mei-Hwa, and his children, Yii-Dauh, Yuu-Dauh, for their understanding, encouragement, as well as the sacrifices they made.

CONTENTS

ABSTRACT

A stochastic model of defects has been developed to explain the electronic properties of dielectric thin film systems. Consequently, a reaction-diffusion (RD) type of equation is obtained. This model considers the dielectric thin film system as an open system, in which nonlinearities play important role for the instabilities of the system. The general experimental observations on the current-voltage characteristics are discussed. The microscopic picture of the conduction processes leading to breakdown is proposed. Several steps of conduction are predicted before the destructive breakdown of the film occurs. These conduction stages correspond to the microscopic states of the system and, consequently, closely related to the defects correlated states. Qualitatively, the microscopic states of the system are correlated with the growth stages of the film. The mechanisms of aging and annealing are also addressed under this reaction-diffusion equation. The following is the chapter by chapter summary.

In chapter one, the general experimental observations and theoretical difficulties encountered in the conventional approaches are discussed. The qualitative properties of

reaction-diffusion equation are discussed. Its relationship with conventional breakdown mechanisms and (quasi-)equilibrium physics are addressed.

In chapter two, nucleation and growth processes are explained by reaction-diffusion equation. The conventional concept of defects has been extended to include all the states inside the band gap. The electronic properties of the dielectric thin films are shown to be closely related to their formation (nucleation, growth) processes, and consequently their microscopic structures. Two examples of the RD model are shown to be equivalent in the theoretical formulation.

In chapter three, further physical insight of reaction-diffusion equation is addressed. General experimental observations in current-voltage characteristics are discussed. Some new features predicted by the stochastic model are briefly described. Modified annealing mechanisms have been used to estimate the total irreversible defect density in the dielectric thin films.

In chapter four, reaction-diffusion model is used to explain the fractional exponential parametric dependence of conductivity and is compared with percolation and variable-range-hopping mechanisms. Mott's predictions are discussed on the basis of Poisson distribution in phase

space. Coulomb's gap is suggested to be caused by the crater-like probability distribution of defects, which is the situation in nonequilibrium.

In chapter five, inverse power law temperature and thickness dependence of breakdown strength are explained by reaction-diffusion model. A microscopic picture of conduction to breakdown suggested by the reaction-diffusion model is proposed. The relation between Weibull's statistics and RD model is addressed.

In chapter six, the reaction-diffusion model is used to explain the experimental data in stearic acid films. Annealing mechanism has been used to estimate the defect density in fatty-acid and S_iO films, and the results are compared with available data.

From the overall point of view, in chapter seven we summarize the main results and discuss how the soliton solutions of the reaction-diffusion equations can be used to explain the nucleation, growth, aging and annealing processes.

LIST OF TABLES

LIST OF FIGURES

CHAPTER I

INTRODUCTION

Potential Application of Dielectric Thin Films

Dielectric thin films, usually less than 1 micron in thickness, have a wide range of applications in electronic and microelectronic industries. For example, the possibilities of development of a variety of miniaturized solid-state devices such as diodes, hot-electron triodes, switching devices, fixed and variable capacitors, piezoelectric transducers, photocells and electroluminescent devices [1, 2]. The deposition methods used in the laboratory are usually thermal evaporation, sputtering, chemical vapor deposition, thermal oxidation, etc. Among the various deposition methods, the films made by Langmuir-Blodgett technique have shown potentional for their application, because this type of films have small and uniform thickness and can be doped, polymerized and functionalized.

Besides their practical applications, the dielectric thin films also have significant fundamental scientific importance. For example, they can serve as model systems to

test the applicability of old mechanisms, and to look for the new ones to interpret the complicated experimental data. Here "model systems" mean systems that exhibit the desired phenomena, and in which the relevant material parameters can be controlled. It is with such model systems that one generally gains the clearest insight and obtains the best quantitative tests of the theories, and it is on the basis of this kind of understanding that more complicated systems can then be understood.

For the above reasons, both theoretical and experimental investigations to understand the properties of the dielectric thin film systems are desirable.

By contrast with the technological approach in which the principle objective is to master a set of processes leading to some desired practical ending, this dissertation is a theoretical research which aims at elucidating fundamental questions regarding the mechanisms or processes. We first analyze the conventional theoretical approaches in electronic conduction and breakdown mechanisms of the dielectric thin films. This is followed by proposing a unique model (theory) to explain the general experimental observations.

Theoretical Difficulties and Experimentally Uncontrolable Problems

The electronic properties consist of (1) electronic conduction, (2) dielectric properties, and (3) electric breakdown. A large amount of literatures has been accumulated on these subjects during the last several decades. Much of these are related to detailed analysis of many physical effects and multiparameter curve-fitting [3-6]. However, no systematic approach has emerged which fully explains the electronic properties and their relationship to inherent defects in dielectric thin films. It is generally believed that the difficulties come from the following:

(a) the uncertainty of the microscopic structure,

(b) the uncertainty of the boundary conditions,

(c) the variable nature of the various experimental preparations, deposition conditions, handling procedures and testing techniques, and

(d) the multiplicity of the various materials' properties.

Several of the above are beyond the control of the experimenter, and even under the most easily controlled laboratory conditions, there is considerable scatter in experimental data due to the unpredictable and unknown nature of defects. Although modern techniques, e.g.,

transmission electron microscopy (TEM), scanning electron microscopy (SEM) and low energy electron diffraction (LEED), are now available to monitor and analyze the microscopic structure in situ, only limited success in gaining a physical understanding with respect to defects has been obtained. Consequently, no simple and clear picture has emerged to explain the electronic properties of dielectric thin films.

A summary of the conventional conduction processes and breakdown mechanisms in the dielectric thin films is given in Table 1 [7] and Figure 1 [8]. In the traditional approach on studying conduction in dielectric thin films the emphasis has been to understand the type, origin, concentration of charge carriers, and the mechanisms of carrier transport. The studies on breakdown have focused on the type and origin of underlying mechanisms. From Table 1 and Figure 1, it can be easily seen that the electronic conduction processes and breakdown mechanisms are quite diverse, and there has been no attempt to present a general and unified approach to explain a host of experimental data in this field.

TABLE 1

Basic conduction processes in insulator films [7].

Process	Expression[a]	Voltage and Temperature Dependence[b]
Schottky emission	$J = A^* T^2 \exp\left[\frac{-q(\phi_B - \sqrt{q\mathcal{E}/4\pi\epsilon_i})}{kT}\right]$	$\sim T^2 \exp(+a\sqrt{V}/T - q\phi_B/kT)$
Frenkel-Poole emission	$J \sim \mathcal{E} \exp\left[\frac{-q(\phi_B - \sqrt{q\mathcal{E}/\pi\epsilon_i})}{kT}\right]$	$\sim V \exp(+2a\sqrt{V}/T - q\phi_B/kT)$
Tunnel or field emission	$J \sim \mathcal{E}^2 \exp\left[-\frac{4\sqrt{2m^*}(q\phi_B)^{3/2}}{3q\hbar\mathcal{E}}\right]$	$\sim V^2 \exp(-b/V)$
Space-charge-limited	$J = \frac{8\epsilon_i \mu V^2}{9d^3}$	$\sim V^2$
Ohmic	$J \sim \mathcal{E} \exp(-\Delta E_{ae}/kT)$	$\sim V \exp(-c/T)$
Ionic conduction	$J \sim \frac{\mathcal{E}}{T} \exp(-\Delta E_{ai}/kT)$	$\sim \frac{V}{T} \exp(-d'/T)$

[a] A^* = effective Richardson constant, ϕ_B = barrier height, $\mathcal{E}$ = electric field, ϵ_i = insulator dynamic permittivity, m^* = effective mass, d = insulator thickness, ΔE_{ae} = activation energy of electrons, ΔE_{ai} = activation energy of ions, and $a \equiv \sqrt{q/(4\pi\epsilon_i d)}$.
[b] $V = \mathcal{E}d$. Positive constants independent of V or T are b, c, and d'.

I. Electronic breakdown process

- Intrinsic breakdown ($\partial F_B/\partial d = 0$)
  - d: sample thickness
  - Theories based on the single electron approximation ($\partial F_B/\partial T \geq 0$)
    - High energy criterion
    - Low energy criterion
  - Collective critical field theories
    - Single crystal ($\partial F_B/\partial T > 0$)
    - Amorphous materials ($\partial F_B/\partial T < 0$).
- Electron avalanche breakdown ($\partial F_B/\partial d < 0$) ($\partial F_B/\partial T \geq 0$)
  - Single avalanche model
  - Collective avalanche model
- Field emission breakdown ($\partial F_B/\partial d = 0$) ($\partial F_B/\partial T = 0$)
- Free volume breakdown ($\partial F_B/\partial T < 0$)

II. Thermal breakdown process

- Steady state thermal breakdown ($\partial F_B/\partial T < 0$)
- Impulse thermal breakdown

III. Mechanical breakdown process

- Electromechanical breakdown ($\partial F_B/\partial T < 0$)

Figure 1: Conventional breakdown mechanisms in dielectrics [8].

General Features of the Dielectric Thin Films

Before we present our model, it is helpful to list the genneral important experimental observations in the dielectric thin films with respect to their physical properties. The general features of the structure in the dielectric thin films are:

(1) usually the combination of amorphous and microcrystalline (small grain size) phases.

(2) commonly to have a much higher defect density than the corresponding bulk material, and

(3) typically large surface to volume ratio.

The common features of electrical conduction in dielectric thin films are the following;

(1) Most of the current (typically 2/3) in the dielectric thin films is carried by the structural defects.

(2) Temperature variation of conductivity is rarely linear (Fig. 2).

(3) The field dependence of DC conductivity is linear at low fields and nonlinear (exponential/power dependent) at high fields (Fig. 3).

(4) The thickness, temperature and field dependence of conductivity are related through exponential-dependence law (Fig. 2-4).

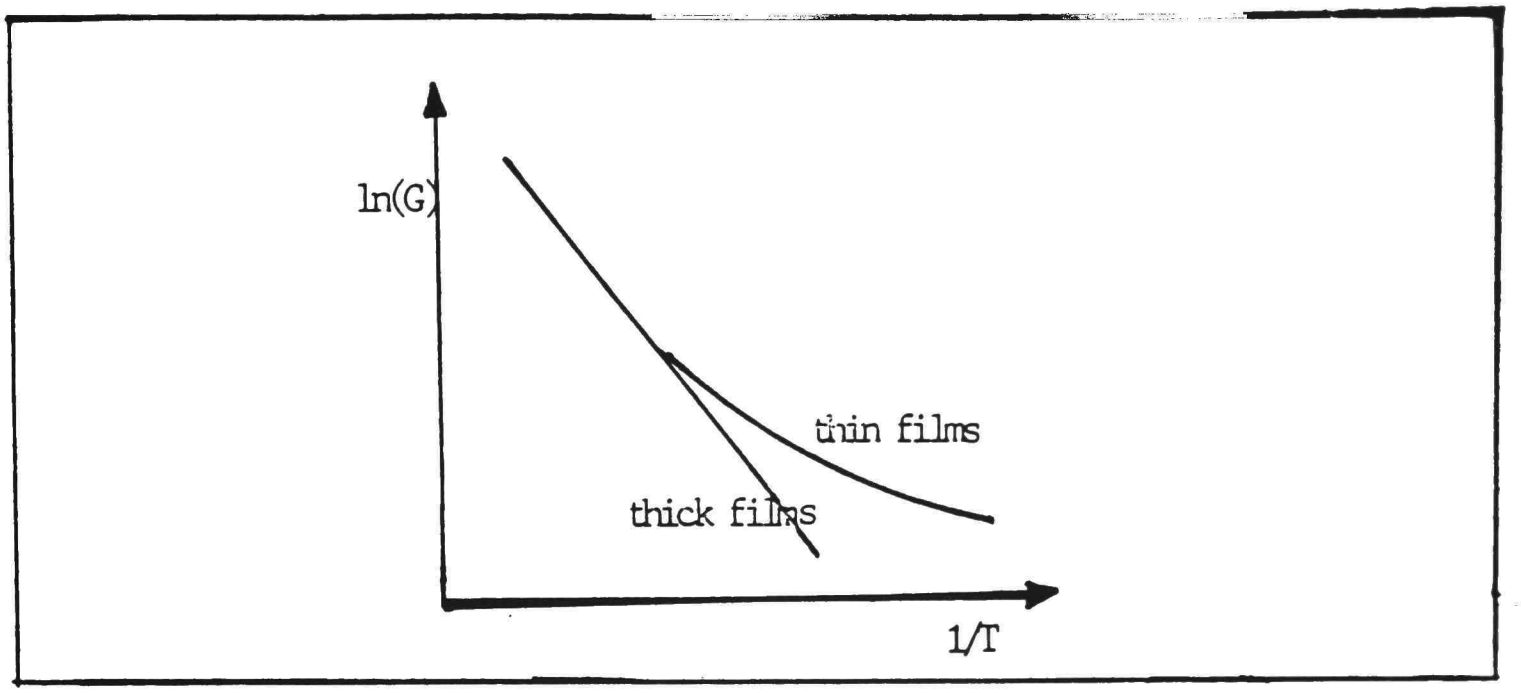

Figure 2: Typical temperature dependence of conductivity in dielectric films.

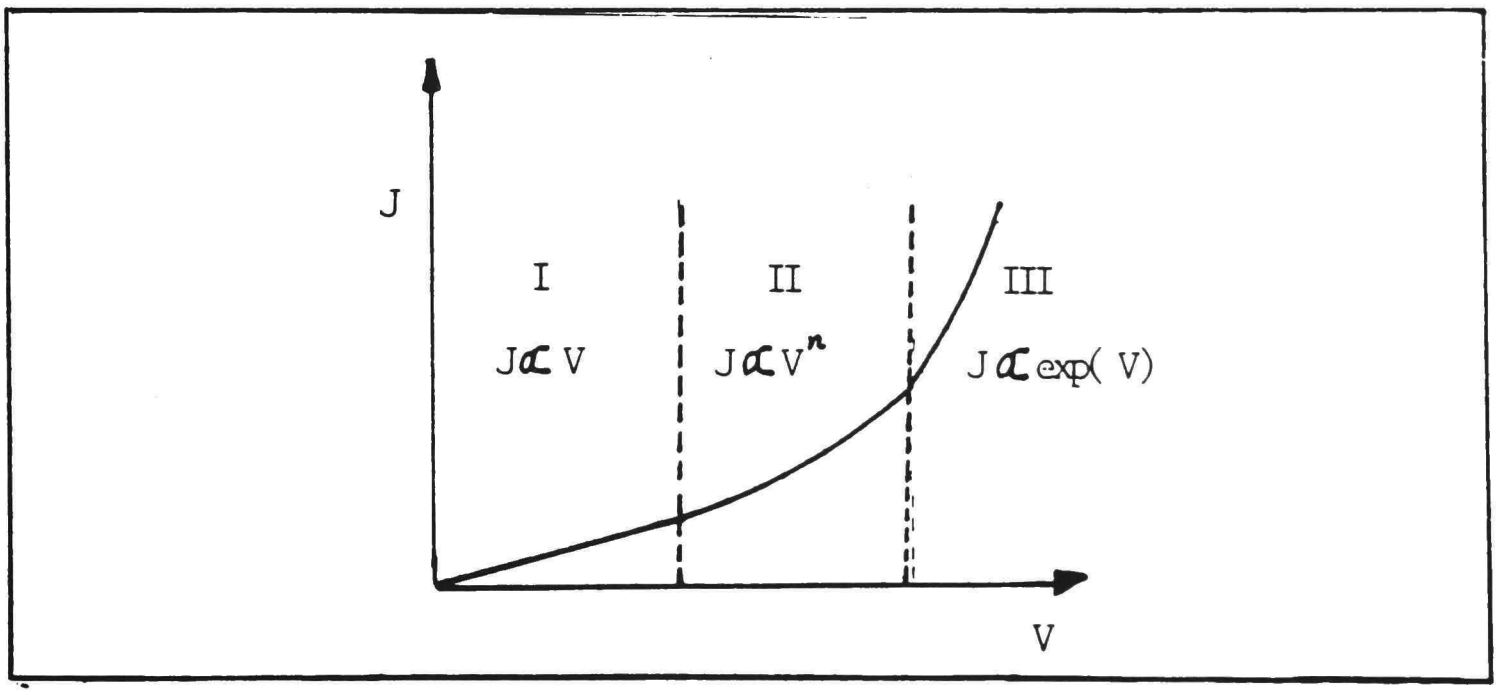

Figure 3: Typical current-voltage relation in dielectric thin films.

(5) Typically, they have low mobility (μ $<<10^{(-1)}cm^2/(s\text{-}Volt)$), high effective mass, narrow band width and large band gap (e.g., > 4eV).

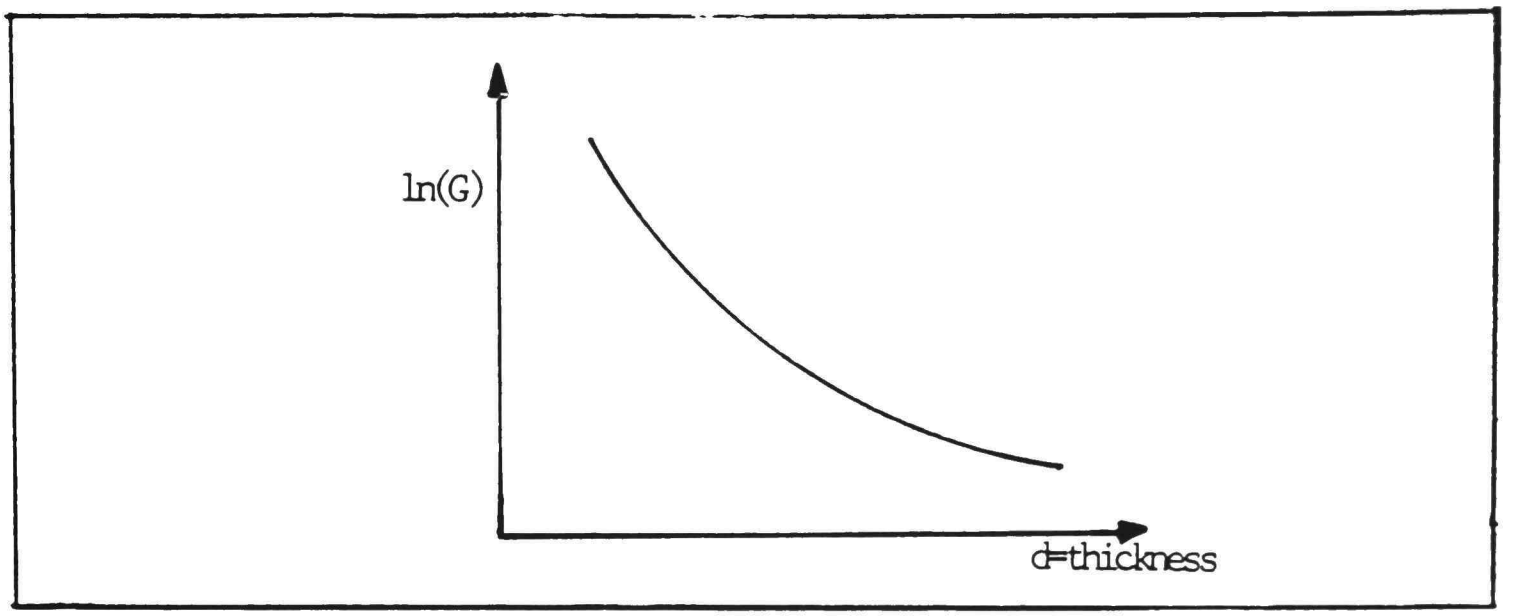

Figure 4: Typical thickness dependence of conductivity in dielectric thin films.

(6) The dielectric relaxation time >> carrier life time.

The common features of breakdown in dielectric thin films are the following;

(1) Breakdown strength increases as the thickness and temperature of the film decrease (Fig. 5 and Fig. 6).

(2) Breakdown strength generally follow Weibull's empirical statistics.

(3) Just before breakdown the conductivity of dielectric material increases dramatically.

(4) Partial discharge of breakdown always happens with light emission in a filament irrespective of material phases (Fig. 7).

(5) Under proper experimental conditions a negative differential resistance is observed (Fig. 8). This

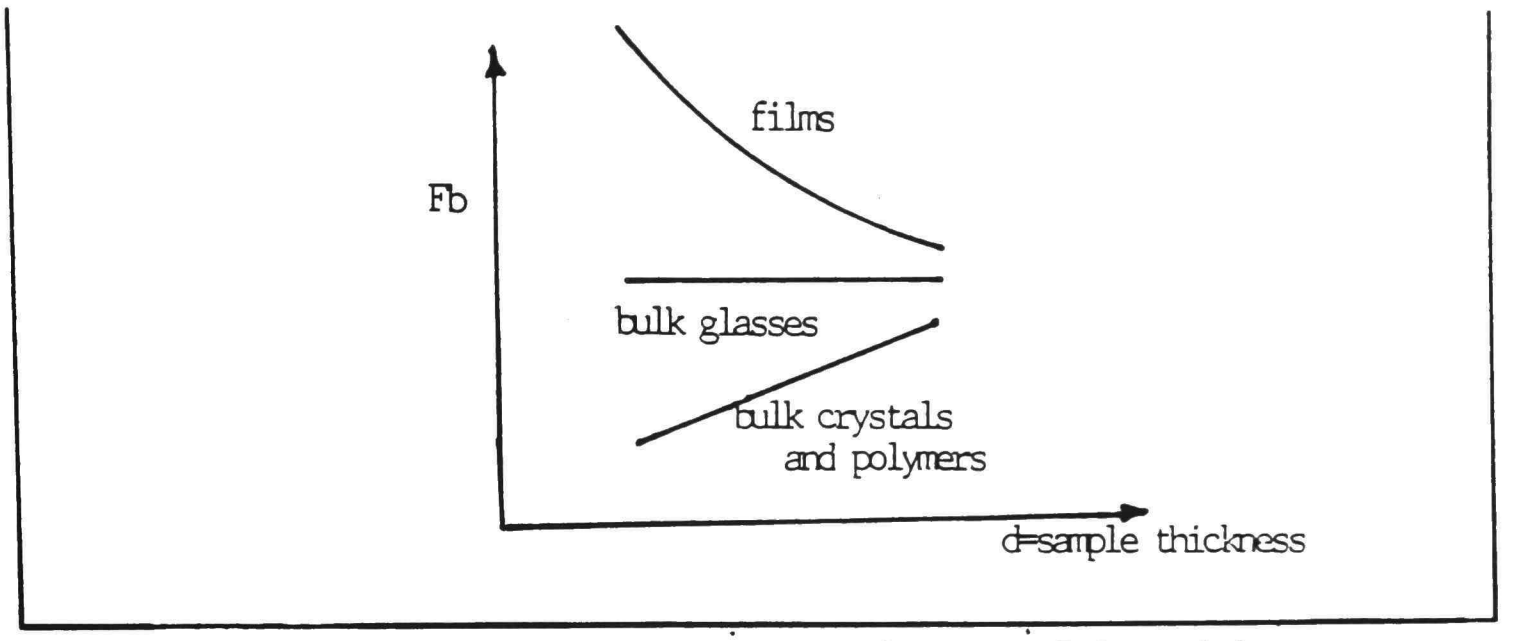

Figure 5: Typical thickness dependence of breakdown strength in dielectric films.

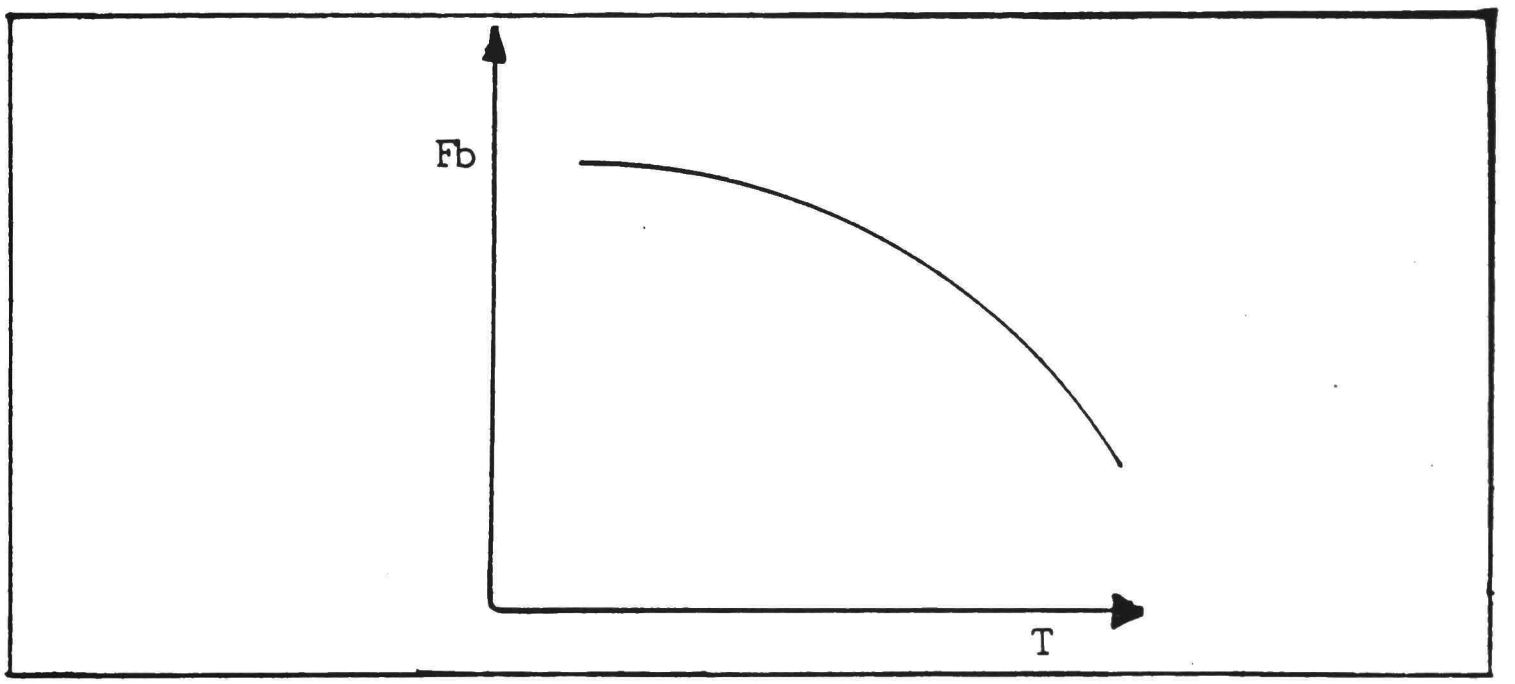

Figure 6: Typical temperature dependence of breakdown strength in dielectric thin films.

indicates that there is a positive feedback mechanism before breakdown occurs.

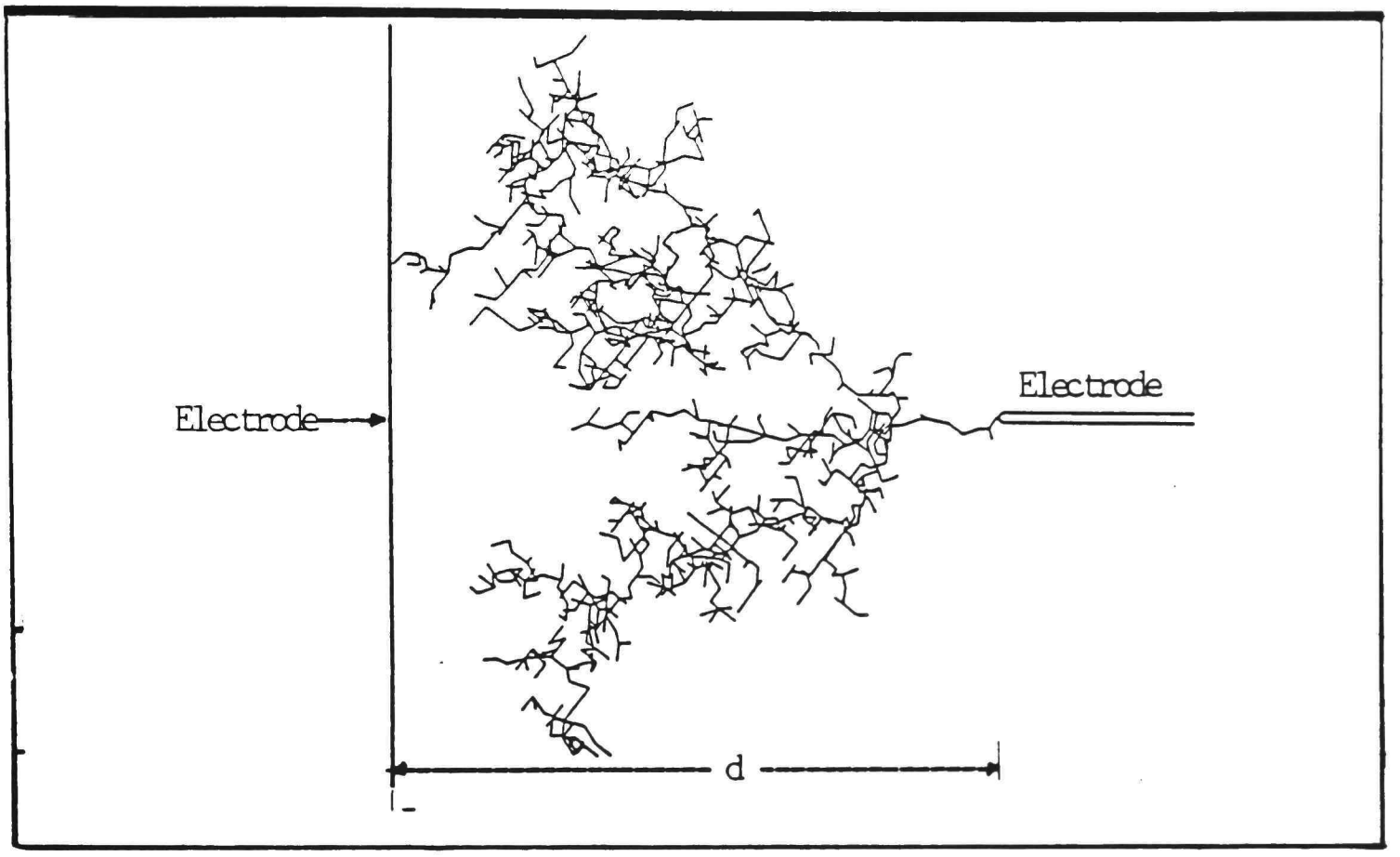

Figure 7: Typical breakdown tree observed between point and plane electrodes in dielectric films.

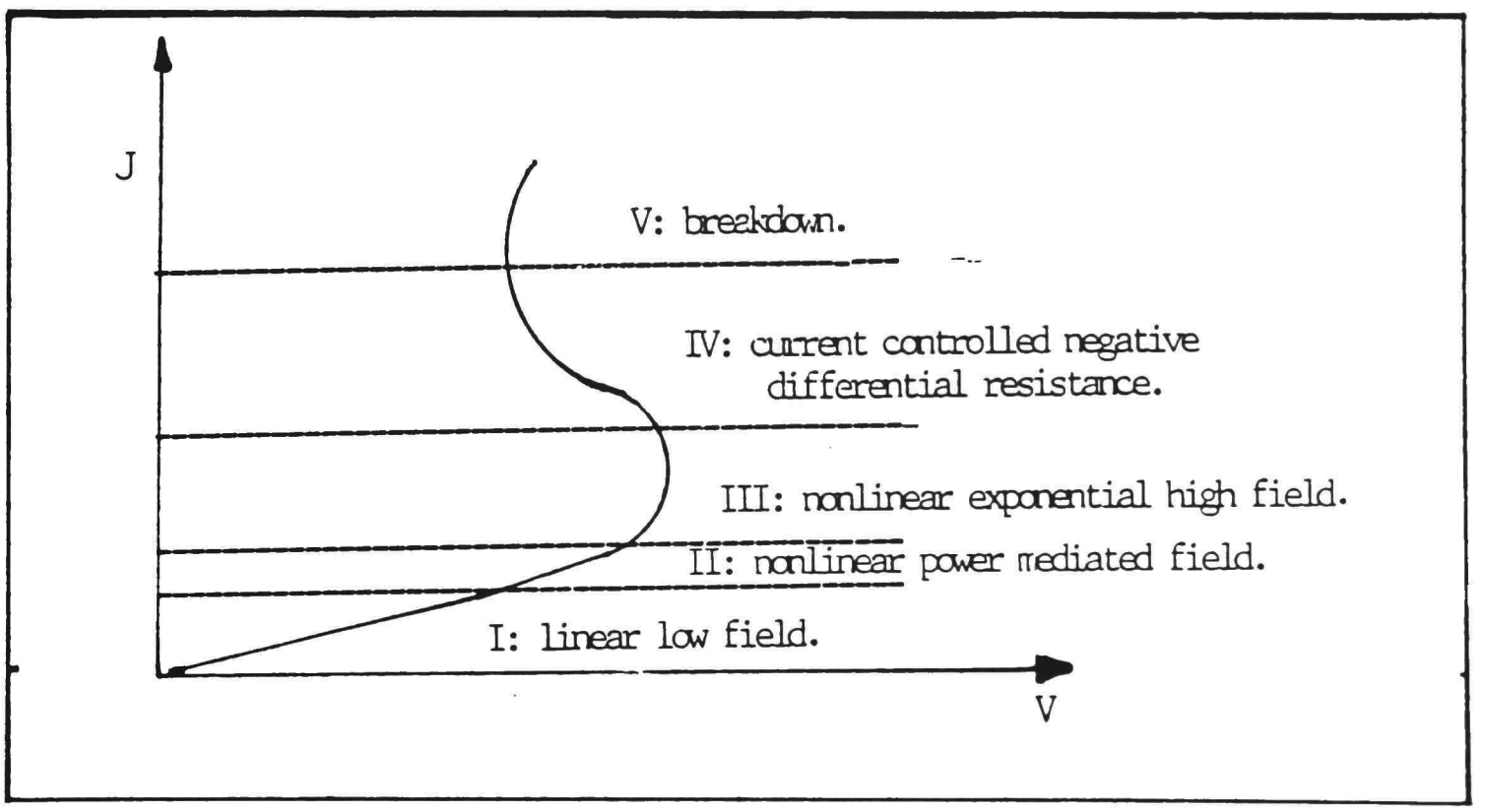

Figure 8: Typical negative differential resistance observed in dielectric thin films.

Defect Model and the Unified Theoretical Approach

According to the above experimental observations, a picture for the charges transportation in dielectric thin films can be envisaged as either the charge carriers (electrons, holes and ions) moving (trap, scatter, diffuse or migrate) from one defect to another, or charged defects jumping from one site to another under the influence of both the external field and the height of defect potentials. The typical high defect density implies short electronic mean free path, and the large surface to volume ratio suggests that the diffusion and the effects of surface states are important. The temperature, thickness and field dependence of the conductivity (Fig. 2-4) can be fitted into a fractional exponential function, and can be explained as a result of the redistribution of position and size of the defects. This also results in the inverse power law dependence of the breakdown strength in Fig. 4 and 5. The influence of other parameters (e.g., aging, geometry of electrodes, pressure, etc.) on the conductivity and breakdown strength can also be explained in this way.

Based on this picture, the next question to be answered is which theoretical approach should be applied to formulate the general conduction and breakdown processes. Before we

answer this question, let us briefly review the available theoretical approaches to see the relationship between the conventional theories and the model we are going to propose.

Depend on the level we are interested in, the change of a physical system in space and time can be described as

(1) a differential equation in macroscopic level (phenomenological approach),

(2) a probability distribution in intermediate (mazoscopic) level (statistics approach), and

(3) a Hamitonian equation in microscopic level (dynamical approach, e.g., classical or quantum mechanics).

In a phenomenological description attention is focused on the average value of some important macroscopic variable which characterizes the physical system. The fluctuations about such average value are neglected in deriving the differential equation which gives the time evolution of this variable. The conventional approaches in breakdown theories belong to this category. For example, Figure 1 shows three breakdown mechanisms, i.e., thermal, electric and electromechanical breakdown. The fundamental equation for thermal breakdown is (e.g., [4])

$$C_v \frac{\partial T}{\partial t} + V\bullet[\kappa(T)VT] = H(T)F^2 , \qquad (1.1)$$

where C_v is the specific heat per unit volume, T is the absolute temperature, κ is the thermal conductivity, G is the electrical conductivity and F is the external electric field. Both κ and G are function of temperature. The numerical solution of equation (1.1) is shown in Fig. 9. If the external field F is small, there is no breakdown as shown in curve (i). As F increase to some critical value, breakdown will occur after a finite time interval, as shown in curves (ii), (iii) and (iv). In order to compare this approach with our model later, let us rewrite equation (1.1) to

$$\frac{\partial T}{\partial t} = DV^2T + H(T,t) , \qquad (1.2)$$

where $H(T,t) = \frac{GF^2}{C_v}$ is the "reaction function" and $D= \frac{\kappa}{C_v}$ is transport coefficient.

The general equation for the electronic breakdown is either the energy conservation [9] or charge conservation expressed by the following set of equations

$$\frac{\partial N_a}{\partial t} = -(\frac{V\bullet J}{e}), \quad J = ev(F)N_a - DeVN_a, \quad V\bullet F = 4\pi e(\frac{N_a - N_o}{\varepsilon}), \qquad (1.3a)$$

where N_a is the density of the conduction electrons which may cause impact ionization leading to breakdown, J is the current density, v is the drift velocity, t is time, N_o is

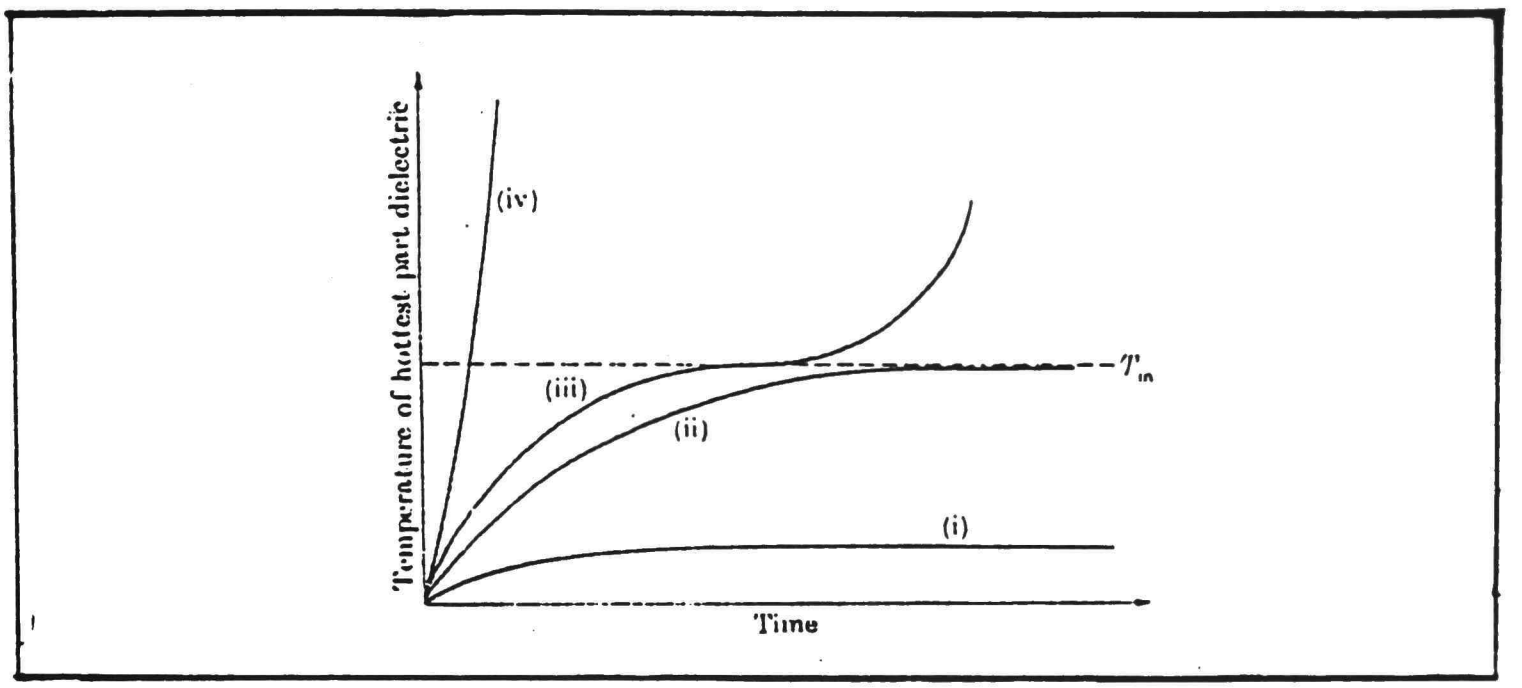

Figure 9: Schematic diagram of solutions to equation (1.1) [3].

the initial density of conduction electrons and ε is the dielectric constant ($\nabla\bullet$ =divergence, ∇=gradient).

The above set of equations can be combined to express reaction-diffusion rate as follows;

$$\frac{\partial F}{\partial t} = -\frac{[4\pi v(F)N_o]}{\varepsilon} + D\frac{\partial^2 F}{\partial x^2} + 4\pi N_o \frac{De}{\varepsilon_o} . \qquad (1.3b)$$

The energy conservation equation suggests that

$$A(F, T, \#) = B(T, \#) , \qquad (1.4)$$

Here A(F,T,#) is the rate of energy gain by the conduction electrons from the field, and B(T,#) is the rate of energy loss (or the rate of energy transfer) of the conduction electrons to their environment. A schematic representation

of equation (1.4) is shown in Fig. 10. From this graph it is found that equation (1.4) can be rewritten as

$$\frac{\partial N_a}{\partial t} = A'(F,T,\zeta) - B'(T,\zeta)\,, \qquad (1.5)$$

where A' is the creation rate of conduction electrons, which is a function of both external and internal parameters. B' is the loss rate of conduction electrons (e.g., dissipation, recombination), which is a function of internal parameters only.

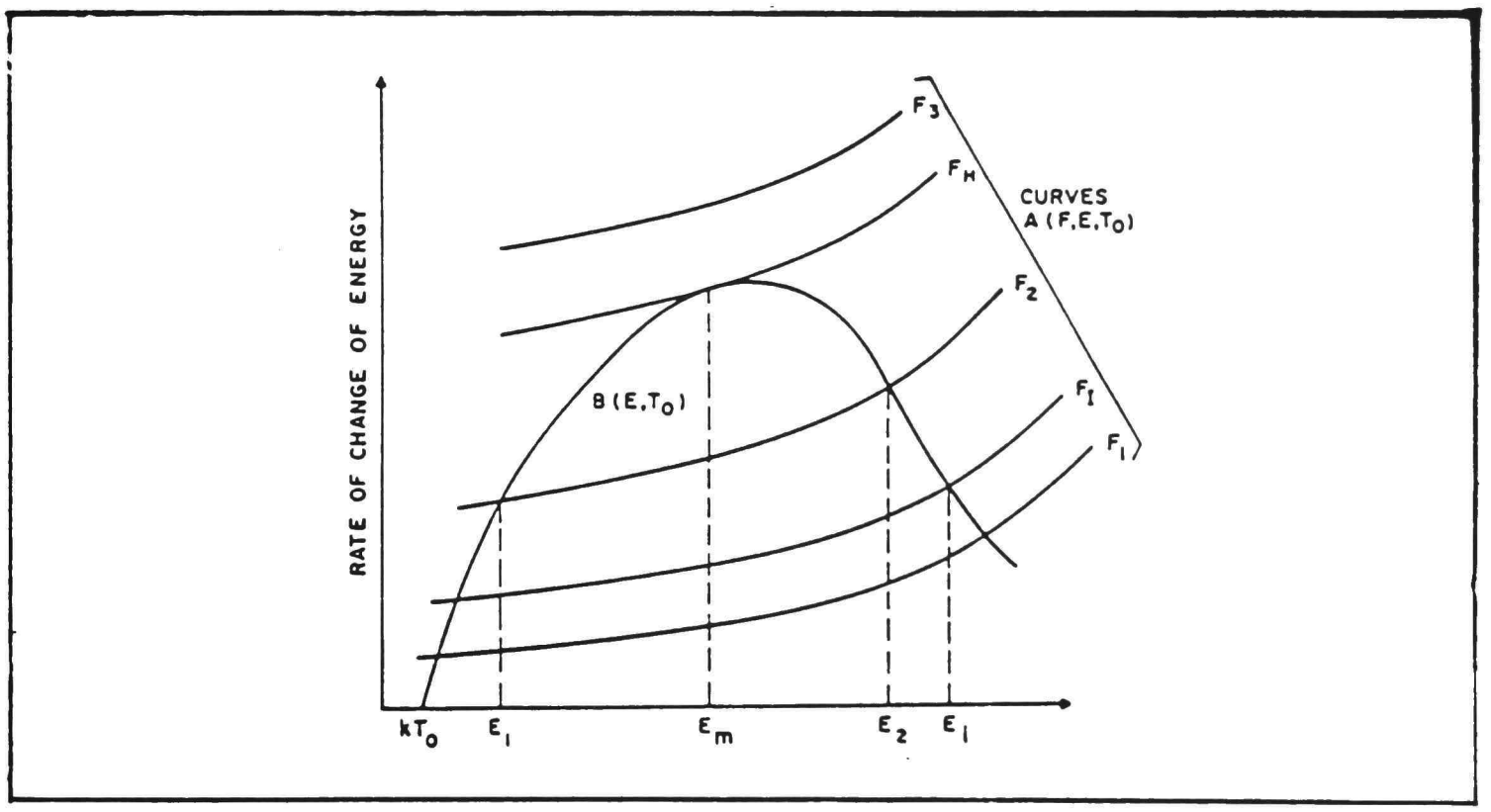

Figure 10: Graphical illustration of conditions for electric breakdown.

The general equation for electromechanical breakdown is (e.g., [9])

$$\frac{\varepsilon\varepsilon_o^2}{2} = Y\ln\left(\frac{d}{d'}\right), \qquad F_b = \frac{V_c}{d'} = \sqrt{\frac{Y}{e\varepsilon\varepsilon_o}}\ , \qquad (1.6a)$$

where Y is the Young's modulus, V_c is the critical field, d is the film thickness and d' is thickness at critical stress. This equation can be rewritten as

$$\frac{dF_m}{dt} = \text{Gain rate} - \text{Loss rate}\ , \qquad (1.6b)$$

where F_m is the mechanical strength.

The advantage of the above phenomenological approach is that the result can be applied immediately to compare with the experimental data without any knowledge of the microscopic processes occuring in the film. However, on the other hand, the microscopic picture proposed by this approach may be unrealistic.

Statistical Approach

In a statistical description, it is assumed that the evolution of the system can be described by transition probabilities at any instant and that these probabilities depend only on the state of the system at that instant. An important assumption of this approach is that the effects caused by the thermodynamical second law (i.e entropy is always increasing) dominate the evolution of the system. In this approach the fluctuations, nonlinear interactions and the effects of nonequilibrium are treated as perturbations.

Since dielectric thin films have typically large surface to volume ratio and high defect density the interactions between defects are in fact significant. In addition, dielectric thin films are usually the good materials for charge and energy storage. This suggests that the energy generation rate from the external field is often much higher than the dissipation rate at high fields. Therefore, the dielectric thin film can usually be considered in a state of far from equilibrium. This implies that the effects of the nonequilibrium may not be suitable to be treated as small perturbations.

Dynamic Approach

In a dynamic approach, the evolution of a system is both deterministic and reversible, in the sense that the final state of the system can be predicted from the given initial state, and the equation of motion is invariant under time inversion.

Table 2 shows the comparison among these theoretical approaches at or near equilibrium. From this table we find that all these approaches may not adequately describe the dielectric thin film systems which have the following features:

(1) at high fields the energy input rate >> the dissipation rate (i.e., far from equilibrium),

(2) the interactions between defects can not be treated as perturbations, and

(3) fluctuations play an important role for the instability of the system.

The system which has the above mentioned features is referred to as open system in the discussion that follows.

TABLE 2

Comparison among theoretical approaches at or near equilibrium.

	Phenomenological	Statistical	Dynamic
level	macroscopic	intermediate	microscopic
evolution variable	macroscopic average	probability	trajectory/wave function
deterministic	Yes	yes	yes
time reversible	no	yes	yes
fluctuation	small	small	small
long-range correlation	no	no	no

The model presented below is a stochastic model. The difference between the statistical and stochastic approach

is that the latter takes the effects of nonlinearities and nonequilibrium into considerations. Besides this, there are two additional reasons for this choice:

(1) the defect related parameters (e.g., size and position of defects) in the film structure are random in nature, and

(2) it is hoped that this approach (which is in the intermediate level) can be extended to the macroscopic level to explain the experimental data and to the molecular level to describe the possible microscopic processes which occur in the system.

We will discuss this model in detail in the following chapters. At present, we follow the picture described at the beginning of this section, and assume that the equation of motion in the macroscopic level is as follows;

$$\frac{\partial O}{\partial t} = \text{Gain}(O) - \text{Loss}(O) = H(O) + F(t) + \frac{\partial}{\partial x}\left(D\frac{\partial O}{\partial x} + CO\right), \qquad (1.7)$$

where H(O) is a polynomial, F(t) represents the fluctuation, D and C are the diffusion and drift coefficient respectively. The evolution variable "O" is the so called order parameter, which is the fundamental macroscopic variable. The various meanings attached to this variable make it possible to formulate a unified description of the order process in different situations. For example,

comparison of equation (1.7) with (1.2), (1.4) and (1.6), may show that the conventional breakdown theories are the special case of this approach, in thermal, electrical and electromechanical breakdown the order parameter is temperature, electronic stress and mechanical stress respectively; and in our model the order parameter will be the defect distribution function or the defect density.

The first term of equation (1.7) gives the change in O(r,t) that results from reactions and is usually a polynomial of the order parameter. In the case of equilibrium and quasi-equilibrium this polynomial is linear, otherwise it is nonlinear. The third term gives the change in O(r,t) due to transport (e.g., diffusion, heat conduction, viscosity, drift). The net effect of transport is to damp the inhomogeneities (e.g., the gradient of local concentration, temperature or field) in the system to reach the stable equilibrium. These tendencies couple with the kinetic nonlinearity of the first term greatly increase the variety of situations that may arise once an instability occurs. The second term represents the fluctuations caused by external fields and internal fluctuations and are connected with the damping term (the 3rd term). This term is therefore a measurement of the coupling strength of the first term and the third term. If this coupling increases to

some critical value, long-range correlation occurs. Some of the properties of each term in equation (1.7), which is also refered to the reaction-diffusion (RD) equation, are shown in Table 3.

Because of the nonlinearity (the first term), equation (1.7) may have several time-independent solutions. One of these is termed as the thermodynamic branch, since it is the continuous extension of the unique thermodynamic equilibrium state. As the external parameters of the system are varied to displace the state of the system away from equilibrium, the final state of the system depends crucially on the stability properties of the various states which are accessible under the changing conditions (especially the external parameters). This situation is indicated schematically in Fig. 11. In this figure we show that the deterministic equation is sufficient at or near equilibrium and the stochastic approach become essential as the bifurcation points are reached. Some typical deterministic and stochastic solutions are also included.

The analytical solutions of the reaction-diffusion (RD) equation are usually very difficult to obtain. However, it is found that the most interesting solutions are the asymptotic solutions which usually show some space-time structures, e.g., solitons or pulse solutions [10-12].

TABLE 3

Properties of individual terms in the reaction-diffusion equation.

	reaction potential drive the system	diffusion resistance factor damp the inhomogeneities		
	kinetics	fluctuations	diffusion	drifting
dN/dt=	H(N) +	F(t) +	d/dx(DdN/dx) +	dN/dx (1.7)
Det.	Yes	No	Yes	Yes
Prob.	Yes	Yes	No	No
L or NL	L/NL	L/NL	L	L
IR or R	R/IR	IR	IR	IR
Unique solution external parameter dependence	No	No	Yes	Yes
	S	S	W	W

Det.=deterministic.
Prob.=probabilistic.
L=linear.
NL=nonlinear.
IR=irreversible.
R=reversible.
S=strong.
W=weak.

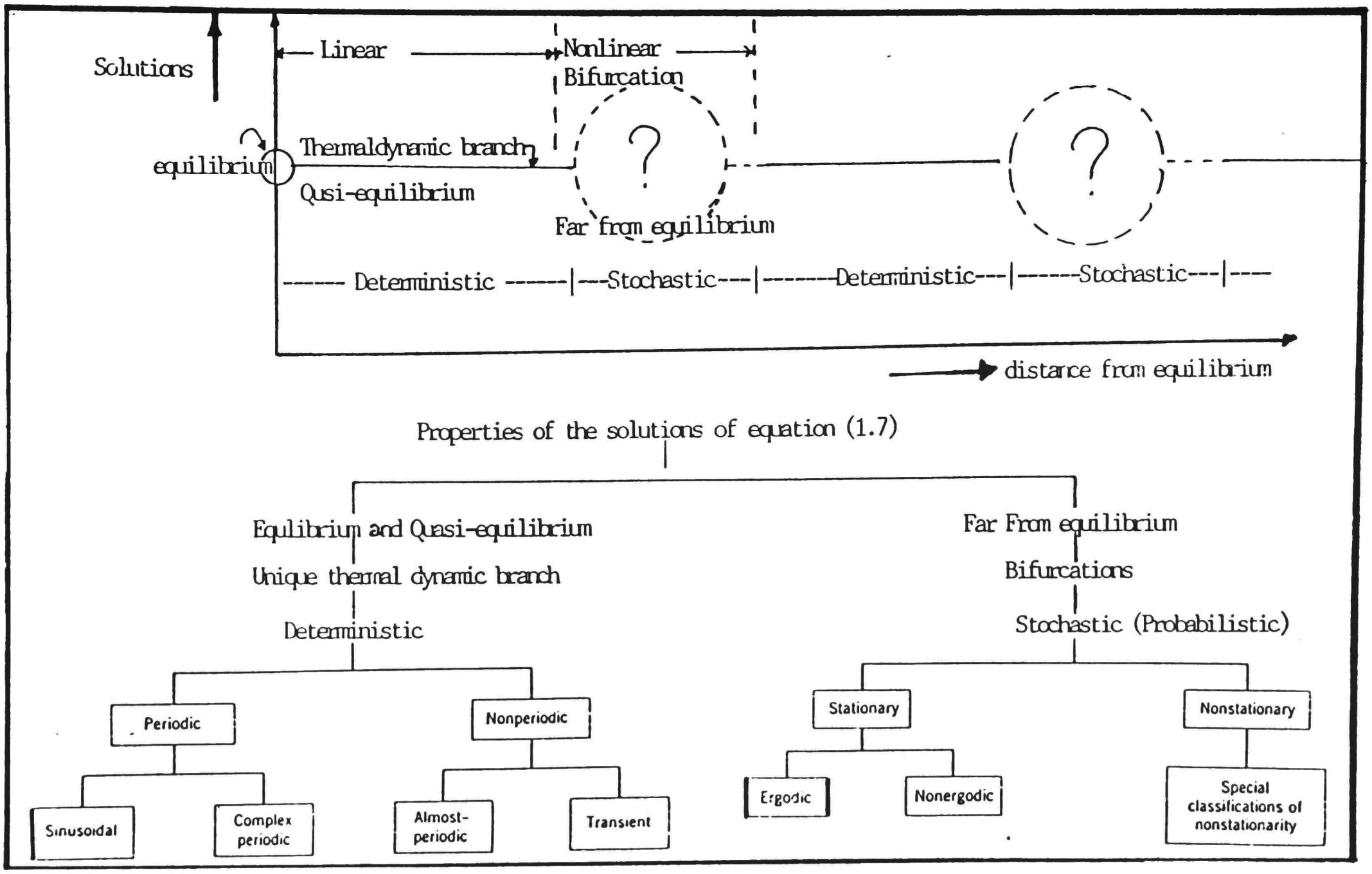

Figure 11: Schematic diagram of solutions of (1.7) versus the distance from equilibrium.

In summary, we have discussed why the dielectric thin film systems have to be considered as open systems when subjected to external sources. We also show that the conventional breakdown theories can be considered as the special cases of equation (1.7), which is a typical equation for the open system.

In the following chapter we briefly review the growth stages during deposition to see how defects are incorporated into the film structure. We further suggest that equation (1.7) can be considered as a model for the nucleation and growth processes, in which the order parameter is the size of the nucleus, or islands. All states inside the band gap have been considered as defects or trap states. Based on this definition, a classical picture of particles moving in the random potential wells under the influence of external field has been applied, and the basic transport mechanism has been considered.

CHAPTER II

DEFECT MODEL IN DIELECTRIC THIN FILMS

Important Experimental Techniques for Monitoring the Film Structure

The close relationship between the structure of thin films and their physical properties has been long recognized. The problem of the formation mechanisms and the structure of the thin films is believed to be the most important parameter in thin films physics.

Because of the lack of a reliable and decisive experimental technique, studying the formation mechanisms and the structure of thin films has been carried out in a complex way by various methods: physical, chemical and structural methods. (For the comparison of these methods see e.g [1, 2]). Among them the high intensity electron-diffraction technique provides the most sensitive and useful tool for the determination of the crystal structure of films down to monolayer thickness. On the other hand the high-resolution transmission electron microscopy (TEM), provides the indispensable technique for the study of microstructure and defect structure of dielectric thin

films. Others like low-energy electron diffraction may provide the valuable information about the shape of the grains, etc. Due to the complex structural states that appear in real dielectric thin films, combination of several methods are often applied. The specialized techniques depend on the type of the thin film material and the information sought.

The Growth Stages of Thin Films

The microscopic structure of dielectric thin films strongly depend on to the nucleation and growth processes. These, in turn, are controlled by a number of deposition parameters such as the deposition rate, chamber pressure, deposition angle, substrate temperature, nature of the impinging species, and the kind of residue gases inside the chamber, etc. The following growth stages are qualitatively the same for all types of vapor-deposited films prepared by a variety of techniques (e.g., vacuum evaporation, sputtering and epitaxy [13]).

(1) The nucleation stage. The impinging species hit the substrate, lose their momentum, and are attached on the substrate surface to form nuclei. These nuclei are thermodynamically unstable and tend to detached in a time depending on the deposition parameters. If the

deposition parameters are such that a cluster collides with other attached species before getting detached, it starts growing in size. After a certain critical size is reached, the cluster becomes thermodynamically stable.

(2) Island stage. The critical nuclei grow in number as well as in size until a saturation nucleation density is reached. The film growth is diffusion-controlled, i.e., adatoms and subcritical clusters diffuse over the substrate surface and are captured by the stable islands.

(3) The coalescence stage (granular structure). As islands increase in size by further deposition and come closer to each other, the small islands start coalescing with each other in an attempt to reduce the surface area. This tendency to form bigger islands is termed agglomeration and is enhanced by increasing the surface mobility of the adsorbed species.

(4) The channel stage (network structure). When the island distribution reaches a "critical" state, a rapid large-scale coalescence of the islands results in a connected network structure, and the islands are flattened to increase surface coverage. Initially, this process is very rapid but slows down considerably following the formation of the network.

(5) The continuous film. The final stage of growth is a slow process of filling the empty bridges and holes between islands to form a continuous film.

These nucleation and growth processes can be described uniquely by equation (1.7), if the order parameter is chosen to be the size of the grains or islands. By changing the external conditions (e.g., deposition parameters) the structure of the film goes from one stage to another, which is predicted by equation (1.7). This interpretation has the similarity with the thermal equilibrium phase transition and nonlinear annealing mechanism. The latter will be discussed in section 3.5, and an overall discussion of this subject will be presented in chapter seven.

Since the electronic properties of the dielectric thin film are closely related to its microscopic structures (island, granular, network or continuous), and hence the deposition condictions (chamber pressure, deposition rate, thickness, substrate temperature, substrate, deposition angle, etc.) and deposition methods (thermal evaporation, sputtering, chemical vapor deposition, etc.), different states of the structure may suggest different conduction stages. These suggest that the desired physical properties of the dielectric (or metallic, semiconductive, etc.) thin film can be obtained by choosing the suitable deposition

methods and controlling the suitable deposition parameters. Some of these will be discussed later in details.

Incorporation of Defects During Growth Processes

When the islands are still quite small, they are perfect single crystals. However, as the growth proceeds from the island stage to coalescence stage, the grain boundaries, point and line defects are incorporated into the film structure due to mismatch of geometrical configurations and crystallographic orientations. The other commonly encountered defects in dielectric thin film are dislocations, which are largely incorporated during the network and channel stages. These type of defects are mainly due to displacement (or orientation) misfits between different islands [14], and are the most important defects in continuous films.

The above mentioned defects are the crystalline defects, which are uniquely defined topologically as certain deviations from the perfect lattice structure. However, for most of the dielectric thin films, the large part of the film is occupied by non-crystalline or amorphous phases. This can be seen from x-ray diffraction pattern which usually show no sharp peak but amorphous-like broad peak.

General Definition of Defect

Because of the absence of a well-defined reference or ideal structure, the defects in amorphous phases can not be defined uniquely. Therefore to distinguish different type of defects at this stage may not be meaningful. For the present purpose, let us define all the energy levels inside the band gap as defect states. Since the dielectrics usually have a large band gap, the electrical conduction is most likely assisted by the states inside the band gap. Thus the above definition immediately connects the electronic properties with the defects. In the present work the defects include the following:

a) point-like defects (vacancy-, interstitials-like, etc.),
b) extended defects (dislocation-like, grain boundaries, melt spots, etc.),
c) undesired impurities (foreign atoms),
d) surface states (on interfaces),
e) disorder (localization),
f) free volume (structure fluctuation), and
g) fluctuations.

The above point-like defects are very different from the point defects defined in the crystalline materials. For example, a vacancy-like defect is not a well defined vacancy, but a collection of split vacancies which then

determine a region of lower density under tension (either electrical or mechanical). This is so because a well defined vacancy is generally unstable in the random structure and splits into partial vacancies. Similarly an interstitial-like defect simply means a crowded region under compression, and dislocation-like defects is similar to that of the crystal dislocation in its core but no long-range field can be ascribed to this defect. And unlike the dislocation in crystalline phase, this defect can terminate in the material and no well defined Burgers Vector, which is the characteristic displacement of a dislocation, can be assigned to it.

Items (a), (b) and (c) are the well-known crystalline-like defects. The rest (d)-(g), which are briefly discussed below, are also considered as defects in the context of proposed defect model.

Surface States

The surface states are critical for thin film systems, because of their large surface to volume ratio. Surface states represent one of the most obvious defects, because the surface has dangling bonds or reconstructions (surface relaxation) which reduce the energy associated with the surface. Quantum mechanically, the surface states are the

travelling wave solutions of the Schrodinger equation situated within the band gap of the bulk solids. These special solutions are waves which can travel parallel to the surface but not into the solid. Thus they are localized on the surface and can have energies within the band gap of the bulk band structure.

Surface states can be associated not only with the termination of a three dimensional potential at a perfect clean bulk exposed plane but also with changes in the potential due to relaxation, reconstruction, structural imperfections (such as emerging dislocations), or absorbed impurities. The surface states can affect the electrical properties of dielectric films by acting as a source or sink of electrons and their chemical reactivity by modifying the affinity of the surface for electrons.

Disorder and Anderson's Localization

When the defect density increases, the long-range order of the system decreases and hence the degree of disorder increases. It was shown by Anderson [15] that as the disorder increases to some critical degree the electrons would be completely localized and no diffusion of charged carriers can occur. This means that the disorder is capable of capturing the electrons and creating localized electronic

states inside the band gap. Based on this finding Mott introduced the concept of mobility edge [16], which is the extension of conduction band. The mobility edge separates the electronic localized states and extended states. Figure 12 shows schematically the mobility edge, surface states and localized states for a metal-insulator-metal system.

Free Volume (Structural Fluctuation)

For an atom or molecular segment to move (or twist) there must be a vacant site for it to move into. The availability of vacant sites may be expressed as an average free volume per atomic or molecular segment V_f, defined by $V_f = V - V_o$. where V is the actual volume occupied by a segment, and V_o is the close-packed-sphere volume. Since free volume can be considered as sites for charged carriers (defects) to move into (i.e., trap the charged carriers), it can be thought as some kind of defect. The relation between the defect density (caused by free volume) and free volume can be expressed as

$$N_f = \frac{e^{\frac{-r\nabla}{V_f}}}{V}$$

where V is the atomic (or molecular) volume, r is a geometrical overlap factor, ∇ is the critical fluctuation size for reaction or relaxation to take place.

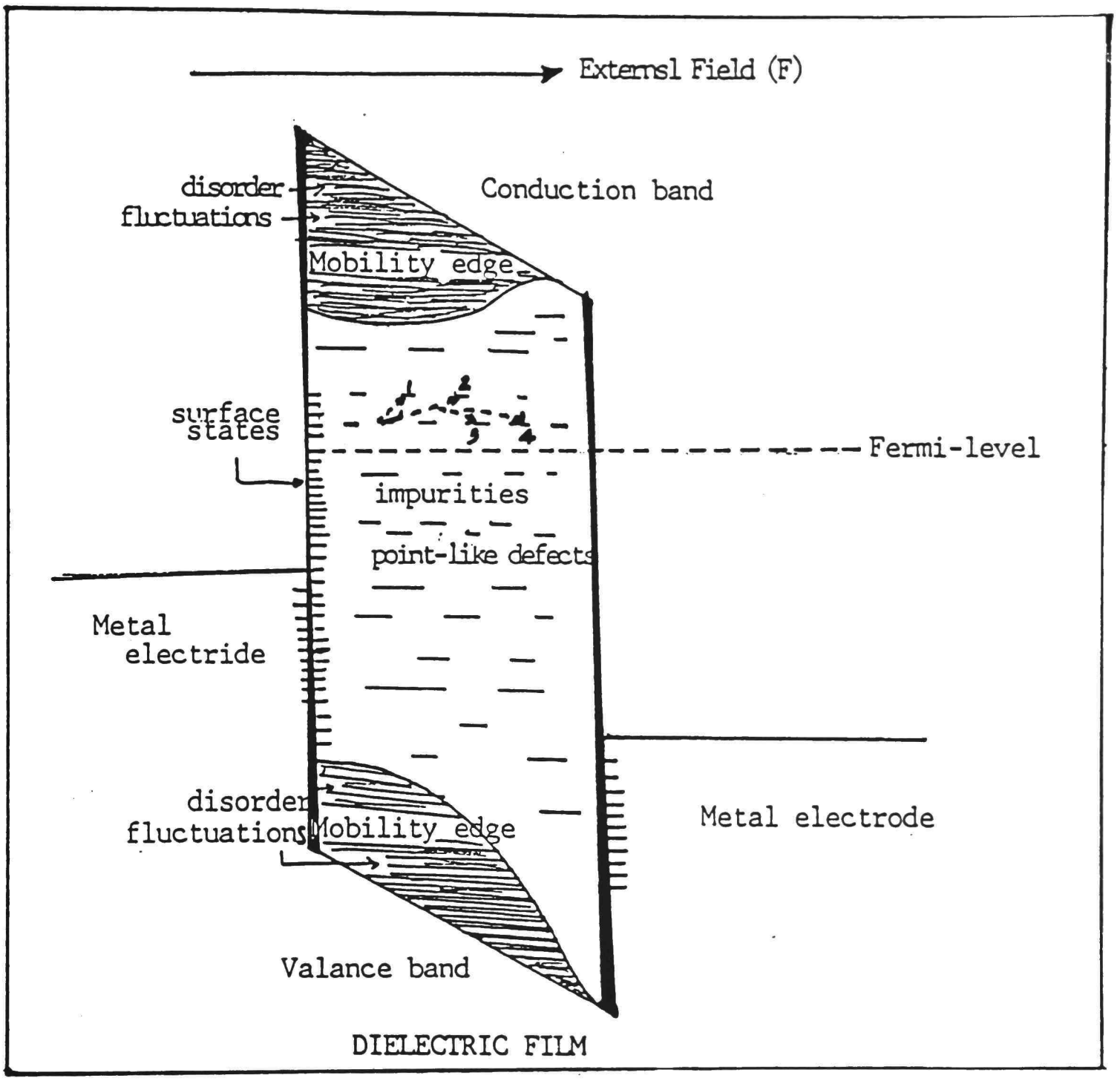

Figure 12: Defect states (traps) in dielectric thin film.

Fluctuations

Besides the structural fluctuation (free volume), other fluctuations caused by, for example, charge density

distribution or defect potential distribution can also localize electrons (or charged carriers) and thus can be considered as defects. It wil be seen later that at a distance far from equilibrium the effects of these fluctuations are in fact responsible for the instability of the states of the system.

Defect Model

In our model the conduction processes can be described as either electrons transport between fixed defects (static case) or by the motion of charged defects (dynamic case).

Static Case

In this case it is assumed that the position and energy distribution of defects in thin dielectric films are random in coordinate and momentum space respectively. In other words the radius of the defects and the distance between them are random in nature. To be more specific, it is useful to think of this defect model as a resistor network (percolative static picture [17, 18]) consisting of randomly distributed defects linked to one another by some conductance, and every defect has some capacitance. Usually, any defect site in the network will be connected by an appreciably large conductance only to its close neighbors in the four-dimensional position-energy space.

In the real film structure, this resistance network can be considered as composed of three regions, (1) high conductivity regions (i.e., high defect density or low material density regions, where G>>Gc, see below), (2) critical conductivity regions (G≅Gc), and (3) low conductivity regions (low defect density or high material density regions where G<<Gc). Here Gc's are overall critical conductances (not the conductance of the individual defect). Conduction and/or breakdown channels can be built up only when the overall conductance reach these critical values (Gc's). If the G>>Gc regions dominate the film structure then the film is in a high conductivity stage. This corresponds to the islands or granular structure of the growth stages in section 2.2. If the G≅Gc regions dominate, the conductivity of the film is in intermediate level (network structure). If the G<<Gc regions dominate, then the film is in low conductivity stage (continuous structure).

The above picture can be reformulated quantitatively via the representation of the energy diagram. The transport of charge carriers (electrons, holes, and/or ions) in the system could be characterized by either a succession of hopping from one defect state to another or by band controlled conduction. The "hopping" process indicated here

includes several basic conduction processes, like quantum mechanical tunneling, activated-tunneling, thermal ionization emission (Table 1), variable range hopping [16], percolation, or diffusion. In either case the position of the Fermi-level (Ef) is of critical importance. For the regions where $E_f << E_c$ (where E_c is the mobility edge), the wave-packet of conducting electrons are localized, and the conduction is mainly due to hopping between defect states. If this process dominates, the conduction is in low conductivity stage. If $E_f < E_c$, then the effect of extended states on the electron wave packet dynamics becomes stronger, and the conduction is dominated by the combination of localized states and extended states. For the regions where $E_f \cong E_c$, the fluctuations of the electronic wavepacket in extended states lead to long-range correlations in the system and to a substantial increase of the electrical conductivity. Finally, If $E_f > E_c$ done can use the standard transport theory based on the Boltzman equation. In this case an electron wave packet, which diffuses essentially as a classical particle, extends all over the system.

By changing the external parameters, e.g., electric field, pressure, magnetic field, and, in some cases, mechanical stress, the position of the Fermi-level and the

structure of the thin film can be changed. Consequently, the transport processes may switch from one stage to another depending on the external parameters. A schematic picture for the dependence of conduction regimes on the external parameters is shown in Figure 13.

As far as the electronic properties are concerned, the main effects of external parameters are to change the distribution of defect potential and position. If the spatial fluctuations of these distributions are large (which is the case at distances far from equilibrium) the effects of the random defect potential and charge distribution may be described as a local variation of the Fermi-level relative to the mobility edge of the system. We therefore suggest that the fluctuations of defect potential and position may be responsible for the different conduction stages and the electronic properties of the films.

For a quantitative evaluation of the important electronic conduction parameters, we should first compute the transition probability. According to quantum mechanics, the transition probability of hopping charge carriers from one defect to another depends on the distance and available energy states of the defect involved, i.e.,

$$P_{ij} = e^{\left[-2aA_{ij} - \frac{(E_i - E_j)}{kT}\right]} \quad \text{for} (E_i - E_j) >> kT \, . \qquad (2.1)$$

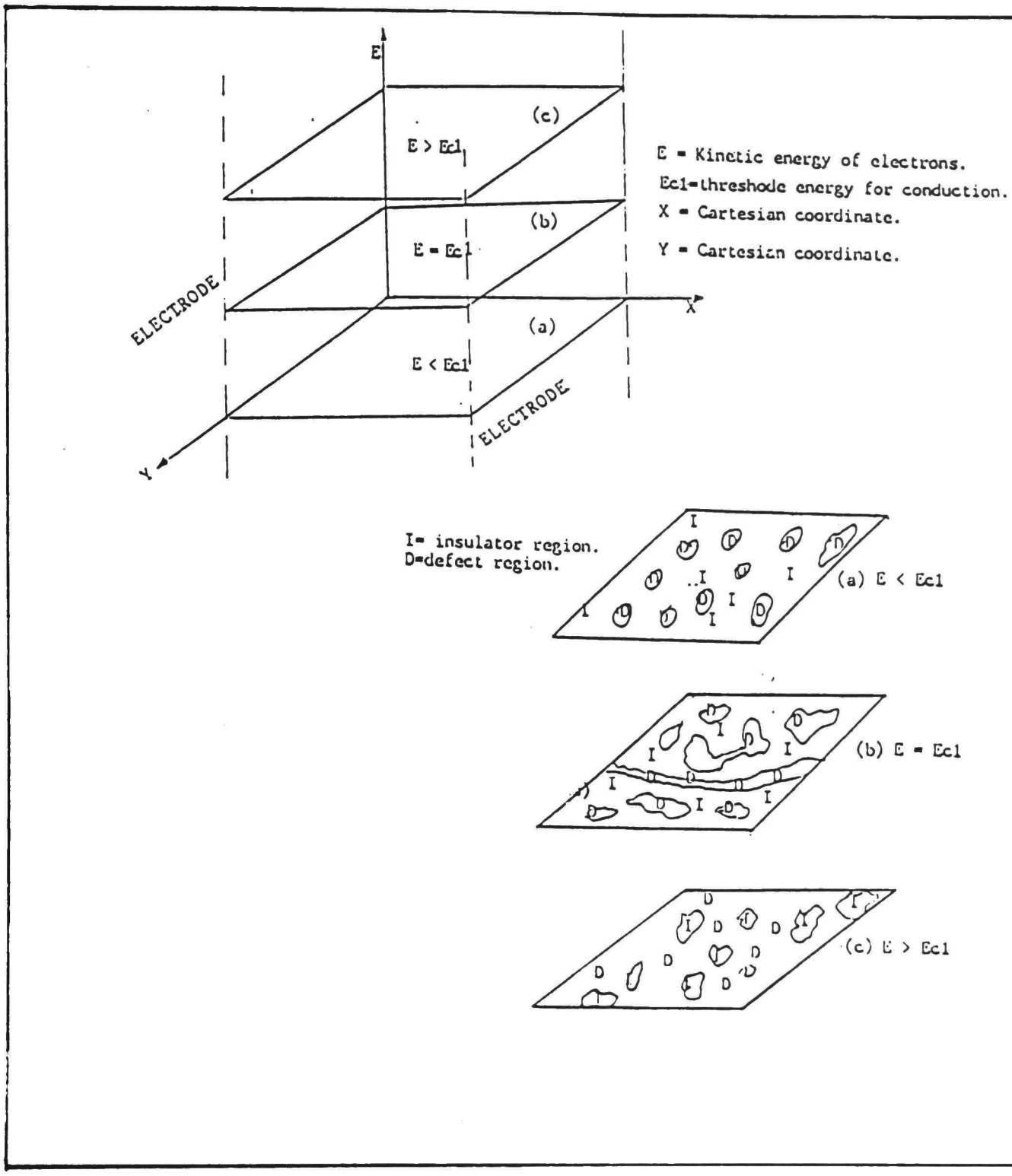

Figure 13: Schematic picture for the dependence of conduction regimes on the external parameters.

Here "a" is the decay constant of the carrier wave function (or the inverse of the localization length), A_{ij} is the effective distance between the defects involved, k is

Boltzman constant, T is absolute temperature, E_i is the initial energy level of hopping and E_f is the final energy level of hopping. For $E_c >> E_f$, $(E_i - E_j) = (E_c - E_f)$, for $E_c > E_f$, $(E_i - E_j) = E_c - E_f + W$,

where W is the mean hopping energy; for $E_c \cong E_f$, $(E_i - E_j) = W$, for $E_f > E_c$, no activation energy is necessary for the transport of electrons.

Therefore the hopping rate which follows from equation (2.1) is

$$\text{Rate} = fP_i(1-P_j)e^{[-2aA_{ij} - \frac{(E_i - E_j)}{kT}]}, \qquad (2.2)$$

where f is the intended-to-jump frequency of charged carrier at the defect i, P_i is the probability density of full states in defect i, $(1- P_j)$ is the probability density of empty states in defect j. The prefactor of tunneling rate $P_i(1-P_j)$ is therefore the probability of initial site i being occupied and the final site j being empty. $e^{-2aA_{ij}}$ is called the overlap factor, because the rate involves the overlap of initial and final state wavefunctions, both falling off exponentially with distance. Then the mobility and conductivity equations are

$$\mu = \frac{De}{kT} = \frac{e}{kT}\frac{A_{ij}^2}{2}\ \text{Rate}\ , \tag{2.3}$$

$$G = N_c e\mu = P_{ij} e \frac{efA_{ij}^2}{2kT} = \frac{N_c e^2 A_{ij}^2 P_{ij}}{2kT}\ , \tag{2.4}$$

where N_c is the number of electrons per unit volume. This depends on the defects present in the structure due to two factors, i.e., the ratio of the defect concentration to the density of state in the conduction band, and the ratio of the defect ionization energy to thermal energy kT. The mobility may also be controlled by defects, either by scattering or by repeated trapping and/or release of the carriers. An important point to note is that the effects of defects on the carrier concentration (N_c) and mobility (μ) are opposite, tending to compensate for each other.

Equation (1.4) can be rewritten as

$$G = Go\ e^{(-2aA_{ij})} e^{\frac{(E_i - E_j)}{kT}} \qquad \text{for}(E_i - E_j) >> kT\ , \tag{2.5}$$

where Go=constant= $\frac{fe^2d^2}{2kT}$.

The important feature of this model is that a distribution of A_{ij} and E_{ij} resultes in a distribution of the relaxation times (or hopping times), and distribution of hopping rates (or release rates). The former comes from the

distribution in hopping distance, and the latter results in the variation of activation energy. Since E_{ij} are influenced by almost all other conduction parameters, e.g., field, temperature, thickness, pressure, electrode, geometry, aging, impurity, order, etc., the relation between conductivity (or breakdown strength) and these parameters can be derived from the knowledge of how these parameters influence the distribution of A_{ij} and E_{ij}. This will explain the parameteric dependence of DC conductivity and breakdown strength, which has been observed experimentally. The details will be addressed in chapter four and five.

Dynamic Case

Another case of the conduction in thin dielectric films is that the defects are moving (diffusion, migration or growth, etc.) under the influence of an external electric field and/or density gradient and temperature gradient [19]. For the energies under consideration the wavelengths of the mobile defects are such that they are much smaller than the characteristic distance of the potential fluctuation. This is because the defects typically have small mobility (high effective mass and narrow band width). In this case, the motion of these defects may be treated classically as particles moving in the random potential wells [20].

Under this approximation the transport process is similar to the ionic conduction. The probability per attempt that the defect succeeds in advancing to the right (along the field), is $e^{\frac{-(2V-qAF)}{2kT}}$, to the left (against the field direction) is $e^{-\frac{2V+qAF}{2kT}}$. If there are f attempts per second then the net probability per second of advancing is

$$\text{Rate} = fe^{\frac{-V}{kT}}[e^{\frac{qAF}{2kT}} - e^{\frac{-qAF}{2kT}}] \text{ , i.e.,}$$

$$\text{Rate} = 2f\, e^{\frac{-V}{kT}} \sinh(\frac{qAF}{2kT}) , \qquad (2.6)$$

here "V" is the barrier height and "A" the distance between defects, q is the charge. Consequently this results in an electric current density J given by

$$J = Nqv = NqPA = 2fAqN\, e^{\frac{-V}{kT}} \sinh(\frac{qAF}{2kT}) , \qquad (2.7)$$

for a charged defect density N. From equation (2.7) it is seen that the mobility μ of the defect is

$$\mu = \frac{v}{F} = \frac{PA}{F} = 2fA\, e^{\frac{-V}{kT}} \frac{\sinh\frac{qAF}{2kT}}{F} . \qquad (2.8)$$

For $qAF << 2kT$ (low fields), $\sinh(\frac{qAF}{2kT}) \cong \frac{qAF}{2kT}$, equation (2.8) simplifies to

$$\mu = fqA^2 \frac{e^{\frac{-V}{kT}}}{kT} \quad . \tag{2.9}$$

Thus at room temperature for fields less than about 10^5V/cm, the conduction current is ohmic. For higher fields, since jumps against the field direction are negligible, (2.7) can be simplified as

$$J = fqAN\ e^{\frac{-(2V+qAF)}{2kT}} \quad . \tag{2.10}$$

In the above formulation, we have assumed that the distance between available jumping sites are the same, i.e., equal to A, and the potential barriers are symmetrical. In real dielectric thin films, however, there is in fact a range of "V" and "A," and there also is a range of attempt to jump frequency, f, and local dielectric constants. Thus to properly derive an expression for current density, J, and hence conductivity, which is a directly measureable physical quantity, all possible conduction paths must be considered. If equation (2.7) is used then for amorphous thin films, it is necessary to consider "V" and "A" to be functions of the field F and temperature T. The precise functional form would depend on the details of the transport network assumed. In general, equation (2.7) leads to a fractional parameteric dependence between conductivity and external field, which will be addressed in chapter four.

Defect Model and the Related Classical Models

The above picture described by the defect model is in some respect similar to the models used to study diffusion in statistical mechanics. For example, random walker, Lorentz model, Brownian motion and percolative motion. The purpose of this section is three-fold (a) to present several different models which are not considered in Table 1; (b) to show the important differences between these models which serve as a guildline for the application of this defect model to other systems or situations; and (c) to extend the range of the applicability of each model.

(1) Random walk. Classical particles move in steps of unit length in either direction with equal probability. The final position to the origin has Gaussian distribution. This is a typical Marcov process (i.e., each process is a function of discrete space and time coordinate). On the other hand, in defect model the jump distance is not constant but a distribution. The distribution function is usually non-Gaussian and the process is non-Marcov.

(2) Lorentz model. Classical particles move in a medium of randomly distributed stationary scatterers, with hard sphere or disk shape, without mutual interactions between themselves. Lorentz model is of special

interest becaused it exhibits nontrivial effects, which are characteristic of diffusion. For example, in normal fluids, there exists several phases, depending on the density of the phase. At low to moderate density phase, diffusion dominates the particles's motion; at high-density phase, localization (no diffusion) dominates the particles' motion. A transition from one phase to another is charactericed by a finite localization length, or a critical density N_c. These critical values are all called the "percolation edge." On the other hand, in defect model the interactions between defects are important and the shape, position and nature of defects are arbitrary.

(3) Brownian motion. Classical particles move under the influence of random fluctuations of the environment. The general equation of motion for this type of motion is the Langevin equation. This equation has been shown to be equivalent to the Foole-Plank equations (Gardiner 1985). Foole-Plank equation is a special case to reaction-diffusion equation. This equation is important in the sense that it is the only exception of reaction-diffusion equation, where stationary solutions are available.

(4) Percolation and Diffusion. (G. Deutscher 1983) There are two types of randomness. (a) the randomness which can be ascribed to the diffusive particles (diffusion process, random walker, Brownian motion, Lorentz model). (b) the randomness which can be ascribed to the medium, and frozen into it. The latter randomness was known as percolative motion. (The percolative motion is therefore determined by the properties of the medium and not the particles.)

Besides this fundamental difference, the following features are important to distinguish these two type of motion.

(a) Percolative motion has threshold properties, which indicate some switching mechanisms. The diffusive motion does not.

(b) Diffusive processes usually take place in a multidimensional medium, the evolution of these processes occur with time, which is one-dimensional. In percolative processes, the randomness is ascribed to the multidimensional medium itself, which is therefore much more complicated.

(c) Diffusive processes do not have memory effect (independent of the previous history), whereas in percolative processes the memory effect can not be neglected.

(d) In percolative process a particle can get trapped and be forced to oscillate between two defects, while the possiblity of trapping does not exist in the diffusive processes.

Despite the similarity and difference between all these models, equation (1.7) suggests that the microscopic processes occurs in the dielectric thin films are the combination of diffusive (Random walker, Brownian motion, Lorentz model, diffusion, etc.) and percolative motion, i.e., the conducting wavepackets in the system should interact with each other as well as with the medium.

Discussion and Conclusion

The reaction-diffusion model has been shown to be applicable to the nucleation and growth processes. Every stage of the growth processes, from nucleation to islands, granular to continuous film via network process, corresponds to different conduction stages. The defects which are incorporated into the film structure during deposition are extended to include all the states inside the band gap. Consequently, defects are responsible for the electronic properties of the dielectric thin films.

Further we have discussed two types of conduction cases, i.e., static case and dynamic case. If we compare the

set of equations (2.1-2.5) with (2.6-2.10) the two cases seem equivalent. In static case, the size of defects, the distance between defects, hopping times and hopping rates have some kind of distribution; and in dynamic case, the activation energy, jumping distance, attempt to jump frequencies and the prefactor of jumping rates have similar distributions.

Besides the basic conduction mechanisms shown in Table 1, the new concept we introduce in this chapter is the Mott's variable range hopping (1979) percolative and diffusive motions. Equation (1.7) takes into account both the diffusive and percolative conductions, and predicts that there are various conduction stages which are functions of the external parameters.

Finally, we point out an interesting feature of this defect model. It is well known that the properties of the crystalline materials depends on their structure. And the structure of the crystalline solid is determined mainly by the chemical bondings between the constituent atoms or molecules. There are three factors which decide the chemical bonding. They are (1) atomic or ionic size, (2) tendency to from covalent bonds and (3) electronegativity. Compare with the defect model, these three factors correspond to (1) size of defects, (2) distance between

defects and (3) formation energy of defects, respectively. This similarity may suggest that the physical properties of the materials are closely related to their microscopic structures, in both crystalline and in amorphous thin films.

In the following chapter, we will discuss some general properties of reaction-diffusion (RD) equation and show their relationship to the electronic properties of the dielectric thin films. Specifically, we will show how these properties may overcome the theoretical difficulties and explain the experimental observation in section 1.2. Several new features predicted by this model are also discussed. Based on RD equation a formalism will be provided to estimate the defect density and its corresponding average activation energy. The results are compared with the available experimental data. Consequently, we suggest that the RD equation may represent new kind of kinetics.

CHAPTER III

ELECTRONIC KINETICS IN DIELECTRIC THIN FILMS

In chapter one the conventional breakdown mechanisms have been formulated as the special cases of the general reaction-diffusion equation. In this chapter we address the following;

(1) How does the reaction-diffusion (RD) model overcome the theoretical difficulties mentioned in section 1.2 ?

(2) Does this model explain the experimental data on electronic conduction and breakdown in dielectric thin films ?

(3) What new features of the electronic properties of dielectric thin films are predicted by this model ?

Reaction-Diffusion Equation

Experience with rate processes of all kinds has indicated that one convenient way to formulate relationship between the rate and the environment is to separate "potential factors" (i.e., the first two terms of (1.7)), which drive the rate processes, from "resistance factors" (the last two terms of (1.7)) which oppose the processes.

The basis for the use and selection of potential factors and resistance factors arises from the second law of thermodynamics. The significant implication of this in the present context is that equation (1.7) contains both the reversible dynamics (Table 2) and the irreversible thermodynamics.

The physics of closed system discussed in Table 2 is well known, in which the equilibrium is the limiting case of the rate process. As the rate approaches zero, the detail balance principle can be applied and thermodynamic potential can be well-defined. On the other hand, the physics of the open system is not well-defined, in the sense that the deterministic laws are not the only operative mechanisms (Fig. 11). The loss of limitation of deterministic laws means that we go from a closed deterministic mechanical universe to a new probabilistic one that is open to fluctuations. This is because the state of the open system is rarely in equilibrium owing to its continuously changing mass, energy or momentum with its environment. Therefore there exists a variety of unpredictable macroscopic states in an open system, which may appear under some special conditions. At best, one can construct approximate expressions for some asymptotic solutions such as stationary-state, periodic, complex periodic, or

quasi-periodic ones without being able to assert that these solutions have exhausted all the possibilities of bifurcations in the system.

General Properties of Reaction-Diffusion Equation

If the order parameter in equation (1.7) is the defect density then one can rewrite that equation as follows

$$\frac{\partial N_i}{\partial t} = \text{Gain}(N_i) - \text{Loss}(N_i) = H(N_i) + F_i(t) + \frac{\partial}{\partial x}\left(D\frac{\partial N_i}{\partial x} + C_i N_i\right), \qquad (3.1)$$

where $N'_i s$ refer to the density of different type of defects and H, F, D, and C have the same meaning as in equation (1.7). The above equation is capable to deal with different kind of defects in the system. However, since it is not easy to distinguish among different type of defects in the dielectric film, we will consider only the total defect density, N, and simplify equation (3.1) to

$$\frac{\partial N}{\partial t} = \text{Gain}(N) - \text{Loss}(N) = H(N) + F(t) + \frac{\partial}{\partial x}\left(D\frac{\partial N}{\partial x} + CN\right). \qquad (3.2)$$

The general properties of RD equation in Table 3 can still be used in equation (3.2), and a flow chart in Figure 14 shows schematically how the external conditions and system parameters influence the states of the system [21].

For a given state, i.e., with a specific reaction function H(N), one generally wishes either to find solutions

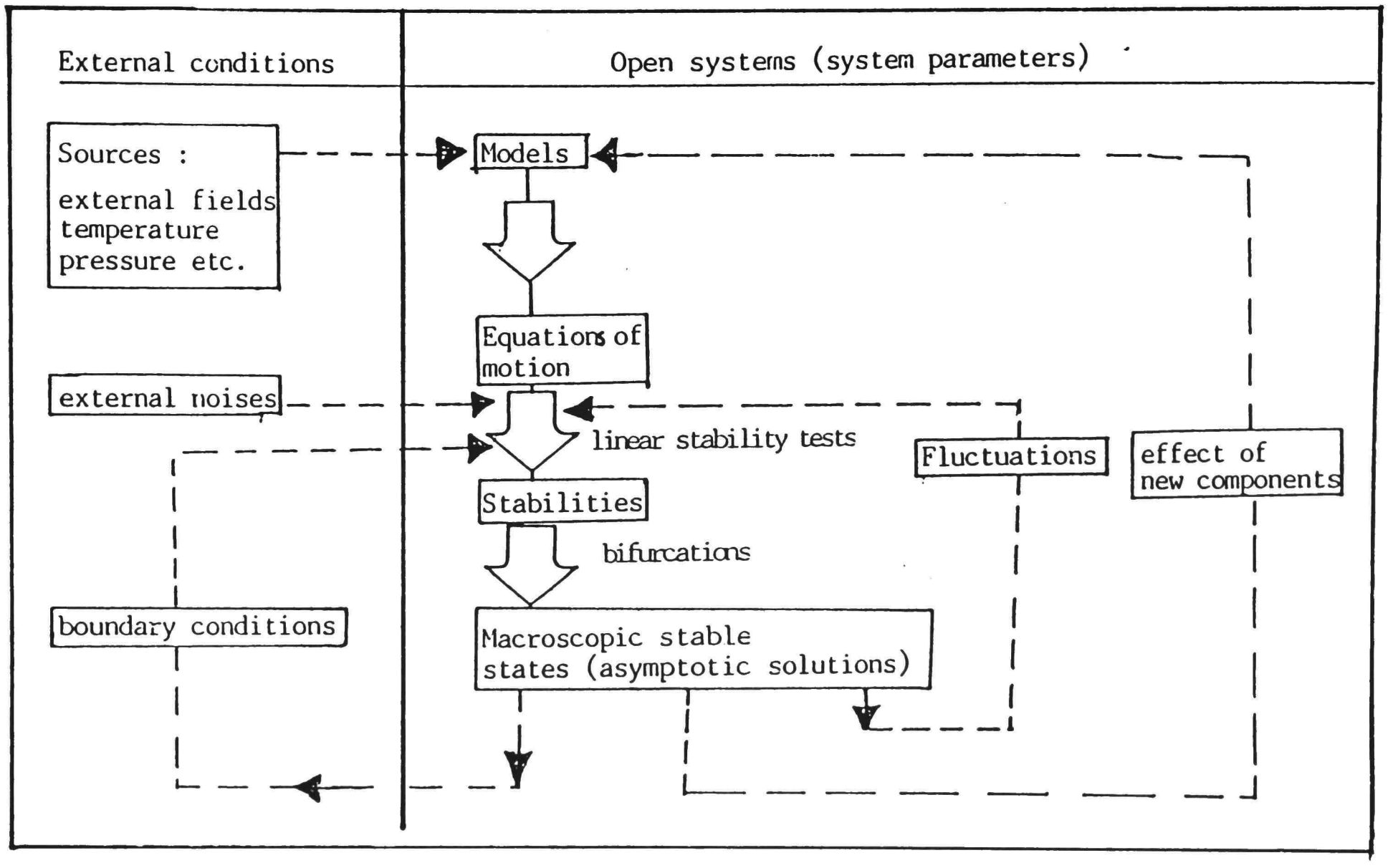

Figure 14: The flow chart for the solutions of reaction-diffusion equation.

satisfying certain subsidiary conditions, or to determine certain qualitative properties of the solutions. At a distance far from equilibrium the RD equation suggests that the analytic solutions are difficult to obtain and only the asymptotic solutions are significant. Asymptotic solutions specify the ultimate behavior of the system while ignoring the transient effects, which implies that the detailed knowledge of the initial and boundary conditions is not important. Since in dielectric thin film the structure is generally nonhomogeneous and is strongly influenced by the environment, only the qualitative results are possible to obtain. Thus the RD equation provides a solution for the difficulties faced by the dielectric thin films mentioned in section 1.2.

In order to see how this equation can be used in dielectric thin film systems, we consider the following important example. Let H(N) in equation (3.2) be one of the canonical ensembles of Thomas' Catastrophe theory [22], i.e.,

$$H(N)=- @N-N^3 . \qquad (3.3a)$$

The coefficient of the polynomial H(N), i.e., @, is called control parameter, which is the function of the external field. This parameter controls the characters of the various solutions of H(N) via the continuous energy or mass

flux input from the outside source. For some critical value of the control parameter the solutions on the thermodynamic branch ($\frac{dH(N)}{dx}=0$) are no longer unique. This can be seen from the steady-state solutions ($\frac{dN}{dt}=0$) of this equation which has been shown in Figure 15(a-d). If @ > 0, we obtain a stable state where the fluctuation F(t) is small. The state of the system in this case is perturbed only in a linear manner (Fig. 14(a)). When @ < 0, the number of states increase. Consequently, the critical fluctuations arise which drive the system from one stable state to another by some diffusion and/or long-range correlation processes (Figure 15(b-d)).

Although the analytic solutions of equation (3.2) are difficult to obtain, the situation can be simplified if certain approximations are made. For example, if the reaction rate is very rapid compared with the diffusion so that in the reaction time scale the diffusion and drift terms in (3.2) can be dropped. This process is called reaction controlled process. On the contrary, if diffusion is so rapid compared with the reaction rate that in the diffusion time scale the reaction terms can be neglected, this is called diffusion controlled process. The solutions for these two extreme cases are relatively easy to obtain

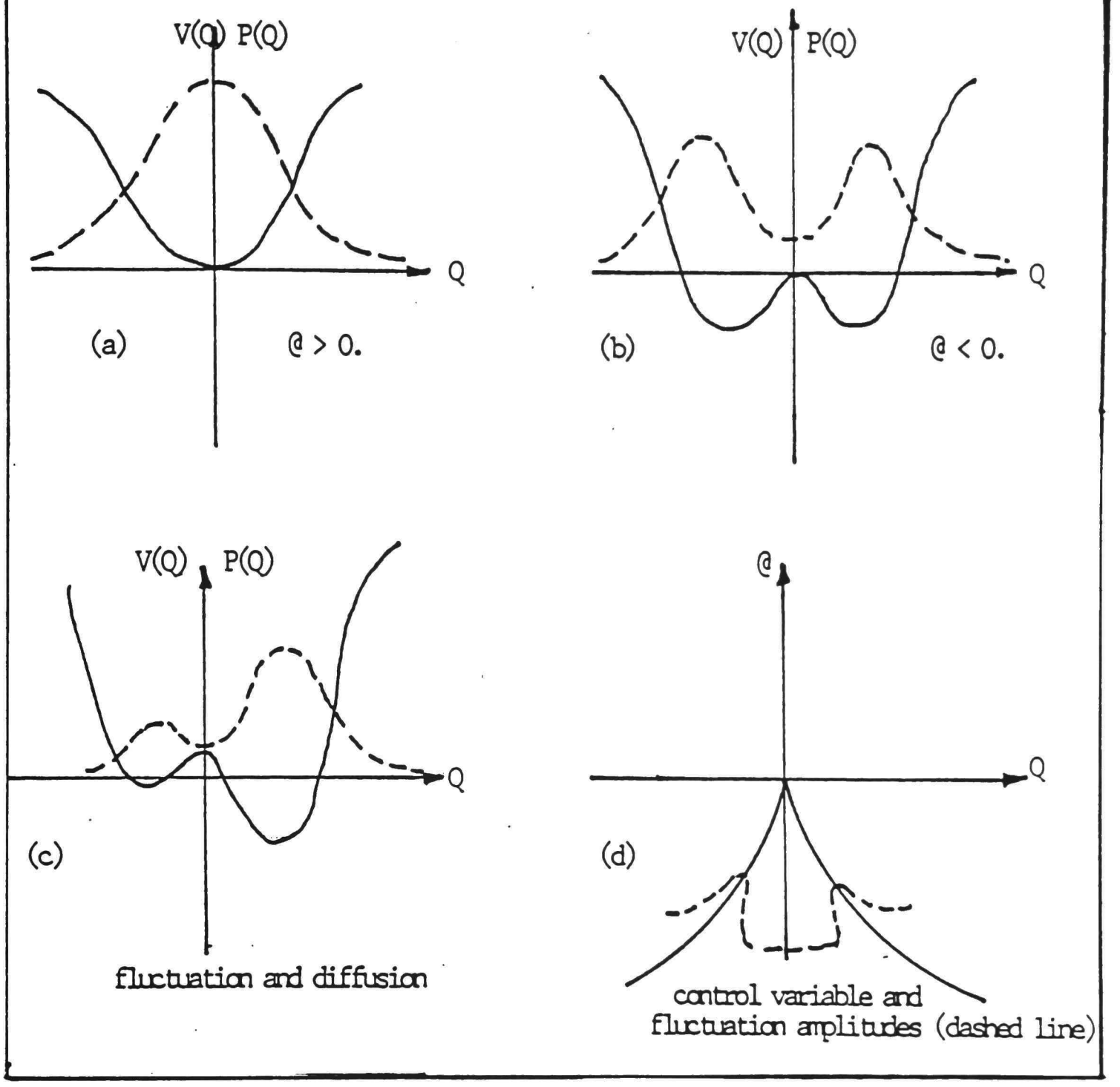

Figure 15: Potential (solid line) and probability density (dashed line) for $dQ/dt = -@Q-Q^3+F(t)+Dd^2Q/dx^2$.

and will be discussed later. Another way to simplify the equation is to transform the original equation to a relatively simple form (e.g., via point transformations), where some terms in equation (3.2) disappear.

It has to be pointed out that some intuitive clarity and accuracy of the original equation may be lost when the original equation is subjected to either elimination or transformation. The simplified equation may no longer have a direct lucid connection with the phenomena being modeled. Thus a restriction of the conditions under which the model is valid may be needed in order to justify the assumption that the neglected terms are small. Although simplification is done at the expense of physical insight and accuracy, such a reduction is advantageous, as it permits many qualitative properties of the solutions without a great deal of difficulty.

Diffusion Controlled Processes and Diffusion Equation

In the diffusion controlled process (i.e., the defects do not interact with each other), the method of rate theory allows one going from the motions of individual defects (under the influence of external and interatomic forces to the average motion of swarms of defects in phase space. This implies a transition from a microscopic deterministic description to a mazoscopic statistical description. Since the defect density is high, we can reasonably assume that the distribution function is continuously diferrentiable in

space-time coordinate. This distribution function will satisfy diffusion equation, which will provide the link between small-scale interactions among the individual defects and large scale motions of the flux of defects. The solution of this diffusion equation is well-known [23]. The formulation of the above description will be presented in section 4.4.

Reaction Controlled Processes and Catastrophe Theory

On the other hand, for the reaction control process, the situation is a little bit complicated. In this case

$$\frac{dN}{dt} = H(N) = \frac{dV}{dx} \quad , \tag{3.3b}$$

where V is the generalized potential, which is the thermodynamic potential at or near equilibrium, at the distance far from equilibrium, the physical meaning of V is not clear. If the generalized potential can be found then Catastrophe theory [24, 25] can be applied to classify the solutions of the kinetic system by looking for the points where there is a change in the stability properties of the steady states, i.e., $\frac{dN}{dt} = \frac{dV}{dx} = 0$. These states form hypersurfaces in the parameter space along which either branching of the solutions of the equations take place, or

stable solutions are obtained where V attains its absolute minimum in at least two distinct points. By crossing these hypersurfaces one switches from a stage where certain dynamics takes place to another where the dynamics is qualitatively different. An example has been discussed in section 3.2 and shown in Figure 15(a-d).

Qualitative Interpretation of Current-Voltage Characteristics

The typical current-voltage (I-V) characteristic curve in thin dielectric films is shown in Figure 8. It is found that at low fields the I-V curve is linear; as the field is increased, it results in nonlinear I-V curve; and as the field is increased further the I-V characteristic shows a negative differential resistance (NDR) regime, which is followed by the breakdown.

These experimental observations can be explained by RD model as follows: At low fields (i.e., below some threshold value) the kinetic energy of electrons U is small and the potential barrier V is high. Furthermore, the correlation between energy levels in defects is not significant, thus the I-V curve is linear. As the field is increased, U increases, V decreases, and the degree of correlation increases. As a result the I-V characteristics are switched

to nonlinear regime. As the field is increased further resulting in high current density, the Joule heating leads the system to a far from thermal equilibrium condition. In this situation the high temperature enhanced fluctuations lead the system to cooperative unstable NDR regime, in which long-range correlation dominates and drives the system to the structural instability (breakdown). We will leave the quantitative formulation and the microscopic description of these general experimental observations to section 4.4 and 5.3 respectively.

Before leaving this section we point out one interesting feature of RD equation. The reaction function in equation (1.5) has the similar form as equation (3.3a). Therefore the qualitative discussion for the instability of the system is similar to Fig. 15(a-d). The analytic solution of equation (1.5) [26] shows hysteresis (or memory) effect for the behavior of the most probable values of current density as a function of external field (Fig. 16(a)).

A good example for the behavior predicted by the RD model is the fatty-acid molecular films (Figure 16(b)), which shows clearly the switching and hysteresis effects.

In the following section we present a formalism to compute the defect density in dielectric thin film.

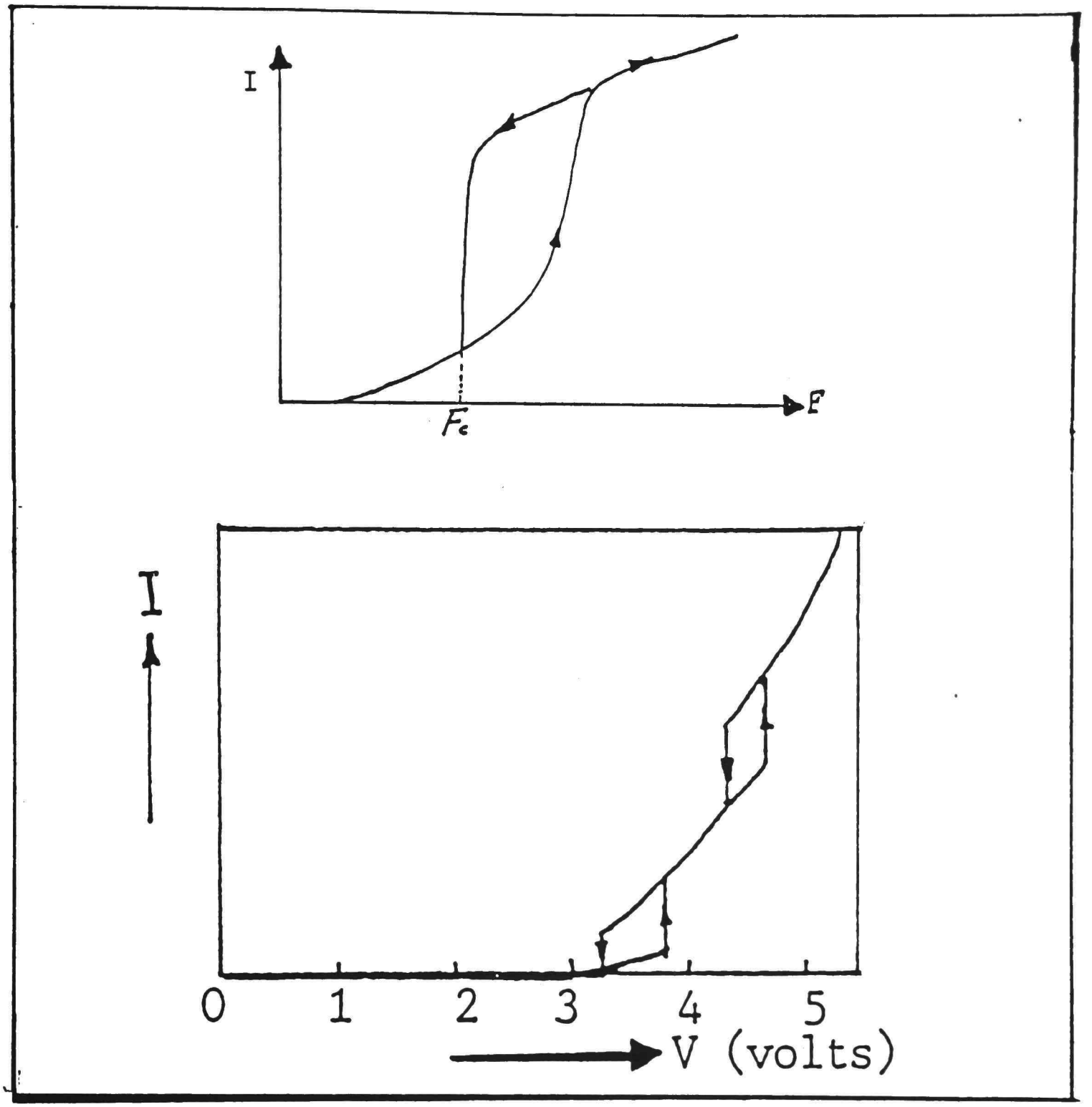

Figure 16: Hysteresis behavior of reaction-diffusion equation. the current switching and memory effects in fatty-acid films.

In the following section we present a formalism to compute the defect density in dielectric thin film.

Annealing Mechanisms: Conventional Electronic Kinetics and Defect Model

In crystalline materials the computation of defect density (e.g., impurities, point defects) is straight forward [16]. However, the computation of defect density in amorphous systems is usually difficult due to the spread in parameter values. These spreads arise mainly from the random variations in, for example, activation energies, distances, positions and hopping times. In general, the defect densities can not be measured directly from experiment. In order to extract the important information of defect densities, suitable physical quantity(ies) which is (are) sensitive to the change of defect densities (e.g., Young's modulus, internal friction, resistivity, diffusivity) has to be monitored. One of the experimental techniques which can be used to obtain the information of defect density is annealing.

Annealing is the processes of disappearance or decay of excess defects. Excess defects may disappear in a system by three different mechanisms:

(1) migration to sinks (dislocations, grain boundaries or surfaces, etc.),

(2) recombination (e.g., impurities and vacancies), and

(3) growth of the grain size.

Using equation (3.2), the annealing mechanisms can be mathematically described as

$$\frac{\partial N}{\partial t} = -C(T)N - b(T)N^2 - \frac{\partial}{\partial x}(D\frac{\partial N}{\partial x} + CN), \qquad (3.4a)$$

where the first term on the right hand side represents the annihilation rate of defects caused by the growth of the grains, and is proportional to the total defect density in the structure. The second term represents the recombination rate of defects, which is proportional to the square of the total defect density. Here we have made a reasonable assumption that the density of the individual defects (e.g., the number of grains, impurities or vacancies) in the structure is linearly proportional to the total defect density. The third term is diffusion caused by the gradient of the defect concentration, and finally the last term represents the drift term, which is the averaged motion of the defects under the influence of the external fields. For the thermal annealing processes the effect of diffusion term is much larger than the drift term, because the diffusion term is proportional to the surface to volume ratio, while the drift term is not, thus the drift term can be neglected from equation (3.4a). Since we are considering only the effect of thermal annealing, we assume the control parameters "c" and "b" to be the function of temperature

only. The annealing effect caused by the small bias voltage will be neglected. After this simplification, equation (3.4a) has soliton-like solution, i.e., as $x \to \infty$,

$$N(x,t) = \frac{1}{\sqrt{x}} \, e^{(x-vt)\sqrt{\frac{b}{D}}} , \qquad (3.4b)$$

where the velocity v is proportional to the annealing rate. The physical meaning of soliton-like solution will be discussed in chapter seven.

Although D can be decided from experiment, the control parameters (a and b) can not. In order to obtain some numbers which can be used to compare with the available experimental data, we take the following alternative approach.

Irreversible Defect Density and Resistance Versus Temperature Data

Let R_j be the resistivity contribution of type j defects (j is a dummy variable) with density $N_j(E_j)$ and activation energies E_j. The total resistivity R caused by all kinds of defects is therefore

$$R = \sum_{i=0}^{i} R_j(E_j) N_j(E_j) \, .$$

Since defects are distributed randomly in the dielectric thin films, the defect density is a continuous function of

activation energies, thus the summation should be replaced by an integral, i.e.,

$$R(E)=\int_{Eo}^{E} R(E)N(E)dE=\int_{Eo}^{E} NN(E)dE \ , \qquad (3.5)$$

where Eo is the lowest activation energy of the defects which are still present in the film at temperature T_o. $NN(E_j)=R(E_j)N(E_j)$ represents unit contribution of defects to resistivity. Differentiating the above equation with respect to temperature, one obtains

$$\frac{dR}{dT}=-NN(E)\frac{dE}{dT} \ . \qquad (3.6)$$

In order to compute NN(E), $\frac{dE}{dT}$ has to be known first. The knowledge of how activation energies of defects depend on the temperature can be obtained via kinetics, i.e.,

$$\frac{dN}{dt}=H(N)=K(E,T)N^m = C(E,T)N^m \ e^{\frac{-E(T)}{kT}} \ , \qquad (3.4c)$$

where we assume H(N) is not a polynomial, as suggested by the RD model, but equal to N^m, where m is called the order of the kinetics and is not necessarily an integer. We also assume reaction constant $K(E,t)=C(E,T)\ e^{\frac{-E}{kT}}$, where C=4fh with f as lattice vibrational frequency ($10^{(12-13)}$), and h is the number of defects in the cluster and is a function of temperature.

Integrating equation (3.4c) we obtain

$$N=N_o[\,1+(1-m)Ct\ N_o^{(m-1)}\ e^{\frac{-E}{kT}}\,]^{\frac{1}{(1-m)}}.$$

By changing the variable from time (t), to temperature (T), separating the variables and integrating from the initial temperature T_o and initial defect density No to T and N in equation (3.4c), we obtain

$$N=No[\,1+\frac{C}{a}(M+1)\ N_o^{(m+1)}\int_{T_o}^{T} e^{\frac{-E}{KT}}dT\,]^{\frac{1}{(1-m)}}\ ,$$

since

$$\int_{T_o}^{T} e^{\frac{-E}{KT}}\ dT=(\frac{KT}{E})^2\ e^{\frac{-E}{KT}}\ ,$$

hence

$$N=N_o[\,1+\frac{C}{a}(M+1)\ N_o^{(m-1)}(\frac{KT}{E})^2\ e^{\frac{-E}{KT}}\,]^{\frac{1}{(1-m)}}=N_oZ\ , \qquad (3.7)$$

where $a=\frac{dT}{dt}$ is the annealing rate, "Z" is the characteristic function of annealing, and is a smooth step function with respect to activation annealing energies as shown in Figure 17. From (3.7) the effective activation energy can be deduced ($\frac{d^2Z}{dE^2}=0$) as

$$E_{eff}\cong kT[\,\ln(f't)\,]\ , \qquad (3.8)$$

here $b=\frac{C}{a}\ N_o^{(m-1)}\ (\frac{KT}{E})^2$, with width $(\Delta(E)=E(Z=0)-E_{eff})$

$$\Delta(E) \cong mKT\ , \tag{3.9}$$

and the inflection point at

$$Z(E_{eff})=m^{\frac{1}{(1-m)}}\ . \tag{3.10}$$

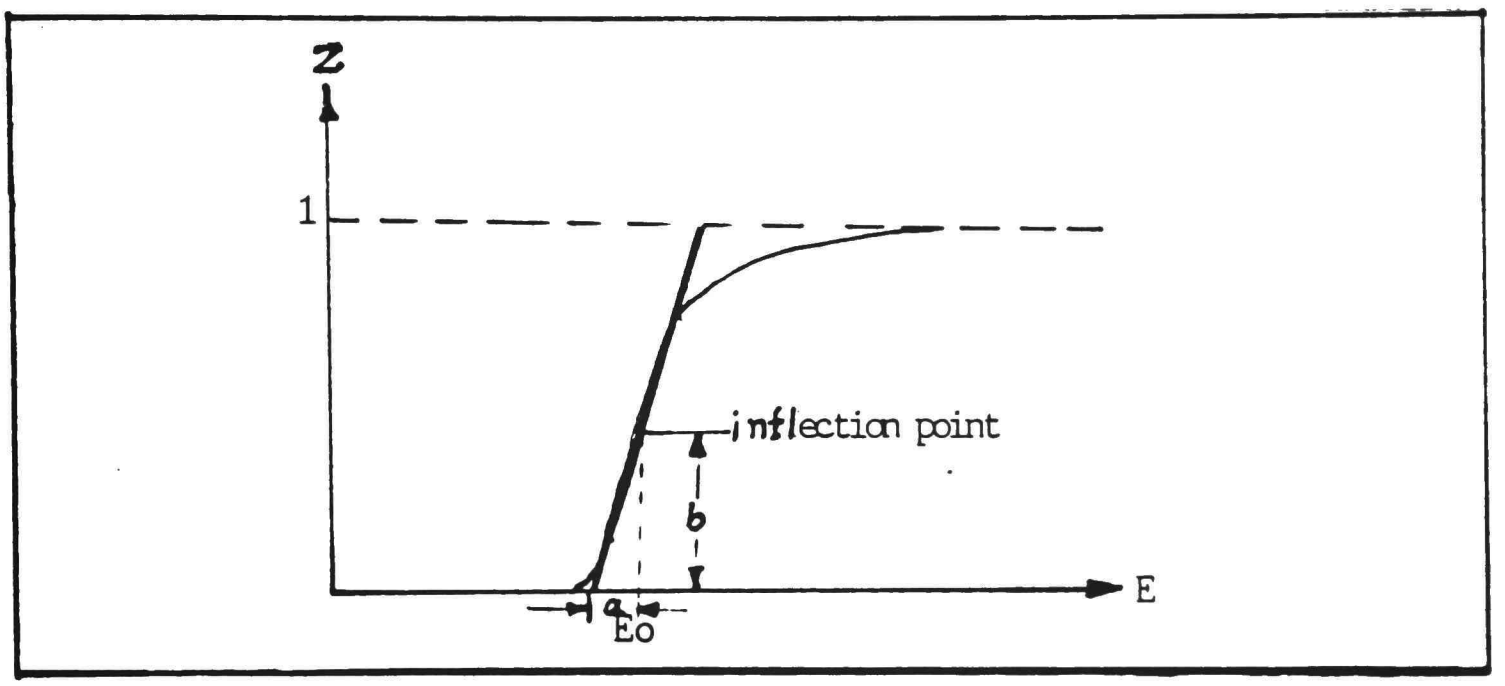

Figure 17: Annealing function versus activated annealing energy.

If equation (3.8) is differentiated with respect to T, we find

$$\frac{dE_{eff}}{dT} \cong \frac{E_{eff}}{T}\ , \tag{3.11}$$

thus equation (3.6) becomes

$$NN(E_{eff})=-\frac{\frac{dR(E_{eff})}{dT}}{\frac{dE}{dT}}=-T\frac{\frac{dR(E)}{dT}}{E_{eff}}\ , \tag{3.12}.$$

Therefore knowing $\frac{dR}{dT}$ at one particular temperature, the function $NN(E_{eff})$ and the corresponding activation energy E_{eff} can be computed from equation (3.6), (3.8) and (3.12). Repeating this procedure at different temperatures, a plot of $NN(E_j)$ versus E_j yields the defect density distribution and corresponding activation energies. This formalism will be applied to estimate the defect density in fatty-acid and silicon-monoxide thin films later in chapter six.

Discussion and Conclusion

In this chapter we have shown that the mechanism of open system has to be applied in dielectric thin film systems. Some important features of RD equation have been addressed. General experimental observations, e.g., typical I-V characteristics and memory effects, can be explained by this model, and a formalism to evaluate the irreversible defect densities and corresponding activation energies is proposed.

It has been shown that the conventional annealing theory (Eq. (3.4c)) did not include specifically the effect of each annealing mechanism. This represents a typical situation of conventional electronic kinetics, which usually

can not be modified easily to include other new type of interactions. From Equation (3.4a) we find that all these interactions can be incorporated into RD equation easily. Therefore the RD equation may represent a new type of kinetics.

In the following chapter we will briefly discuss the relationship between defect RD model and the basic conduction processes in dielectric thin films. New conduction processes, e.g., variable-range-hopping and percolation, will be introduced to explain part of the experimental data. After comparing these new conduction processes with defect RD model, an interpretation of the general fractional exponential parameteric dependence will be proposed. A nonlinear superposition principle is discussed and an interesting interpretation of Coulomb's gap, insulator-metal transition and minimum conductivity will be addressed.

CHAPTER IV

CONDUCTION PROCESSES IN DIELECTRIC THIN FILMS

In this chapter we are going to show quantitatively the role of defects played in the conduction processes and the relation between this process and the existing transport processes in dielectric thin film.

We consider a metal-insulating thin film-metal (MIM) system, which is subjected to an external electric or other fields (temperature or magnetic field). We are concerned mainly with conduction through, rather than along the plane of the film. Since the impedance of dielectric films is usually very high, the dominant electrical conduction is not likely along the film plane or the edges (this situation is different from metal films, in which the edge conduction is important). Furthermore, since dielectrics usually have relatively large band gap, we will concern primarily with the conduction caused by electrons rather than the holes or ionic carriers (the effective mass for the later is large), although the result can be applied equally well to any type of charge carriers.

Basic Conduction Processes and Their Relation with Defect Model

Table 1 lists the well established conduction processes in the dielectric thin films. None of them alone, however, can explain satisfactorily the experimental data. Usually, in different temperature and applied voltage ranges, one or more conduction processes in Table 1 may be used. In order to see the role of defects played, let us first consider the possible relationship between defects and these conduction processes.

It is well known that for a given voltage, the current is a function of impedance. This suggests that the electrons, which are responsible for the conduction, are trapped somewhere in the system. If electrons are trapped mainly by the defects on the metal-insulator interface then either Schottky or tunneling conduction dominates. If electrons are mainly trapped by the defects inside the dielectric film, then space-charge-limited conduction dominates. Others like Ohmic and Poole-Frenkel conduction are directly related to defects, and ionic conduction can be considered as the drift of structural defects under the influence of an applied electric field. The brief relation between defect model and the basic conduction processes are shown in Table 4.

TABLE 4

The brief relation between defect model and basic conduction processes.

Processes	description	relation with defects
Schottky emission	* Electrons emitted from * the cathode jump (or * thermally assisted) over * the potential barrier at * the interface.	* surface states *modification leads to * lowering of barriers
Poole-Frenkel emission	* At high field the trapped * electrons are responsible * for the conduction.	*defect states control * the conduction.
Tunneling or Field emission	* the electrons from the * cathode tunnel through the * potential barrier without * thermal excitation. * (the position of the * Fermi-level is varied.)	* the electrons tunnel *from defect to defect *(the position of Fer- * mi level is fixed.)
Space-charge limited	* Charged carriers are trap- * ped by the deep level * defects, and there are no * free electrons in dielect- * ric to balance these * trapped charges.	* trapped charges * control the conduc- * tion.
Ohmic	* the electrons hop from * one defect state to * another.	* defect states (at * the same energy * levels) control the * conduction.
Ionic conduction	*Conduction is controlled by * the hopping or diffusion * of the ions.	* ions behave as * charged defects.

The Candidate of Electronic Conduction in Dielectric Thin Films

The tunneling conduction in Table 1 is the tunneling between electrodes; the defects related tunneling is the tunneling between defects. The difference is that the Fermi-level in the former is fixed, and in the latter it varies. In real thin film system the direct electrode to electrode tunneling rarely occurs, because the effect of the surface states. Recent tunneling investigation in molecular films indicates that this is the case [27, 28].

The transportation of charge carriers from one defect to another can take place through either of the following (neglecting the fine structure of defects band):

(1) field emission (quantum mechanical tunneling) which should be responsible for the main conductivity process at low temperature,

(2) thermally assisted tunnelling which may be responsible for the conduction process at moderated temperature,

(3) thermal emission which contributes to the conduction process at high temperature.

Among these three possible processes, quantum mechanical tunnelling is much more sensitive to the distance between defects (a typical tunneling distance in dielectric thin film is 50-100A. This distance can be extended further

if the structural defect density is high). Because the high defect density and many potential barrier lowering mechanisms strongly depend on these structural defects [29], the tunnelling may be the most important conduction mechanism at any temperature range in the dielectric thin films.

Multiple-Range-Hopping and Percolative Process

In 1969 Mott [30] had predicted that the temperature dependence of conductivity in the amorphous semiconductor (or dielectrics maybe) is $\langle G\rangle=\langle Go\rangle\, e^{(\frac{T_o}{T})^{\frac{1}{4}}}$ at low temperature. Later this type of fractional temperature dependence was derived by Ambegaokar et al [31] which can be understood from the following argument.

At high temperatures, the temperature factor of the transition probability in equation (2.2), i.e., $e^{\frac{E_j-E_i}{kT}}$, is relatively unimportant. Thus the short range jumping, which maximizes the overlap factor of the electron wave-function ($e^{-2aA_{ij}}$), dominates. On the other hand, at low temperatures both the temperature and overlap factor are important. The most possible transition is therefore the

optimization of these two factors. Because of the random distribution of the defect sizes, there will be a distribution in activation energies E's. Within the radius of jumping distance A, the average spacing of the energy intervals $\Delta(E(A))$ is related to defect density $N(E_f)$ by $\Delta(E(A)) = \frac{1}{[N(E_f)4\pi A^3]}$. As A becomes larger, $\Delta(E(A))$ become smaller. The most probable transition probability of the charged carriers is thus to minimize $(\frac{\Delta(E)}{kT} + 2aA)$. This indicates that the hopping is not restricted to the neighborhood sites, but sites at some "considerable" distance (e.g., 200A) which are energetically favorable. This property gives this model the name of variable-range hopping, as shown in Figure 18. Consequently, one readily finds that $A_m(T) = [8aN(E_f)kT]^{\frac{1}{4}}$, and that $e^{\frac{-E}{kT} - 2aA}$ takes the form of $e^{(\frac{-T_o}{T})^{\frac{1}{4}}}$. Combining the above three equations and assuming defect density proportional to kT, we find that the total conductivity $\langle G \rangle = \langle Go \rangle\ e^{(\frac{-T_o}{T})^{\frac{1}{4}}}$, where T_o and Go are constants.

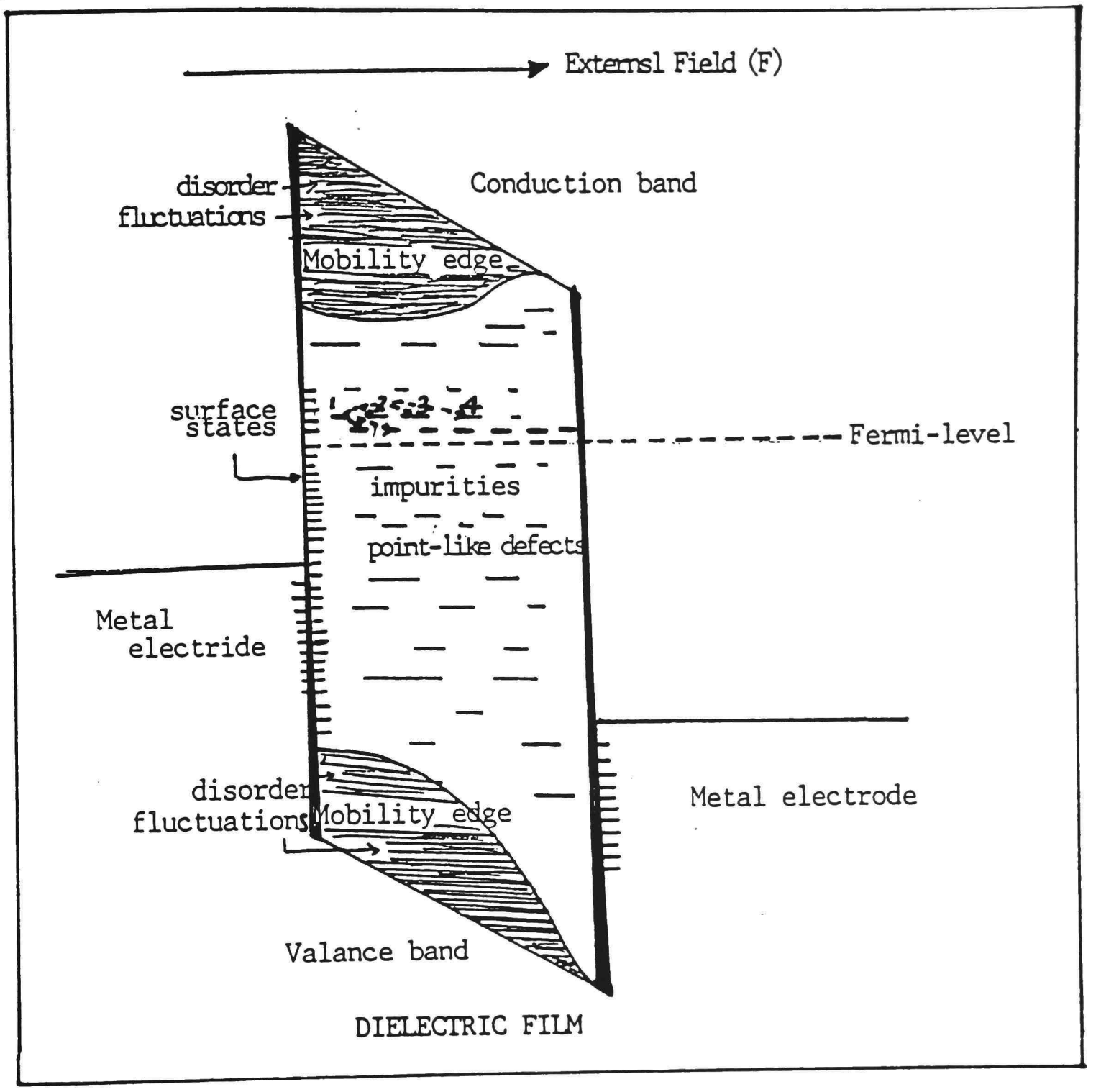

Figure 18: Variable-range-hopping in dielectric thin films.

The above model assumes that the density of states at Fermi-level is constant and has the following features: (1) the transition rate is determined by equation (2.2), (2) the

correlations between the energies of the neighboring sites are neglected, (3) the interaction between electrons on different sites is neglected, and (4) the fluctuations of the states density near Fermi-level are neglected.

A detailed consideration of all these features suggests that any of them may introduce nonlinearity into the system and therefore affect the transition probability. For example, take the electron-electron interaction on different sites into consideration, the transition probability become proportional to $e^{-2aA_{ij}-\Delta\frac{(E)}{kT}-\frac{e^2}{\varepsilon AkT}}$. Optimizing the exponential factor, Efors found that there is a soft Coulomb gap at the Fermi-level and the temperature dependence of the conductivity is $e^{(\frac{-T_o}{T})^{\frac{1}{2}}}$ [32, 33] instead of Mott's $e^{(\frac{-T_o}{T})^{\frac{1}{4}}}$. Since both of these are supported by the experimental data at low temperature in, for example, amorphous semiconducted films and spin glass systems [16, 34] respectively, the question is whether any of these can be used in dielectric thin films systems. This question will be addressed in the next section.

Besides the variable-range-hopping model, the percolation theory has also been applied to explain the

conduction processes in amorphous systems. As far as the fractional temperature dependence of conductivity is concerned, the percolation theory predicts that

$\langle G\rangle=\langle Go\rangle\ e^{(\frac{-T_o}{T})^{\frac{1}{(d+1)}}}$, where d is the dimensionality. The relation between multiple-range hopping and percolation theory is that the long-range hopping process can be treated as a near-neighbor bond percolation problem in a (d+1) dimensional hyper-space in which energy is the additional dimension. This suggests that for quasi-one dimensional finite chain systems at low temperature, the temperature dependence of conductivity should be $e^{(\frac{-T_o}{T})^{\frac{1}{2}}}$ (e.g., [35]) and $e^{(\frac{-T_o}{T})}$ for quasi-one dimensional infinite long chain systems (zero dimension, see e.g., [37]), and $e^{(\frac{-T_o}{T})^{\frac{1}{3}}}$ for two-dimensional systems (e.g., [38]).

Although the above models can, more or less, explain part of the experimental data, the observed values of the fractional exponential factor, n, in dielectric thin film systems are in fact some kind of distribution.

Defect Reation-Diffusion Model and the General Fractional Exponential Dependence

According to the RD model, an explanation can be easily given to the difference between n=.25 and n=.5. Mott's assumption (n=0.25, i.e., constant density of defect states at Fermi-level) corresponds to the situation of thermal equilibrium and quasi-equilibrium, where the density of the distribution function is Poisson distribution at the Fermi-level. On the other hand, Erof's consideration (n=0.5) represents a special case of far from equilibrium, in which the nonlinear interaction (i.e., $e^{\frac{-e^2}{\epsilon AkT}}$ enhances some of the fluctuations. The density of the distribution function in this case is no longer Poisson, but crater-like, with its minimum density at Fermi-level. An example of the latter situation can be obtained directly by adding a fluctuation term in equation (3.3a), i.e.,

$$\frac{dN}{dt} = -N^3 - @N + F(t) \ . \qquad (4.1)$$

The steady state solution is then given by the third-order algebraic equation

$$N^3 + @N = F(t) \ . \qquad (4.2)$$

As F(t)=0 we find equation (4.2) has only one root, N=0, if the control variable @>0. On the other hand, if @<0 there

are three roots, N=0, N=$\sqrt{(-@)}$, and N=-$\sqrt{(-@)}$. As shown in Figure 19. For @ < 0, the distribution function has double-hump with peaks centered on N=$\sqrt{(-@)}$ and N=-$\sqrt{(-@)}$ (for the detailed discussion of probability density peaks referres to [39]).

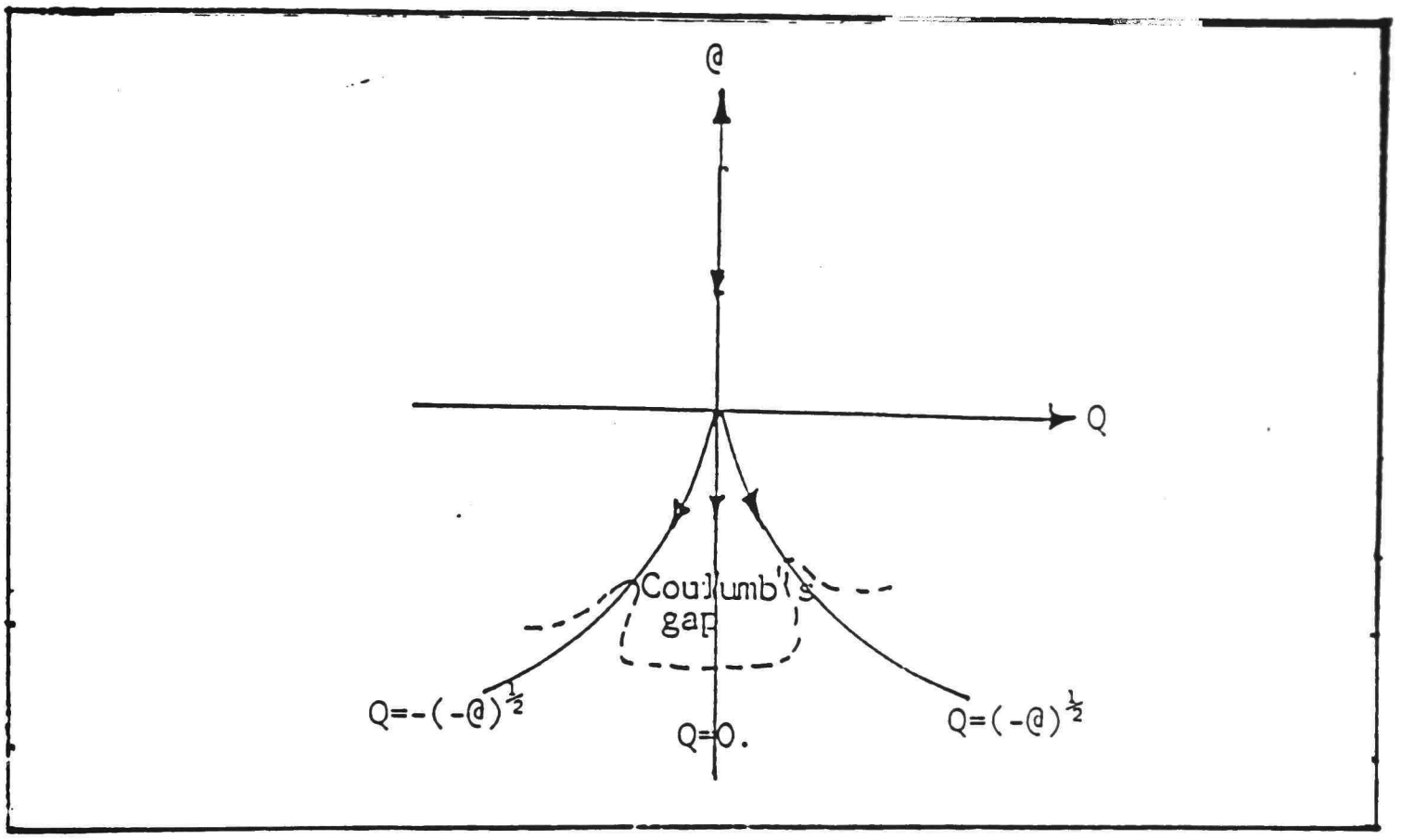

Figure 19: Coulomb's gap and non-poisson distribution.

Between peaks, the density of the distribution function is zero, and the separation increases as the fluctuation increases (i.e., as @ becomes more negative). This gives Coulomb's gap a simple physical explanation.

The Coulomb's gap has been observed in many physical systems, e.g., granular metal films [40], TCNQ (salts of organic ion-radical tetracyanoquinodimethan [41]), and doped polyacetylene [42].

Asymptotic Solution of RD equation in Phase Space

Let us envisage that the thin film system is divided in a number of cells. Each cell contains an arbitrary number of defects, x. Reaction (e.g., recombination, scattering, annihilation, trapping and growth of the size of the defects) occurs each cell, and the energy and matter transport (diffusion, hopping, inside percolation, etc.) take place between two or more cells. The Master equation for describing this process is as follows;

$$\frac{dP(x,t)}{dt} =$$

$$H(P)+D\langle x\rangle[P(x+1,t)-P(x,t)]+D[(x+1)P(x+1,t)-xP(x,t)], \quad (4.3)$$

where P(x,t) is the defect distribution function in phase space as described in section 3.2. H(P) and D are the macroscopic reaction and diffusion function, respectively.

$\langle x\rangle = \sum_{i=0}^{i} x_i P_i(x,t)$, reflects the averaged influence of the environment on the fluctuations. Under a continuum approximation (i.e., assuming the size of the system is much

larger than the size of the cell) equation (4.3) can be shown equivalent to equation (3.2) in the macroscopic level [12].

One of the asymptotic solutions of this equation is the stable distribution function, which has the following form [43]

$$P(z,n)=\int_{\infty}^{\infty} e^{-izu-u^n}\,du\,, \tag{4.4a}$$

where z and u are conjugate coordinates, $i=\sqrt{-1}$, and n is the correlation index, which has value between $0\le n\le 2$. For n=2,

$$P(z,n)=2\sqrt{\pi}e^{\frac{-z^2}{4}} = \text{Gaussian distribution.}$$

For n=1,

$$P(z,n)=\frac{1}{\pi}\frac{1}{1+z^2}= \text{Cauchy distribution.}$$

For n>2,

P(z,n) may diverge at some z, therefore it is not well-defined.

For $0<n<1$, [43, 44]

$$P(z,n)=\frac{n}{\pi}\sum_{j=0}^{j}\Gamma(1+j)\sin\frac{j\frac{\pi}{2}}{z^{(1+j)}}\,. \tag{4.4b}$$

One of the important properties of this stable distribution is that the linear combination of a set of

stable distributions, with a particular value of n, also has the same distribution and n. For example, if

$X=C_1X_1+C_2X_2+....+C_iX_i=\sum_{i=0}^{i}C_iX_i$ are random variables which has stable distribution with correlation index n, and $C_1, C_2, ...C_i$ are real constants, then the linear combination

$$X=C_1X_1+C_2X_2+....+C_iX_i=\sum_{i=0}^{i}C_iX_i \ ,$$

also has stable distribution with the same n. The physical meaning of this property is that the stable distribution satisfies some kind of superposition principle which may not be linear. For example, if M_o is the moment of any order of stable distribution then [45]

$$M_o^n=C_1M_o^n(1)+C_2M_o^n(2)+.....+C_iM_o^n(i)=\sum_{i=0}^{i}C_iM_o^n(i).$$

In case of Gaussian distribution (n=2),

$$M_o^2=C_1M_o^2(1)+C_2M_o^2(2)+.....+C_iM_o^2(i)=C_iM_o^2(i).$$

Thus the superposition of X_i is linear as n=1, and nonlinear as n not equal to 1.

General Fractional Exponential Temperature Dependence

The fractional exponential temperature dependence can be obtained readily from the assumption that the defects, which are responsible for the conduction, have a distribution in activation energies. Under this assumption the conductivity can be expressed as $G=\sum G(i)\, e^{\frac{-E_i}{kT}}$. If the activation energy is not correlated with other factors which determine the individual conductivity, the above equation may be written as

$$\langle G\rangle = \langle Go\rangle \int_0^\infty ff(E)\, e^{\frac{-E}{kT}}\, dE\,, \qquad (4.5)$$

where ff(E) is the distribution function of defect potential (or activation energies), <G> is the macroscopic average of the total conductivity, and <Go> is constant.

If we assume that ff(E)=P(E, n), substitute this into (4.5), and do the Laplace transformation [43], we obtain

$$\langle G\rangle = \langle Go\rangle\, e^{(\frac{-T_o}{T})^n}\,, \qquad (4.6)$$

where Go and T_o are constants.

If ff(E) is a Cauchy (Delta-like function) distribution (i.e., n=1), centered at Eo, then from equation (4.5) we find

find the conductivity is proportional to $e^{(\frac{-B}{T})}$, where B is constant. This distribution corresponds to the simple activated process, which suggests that there is only narrow defect energy band, not a broad distribution, inside the band gap. This situation appears to be associated with higher temperature and with films having small grains of relatively uniform size, and is usually observed in the growth stages of the thicker films, when the islands are just about to grow together to give a continuous film. For thinner films, the size of the grain is usually a linear function of thickness, unless they are annealed for a long period at high temperature.

If ff(E) has Gaussian distribution (i.e., n=2), centered at Eo, then from equation (4.5) we find

$$<G(T)> = <G'> e^{(\frac{-T_o}{T})^2},$$

with $T_o = \frac{Eo^2}{k}$. This suggests that special type of defects strongly dominate the film structure similar to the situation of n=1, however, there exist considerable broadening mechanisms.

If ff(E) has the form of equation (4.4b), i.e., $0<n<1$, then at low temperature and small n, equation (4.5) suggests that

$$\langle G \rangle = \langle G_o'' \rangle \, e^{(\frac{T_o}{T})^n} + C,$$

here G" and C are approximately constants. For n=.25, the first term was predicted by Mott's multi-variable-range hopping model, and the second term represents the minimum conductivity which was also predicted by Mott [30].

A physical picture of this fractional exponential temperature dependence of conductivity is that in the beginning there exists a variety of conduction channels for competing in parallel, and later the nonlinear interactions come in to play. The main effect of these nonlinear interactions is to enhance the amplitude of fluctuation which in turn drives the system to one of its macroscopic stable states. Each of these states corresponds to a specific value of n. The important feature of the stable distribution is that a number of n values are possible. This implies that there exists various conduction stages with respect to the different temperature ranges.

Fractional Exponential Field Dependence

For an open system, the source of the energy (or matter) input is a very important and convenient parameter for the characterization of the macroscopic stable states of this system. The main effects of the applied field in a MIM

system are

(a) to lower the potential barriers between defects at the metal-insulator interface along the field direction, and

(b) to increase the kinetic energy (or mean free path) of charged carriers, which are responsible for the conduction, and

(c) to enhance the amplitude of some of the fluctuations which may lead the system to a new stable state.

The typical experimental observation of field dependence has been shown schematically in Figure 3. This curve can be fitted approximately by the expression

$$J \propto V^m . \qquad (4.7)$$

For m=1, equation (4.7) represents the linear ohmic regime. It occurs when (a) there is no space charge in the sample, and (b) the electric contacts are ohmic for carrier injection or extraction. For m>1, equation (4.7) represents nonlinear conduction stage. It occurs at high field, when nonlinear interactions become important. For m<0, equation (4.7) represents the negative differential resistance regime. It occurs as the long-range correlation effects dominate.

At high fields (e.g., > 1MV/cm) the increase of the conductivity is usually exponential. For example, the Poole-Frenkel model (i.e., thermally assisted field

ionization, [46]) predicts n=.5 in the field dependence of conductivity, and Mott-Shklovoskii model (i.e., activationless variable range hopping, [47, 48]) predicts n=.25. The fractional field dependence of conductivity implies that there is a distribution in jumping distances A's. Thus the equation (4.5) becomes

$$\langle G \rangle = \langle Go \rangle \int_0^\infty ff(A)\, e^{\frac{qAF}{2kT}}\, dA \,. \qquad (4.8)$$

If ff(A)=P(A,m).

$$\langle G \rangle = \langle Go \rangle\, e^{(\frac{F}{F_o})^m} \,. \qquad (4.9)$$

The fraction m in equation (4.9) may be different from n in equation (4.6). The relation between m and n has to be decided from the precise field dependence of potential barriers and kinetic energies. The former, i.e. V(F), has been addressed by Schulter [29] and Frenkel [49]; and for the latter, i.e., U(F), more experimental data are needed.

Thickness Dependence of Conductivity

The defect model developed so far did not include the effects of film thickness directly. However it is well known that the thickness can influence, for example, the grain's size and the electron mean free path. As a result,

it influences the total resistivity (or conductivity) of the dielectric thin film. If the potential of the defects have stable distribution, i.e., ff(V)=P(V,n), then

$$<G> = <Go> \int_0^\infty ff(V)\, e^{\frac{-2aA\cdot qAF}{2kT} \cdot \frac{q^2}{\varepsilon AkT}}\, dV \ . \qquad (4.10a)$$

The Laplace transformation of the above equation yields,

$$<G> = <Go>\, e^{(\frac{d_o}{d})^{\pm n"}} \ . \qquad (4.10b)$$

It is noted that, at thermal equilibrium, the stable distribution function (e.g., n"=2, Gaussian distribution) is not sensitive to the redistribution of both activation energies and jumping distances caused by the small perturbation of, for example, F, T and thickness d. Under perturbation, the Gaussian distribution may change to Maxwell (assume n"=1.8) distribution, or simply move the maximum of the distribution to a new location without changing its shape (n"=2).

At a distance far from equilibrium the stable distribution function with 0<n"<1 is sensitive to its redistribution, because different n" in this range may indicate different conduction stages. Therefore a small change in n" (say from n"=.5 to n"=.6) may result in changing the conduction from one stage to another. Although

the value of n" may change, however, the fractional exponential parameteric dependence will not change under redistributions no matter in equilibrium or nonequilibrium.

Aging Effect and Other Parameteric Dependence

Aging effects constitute complex combinations of the inference caused by, for example, electromagnetic radiation, applied fields and temperature. Based on our model, the effects of aging are to change the distribution of activation energies and jumping distances (or the size and the position of the defects). From the discussion in the last few subsections we predict that the net effects of aging in conductivity is the following

$$\langle G \rangle = \langle Go \rangle \, e^{-(\frac{t_o}{t})^n}, \qquad (4.11)$$

where t is the aging time and t_o is constant. In thermal equilibrium and quasi-equilibrium (i.e., the reaction function in equation (1.7) is either constant or linear function of order parameter) t_o is not a function of order parameter. On the other hand, when the system is at a distance far from equilibrium (or the reaction function has the order higher than the second) t_o depends on the order parameter. The aging effects will be discussed further in the chapter five and seven.

Discussion and Conclusion

We have shown quantitatively how the defect reaction-diffusion (RD) model can consistently explain the observed experimental dependence of conductivity on T, F, and d, and gives an unique description of conventional conduction processes in dielectric thin films. This includes Mott's variable range-hopping model and percolation theory. n=0.25 temperature dependence has been suggested as the result of Poisson distribution at Fermi-Level, and n=0.5 temperature dependence is the result of a crater-like distribution, which shows a Coulomb's gap at the Fermi-level.

Furthermore, assuming that the defect related parameters have stable distribution, we propose an explanation for the general fractional exponential parameteric dependence of conductivity. According to this model, the main effects of external parameters (e.g., F, T, d, aging and any other parameters which has effects on the conductivity), are to redistribute the distribution of activation energies and/or jumping distances. Consequently, these result in the redistribution of hopping time and hopping rate. The properties of the stable distribution function suggest that the effect of redistribution is not important in the situation of equilibrium and

quasi-equilibrium. However, it may be crucial at the distance far from equilibrium. The redistribution in the latter case may switch the system to a new conduction stage.

In the following chapter, we will discuss (1) the relation between defect model and the conventional breakdown mechanisms, (2) the inverse fractional power parameteric dependence of the breakdown strength and compare it with the available experimental data, (3) microscopic processes of breakdown phenomena proposed by the RD model, and (4) Weibull's statistics.

CHAPTER V

ENERGY TRANSFER AND BREAKDOWN MECHANISMS

Introduction

In chapter one and four we have shown that the defect RD equation is capable to generalize the conventional breakdown mechanisms and give a consistent description for breakdown and electrical conduction. Based on this model, the extension of the old theories is easy to see. For example, in thermal breakdown theory, the term $H(T)F^2$ in equation (1.1) is replaced by a polynomial in equation (1.3). The latter approach can easily incorporate, for example, the effects of space charges, recombination, annihilation and multiple trapping. In addition, the nonlinear interactions and cooperative behavior can also be taken into consideration.

In this chapter we extend the conclusions obtained in last chapter to explain the parameteric dependence of the breakdown strength, and compare it with the available experimental data. From the energy transformation point of view we consider some detail of the microscopic processes of conduction to breakdown, and emphasize the role of the

fluctuations at a distance far from equilibrium. Finally, we apply the concept of the open system to explain the Weibull's statistics.

Thickness and Temperature Dependence of Breakdown Strength

In section 4.5.3 we have shown that at high fields the experimental data of the field dependence of the conductivity can be best explained by

$$\langle G \rangle = \langle Go \rangle e^{BF}, \qquad (5.1)$$

in which Go and B are constants at a given temperature. For breakdown to occur the field F in equation (5.1) should be larger than breakdown strength Fb. Therefore comparing (4.10) (i.e., $\langle G \rangle = \langle Go \rangle e^{(-d)^n}$), and (5.1) one finds that

$$F_b \propto d^{\pm n} \quad \text{with} \quad 0 \leq n \leq 2 . \qquad (5.2)$$

For bulk crystals and polymers +n are applied ; for thin dielectric films -n are applied (Fig. 5). The experimental data of F_b versus d^{-n} in dielectric thin films have been collected in Table 5, which shows that the correlation index, n, is always between $0 \leq n \leq 2$.

Similar data are also observed in temperature dependence of the breakdown strength, i.e.,

TABLE 5

Thickness dependence of breakdown strength.

dielectric	Deposition methods	exponent n	thickness range (A)	temperature range (k)	reference
BaSt	(LB)	.59	250-2500	300	[59]
BaSt	(LB)	1.01	25-250		[60]
Fatty acid	(TE)	0.65	1000-7500	300	[61]
Fatty acid	(TE)	1.0	< 1000 and > 7500		[61]
Stearic acid	(TE)	0.8	600-2000	300	[62]
Stearic acid	(TE)	1.3	200-600	300	[62]
SnO2	(TE)	2.1	480-1200	328	[63]
SnO2	(TE)	0.21	1400-2000	328	[63]
p-type Te	(TE)	1.8	1000-2000	300	[64]
La2O3	(TE)	0.66	40-400	300	[65]
ZnS	(TE)	0.2	< 800	300	[66]
ZnS	(TE)	0.5	> 800	300	[66]
ZnS	(TE)	.12	200-1000	77-300	[67]
Si2N3	(CR)	.0	300-3000	128-200	[68]
SiO2	(TD)	.47	300-700	77-323	[69]
SiO2	(TD)	1.55	800-2000	77-323	[69]
SiO2	(TO)	.21	< 800	300-527	[57]
SiO2	(TO)	.0	1000-2000	300-527	[57]
SiO2	(TO)	0.47	300-700	300-723	[70]
SiO2	(TO)	1.55	800-2000	300-723	[70]
SiO	(TE)	.5	900-16000	80-380	[54]
CeO2	(TE)	.5	900-16000	80-380	[54]
CeF3	(TE)	.5	900-16000	80-380	[54]
CaF2	(TE)	.5	900-16000	80-380	[54]
MgF2	(TE)	.5	900-16000	80-380	[54]
LiF	(TE)	.5	900-16000	80-380	[54]
NaF	(TE)	.5	900-16000	80-380	[54]
Teflon	(SP)	.5	900-16000	80-380	[71]
Vinyl chloride acetate		.0	1200-50000	80-380	[71]
Al2O3	(TD)	.45	800-2000	773-823	[70]
Ai2O3	anodic(TO)	.85	2000-5000	773-823	[70]
Ai2O3	anodic(TO)	.30	134-1540	290	[72]
Sb2O3	(TO)	.5	> 800	300	[73]
Sb2O3	(TO)	.0	< 800	300	[73]
SnO2	(TO)	2.1	480-1200	308	[74]
SnO2	(TO)	.21	1400-2000	308	[74]

Bi2O3	(TO)	.78	1300-2750	300	[75]
Bi2O3	(TO)	.74	230-900	300	[76]
Nb2O5	(TE)	.65	266-2150	300	[77]
Sb2O3	(TO)	.5	> 750	300	[77]
Sb2O3	(TO)	.0	< 750	300	[77]

BaSt = Barium-stearic.
LB = Lagumuir-Blodgett method.
TE = Thermal evaporation method.
CR = Chemical reaction.
TO = Thermal oxidization.
SP = Sputtering.
TD = Thermal decomposition of
$Al(C_5H_7O_2)$ or
$Al(C_2H_5O)_3$.

$$F_b \propto T^{-m} \quad \text{with} \quad 0.1<m<1.9 , \tag{5.3}$$

with m=.68 for S_iO film [50], m=0.74 for Si_3N_4 film [51], m=1.83 for Ta_2O_5 film [52]. For many other dielectric thin films the reference should be made to [53-58].

The m value decreases as the defect density increases and increases as the degree of interaction and correlation between density fluctuation increase. The experimental m value is thus determined by the balance of these two factors. The n value in equation (5.2) has the similar tendency.

Energy Storage and the Propagation of Defects

When the field is applied, the electrons and/or holes injected from the electrodes into the dielectrics. These charge carriers are likely trapped by defects to form space charges, which in turn polarize the cells, change the charge distribution and modify the electronic energy levels inside the band gap. Similar hopping and trapping processes continue to occur when the electrons proceed inside the system.

The energy stored in the system (mainly in defects) can be used in one of the several ways, e.g., for creating new defects, for the migration (diffusion, drift) and growth of defects, and/or dissipated as heat. Since we expect that the Coulomb's interaction will be the dominant long range interaction, the energy stored in the defects should be of the order of $\frac{e^2}{\varepsilon r}$, here e is electric charge, ε is dielectric constant, and r is the average radius of the defects. Thus the larger the defects the lower is the formation energy (the energy required to grow the defects), and thus easier for them to attract the smaller defects (Smaller defects usually have relatively higher mobilities than the larger defects). As the external field increases to some critical value, growth mechanism of defects (e.g., create new

defects, enlarge the old defects, combination of defects, etc.), which is independent originally, becomes coupled together. At this stage the external energy quickly get into the system via, e.g., potential barrier lowering mechanisms [29], high defect density enhance tunneling, and high field enhanced charges transfer at surface states [78]. The defects and current growth rate at this stage will be nonlinear (Fig. 3). The macroscopic current caused by the fluctuations of local charges distribution are enhanced. As the field increases further the growing defects, which are separated formerly, are now linked together. The memory effect is enhanced, spatial correlation length is extended by the cooperative nature of the local fluctuations. The defects therefore propagate (diffuse, hopping, percolation) from one cell to another. At this stage the energy flow through the system is used to a maximum degree in extending the defects to form channels. This corresponds to the filament (or tree) stage (or NDR regime). It should be pointed out that the filamentary paths (trees) may not be fully in the direction of external field due to the similar nature of percolation or multiple-range-hopping. In the final stage of breakdown the channel is formed across the dielectrics and high joule heating along the channel leads to the destruction of the dielectric material.

Energy Transfer Mechanisms

The systematic investigation of energy transfer mechanisms in dielectric thin film systems are so far not available in both theory and experiment. Although we expect its importance on the understanding of their microscopic conduction processes. Below we apply some well known energy transfer mechanisms in solid state theory to the dielectric thin film systems, and show their relations with the assumption of the conventional breakdown theories. There are several purposes for doing this: (1) to show what kind of interaction is believed to be important, (2) to see what kind of formalism can be used to distinguish competing energy dissipation mechanisms (e.g., diffusion, defect creation, relaxation and luminescence), and (3) to understand why the competition of energy transfer mechanisms can induce the instability or switch the conduction stages of the system from one to another.

The energy transfer mechanisms can be roughly divided into two categories: (1) radiative energy transfer (photons related), and (2) nonradiative energy transfer (non-photons related). Generally, the probability for these two mechanisms to occur is 50% each. However, since it is the nonradiative energy transfer (NRET) which diverts energy into breakdown channels, in the present context, we will consider only the NRET.

NRET can be further classified into four categories depending on how the excitation energy (both external and internal) is dissipated in the system. The electronic excitation energy may be transferred to (a) another electrons (free or trapped electrons) via Coulomb's interaction (range 50-100A) or exchange interaction (range less than 20A), (e.g., Kao's model [79]), (b) optical phonons (von Hippel's breakdown model [80]) or acoustic phonons (Seitz's breakdown model [81] and Minnaja's model [82]), (c) its environment (to create defects or increase the diffusion rate, etc.), (e.g., Jonscher and Locase's model [83]). Let us consider an example to see how the competition between these processes leads to the instability of the system. Let U' represent the electrons-electrons correlation energy between two adjacent defects, T' represent the migration (or diffusion) energy of defects from one place to another, S' represent the structural distortion energy (or relaxation energy) caused by this migration. Similar to Toyozawa's analysis [84], we conclude that

(1) if S'>>T', small polaron conduction (hopping and/or diffusion) is favored; if S'<<T' large polaron (delocalization,) is preferred. However, it is believed that the random potential fluctuations of defects will

smear out the very narrow polaron bandwidth so that at the initial stage the hopping-type transport is likely to dominate at any temperatures. In other words the former situation (S'>>T') is more likely in dielectric thin film systems at the initial stage.

(2) if S'>>U', electrons prefer to share sites to gain structural relaxation energy. In this case conduction can occur without inhibiting activation energy. This implies a high conductivity; if S'<<U' electrons prefer to remain on separated sites, i.e., hopping type conduction is preferred.

(3) if U'>>T', the energy gain from forming extended states increases and the screening reduces the energy needed for electron to transfer, at a critical spacing the state of high conductivity is favored; if U'<<T', Mott's n=.25 law results.

Another NRET is phonon-phonon interaction. The important application of this type of interaction is to distinguish several competing processes (e.g., diffusion, defect creation, relaxation and luminescence) without knowing the detail of the interactions. This can be seen from the following consideration. In Figure 20 we show an asymmetric double minimum potential well, which represents two defects (or group of defects) in an external field.

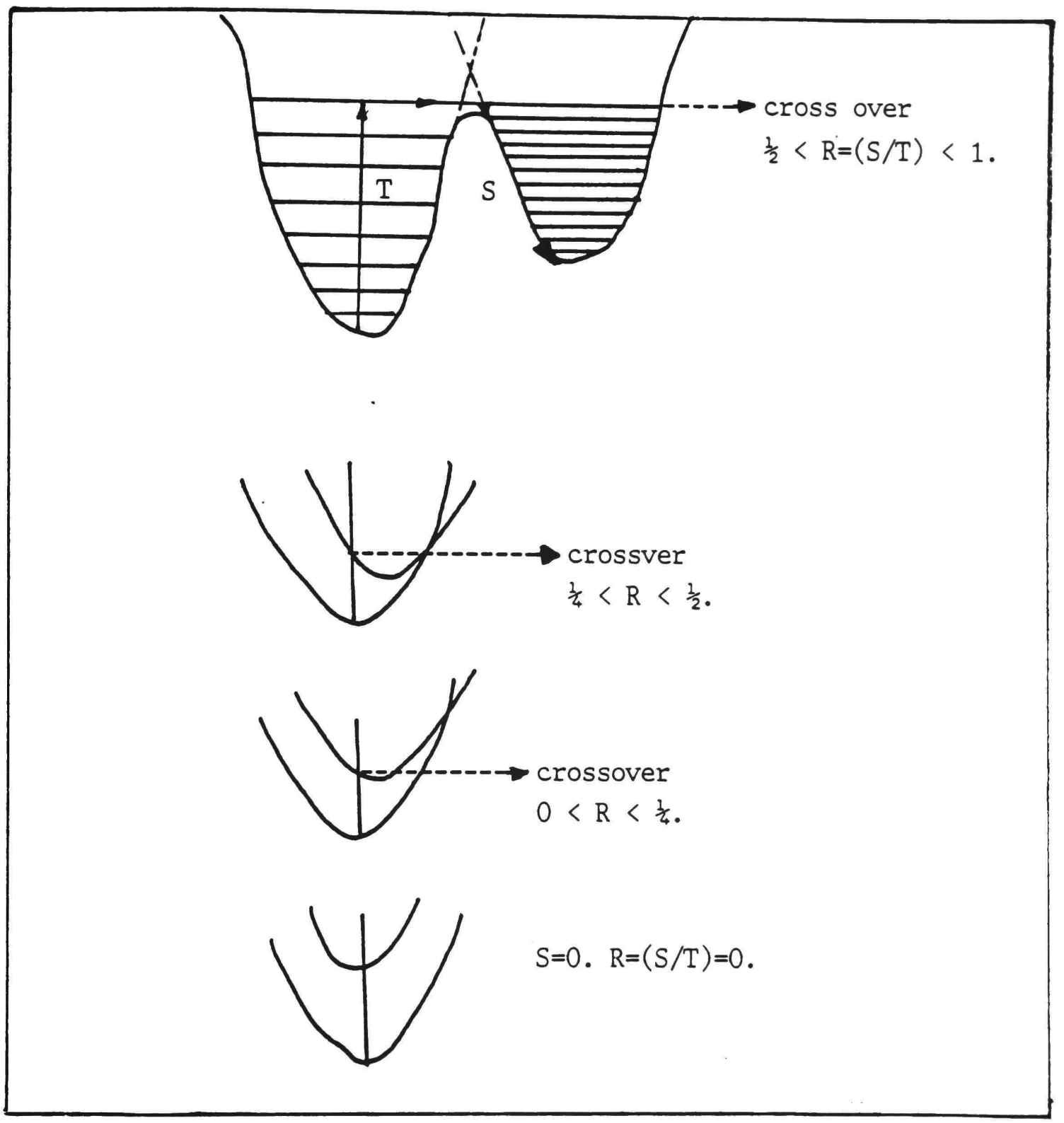

Figure 20: Defect potential surfaces and the energy transfer mechanisms.

For the phonon-phonon interaction we are interested in the vibrational energy levels inside each defect potential well.

Let R be the ratio of relaxation energy and excitation energy. If 0<R<.25, according to Dexter's rule [85], the energy transfer is via luminescence emission completely. If .25<R<.5, excitation energy is partly diverted to create defects or enhance diffusion, only weak luminescence is expected (e.g., [86]). If 1>R>.5, no luminescence will be observed, all the excitation energy is used for creation and diffusion of defects. If R>1, this is an exothermic process the released energy can be used to generate hot electrons, Auger electrons, or heat. Since the value of R can be decided from the defect potential surfaces in question, the information about these potential surfaces is desirable.

Fluctuation and Instability

Fluctuations of various kinds (e.g., in jumping distances, activation energies, hopping times, defect densities and charges distribution, etc.) are present in the cells and therefore in the system. The stability of an existing structure is constantly threatened by these inevitable fluctuations (both internal and external). As far as the electronic properties are concerned, let us assume that the fluctuations are caused mainly by local random electric fields, arising presumably from the Coulomb's potentials due to charged defects. The effect of the

fluctuations is to distinguish different conduction stages. For example, let φ be the fluctuations of the system (caused by e.g., T, F, P, or Potentials). The usual way to determine whether the fluctuations will introduce instability, is to apply the criteria of the linear stability test [87]. According to this theory if the amplitude of the fluctuation increases with time the system is not stable, otherwise it is stable. Let the solution of equation (3.2) be

$$N(x,t) = N(x)\varphi(x,t) , \tag{5.4}$$

where N(x) represents the thermal dynamic branch and assume at t=0, φ is small. Substitute (5.4) into (3.2) we obtain a set of linear equations in φ. i.e.,

$$\frac{\partial\varphi}{\partial t} = \frac{dH(N,t)}{dN}\ \varphi\ +\ D\frac{\partial^2\varphi}{\partial x^2} , \tag{5.5}$$

where we neglect the drift term, and apply the result H(N(r,t))=0 (i.e stationary solution). These equations are then analyzed in terms of normal modes of the form

$$\varphi\ =\ \varphi_o\ e^{(wt+ikx)} , \tag{5.6}$$

where φ_o is some constant; w's are the frequencies of fluctuation, and are complex numbers with real part Re(w) and imaginary part Im(w); k's are the wavenumbers, and are also complex numbers. Combine equation (5.5) and (5.6), we get

$$[w + D\,k^2 - \frac{dH(N,t)}{dN}] = 0 \ . \qquad (5.7)$$

The stability of the thermodynamic branch N(x) and therefore the whole system depends on the sign of the Re(w). If all Re(w)<0, then all normal modes decay, as can be seen from (5.6). The system is therefore stable. If at least one of the Re(w)>0, then the system is unstable. The mode with Re(w)>0 will grow exponentially with time. If at least one of the Re(w)=0, and all other Re(w)<0, then the system is in a metastable state. Re(w)=0 mode will be stable if k is positive imaginary number; unstable if k is negative imaginary number; and oscillate if k is real number.

From this discussion, the thickness dependence of the breakdown strength can be understood easily from the following consideration: The instability occurs as the energy generating rate is larger than the dissipative rate. For short wave length fluctuations (high frequency), the adjacent half cycles can exchange energy (heat, etc.) with each other and is therefore able to dissipate energy (heat) more effectively than long wavelength fluctuations. This suggests that the long wavelength fluctuations are more effective for causing the instablity. Since the longest permissible value of wavelength is determined by the size (thickness) of the system, thus the smaller the thickness,

the larger the onset breakdown strength. Although the long wavelength fluctuations become unstable first. The filaments formation can not go without the cooperation of the instability of the short wavelength fluctuations.

Reaction-Diffusion Model and Weibullton Statistics

Weibull's statistics has been commonly used to interpret the probability distribution of breakdown strength. Recently, Dissado and Hill have proposed a model to explain its physical origin [88]. One main feature of their model (i.e., many-body correlated model (MBCM) [89]) is to assume that the structural fluctuations have stochastic nature, and it is these fluctuations that are responsible for the structural relaxation and the Weibull's statistics. This interpretation strongly supports the general views (e.g., fluctuations dominate the system beyond the bifurcations) provided by the RD equation, although there exists no similarity about the fundamental theories behind these two models. The RD model is based on the mechanism of open system; whereas the MBCM model is based on the fluctuation kinetics. RD equation deals with, mainly, the situation of far from equilibrium; MBCM model restricts its application to the (quasi-)equilibrium condition. In RD

model the role of the fluctuations at a distance far from equilibrium are clear, however, it does not seem so for the MBCM model. According to the RD model the Weibull's empirical relation can be easily seen by comparing equation (4.9) and (4.11), i.e.,

$$F_b^n \propto t^{-m} \quad \text{or}$$

$$F_b^n \, t^m = \text{constant} . \tag{5.8}$$

The main features and difference of these two models are summarized in Table 6. Briefly, in RD model we consider the fluctuations dominate the average as the special feature of an open system or the nature of the far from equilibrium. If the fluctuations are caused by, e.g., thermal, electrical, or mechanical origin then the corresponding breakdown (or instability) is called thermal, electrical or mechanical breakdown respectively. Another difference is that the local currents caused by the fluctuations of charges is distributed as g(y)dy (see Table 6), and in RD model the distribution function is suggested as a stable distribution which is one of the asymptotic solution of RD equation with upper and lower limit, $0<n<2$. The interested readers are referred to [88, 89] for more details.

TABLE 6

Comparison of many-body correlation model (MBCM) and reaction-diffusion (RD) model.

	MBCM	RD
level	(quasi-)equilibrium	(non-)equilibrium
equation of motion	rate equation [89]	RD equation (1.7)
solutions. (distributions)	++	stable Eq. (4.4a)
correlation index	m	n=2(1-m)
noise spectrum	$w^{(-2(1-m))}$	w^{-n}
applications	*dielectric relaxation *Weibull's Statistics, * etc.	*electric conduction * relaxation, *breakdown processes * annealing, * aging, growth and * nucleation * processes, and * Weibull's * Statistics, etc.

$$+g(y)dy=y^{\left(\frac{(1-m)}{m}\right)}_{[1+y^{-1}]^2}\,dy \quad \text{with} \quad 0\le m\le 1.$$

for m=0, g(y) is Delta function;

for m=1, g(y) decays quasi-exponentially.

Discussion and Conclusion

The defect RD model has been applied to explain the fractional temperature and thickness dependence of the breakdown strength. Similar to the conduction, the exponents m and n in equation (5.2) and (5.3) are inversely proportional to the defect density and proportional to the nonlinear interaction and correlation. The balance between these factors, which determine the m and n, is investigated further via the consideration of energy storage and transformation mechanisms. Several conventional breakdown models have been correlated to RD model. A microscopic picture is proposed which suggests that there exists several defect correlated states in the film structure during conduction to breakdown. Each correlated state corresponds to one conduction stage. In every stage we discuss the possibility of instability induced by the fluctuations. The Weibull's statistics, which is based on a stability postulate [90], is shown to be the result of stable distribution in defect related parameters.

In the following chapter, we will apply RD model to explain the experimental data in stearic acid molecular films. These include (1) temperature dependence of conductivity, (2) band-gap across the Fermi-level, (3) thickness dependence of breakdown strength, (4) various

conduction stages, (5) negative differential resistance, and (6) the defect density and the corresponding energy level.

CHAPTER VI

THE ELECTRONIC PROPERTIES OF FATTY-ACID LAGUMUIR-BLODGETT FILMS

Fatty acids dissolved in benzene solvent can spread quickly on the water surface to form a monolayer with thickness about 25A [91, 92]. By transfering this mono-molecular layer on to a solid substrate, like glass or polished semiconductor, and making contacts (electrodes), a good quality capacitor (MIM or MIS) is obtained. Here good quality means

(1) good thermal stability from 4K to 330K, and low thermal expansion coefficient.

(2) high dielectric strength ranging from 10^6-10^7 V/cm.

(3) uniform, controllable thickness and almost structural defects free nature.

(4) good dielectric properties (low loss).

(5) low optical attenuation.

(6) easy reproducibility.

Although fatty-acid molecular films have well-defined lattice and are relatively defect free, there are unavoidable nonstructural defects, which may have an important influence on the electronic properties of the

films. Table 7 lists the possible types of defects in these films.

TABLE 7

The defects in fatty-acid molecular film.

defects	origin	function	remark
(1) surface states	(a) metal-insulator interface.	traps	unavoidable
	(b) Al oxide layer.	traps	unavoidable
(2) impurities	solvent	contribute conduction electrons	unavoidable
(3) water	during deposition	source of ions.	avoidable
(4) methyl group	internal (polar group)	traps	unavoidable
(5) dust	during deposition	traps	avoidable
(6) dislocation	internal	traps	avoidable
(7) pinholes voids.	during deposition	traps	avoidable
(8) disorder	intrinsic	localization	unavoidable
(9) fluctuations	internal and external	localization	unavoidable

Because of the random presence of the charged defects and/or dipoles, the conduction electrons experience a potential which varies randomly along and perpendicular to

the chain's direction. Due to these potential fluctuations, most of the electronic states are possibly localized (Anderson localization) and consequently the electronic conductivity is likely due to phonon-activated hopping from one localized (defect) state to another.

Tunneling or Traps Control Conduction

The conventional interpretation of the electronic conduction process in fatty-acid monolayer film was proposed by Kuhn and Mann [93] as a direct tunnelling from electrode to electrode. This conclusion came from the observation that the variation of tunnelling current with thickness correlated well with the values predicted by Quantum mechanical tunnelling theory. In this explanation defects (structural or nonstructural) played no role. The first evidence for the importance of defects in conduction was suggested by Procarione and Kauffman [94]. They studied Phospholipid layers and discovered that the apparent tunnelling currents in monolayers could be varied several orders of magnitude by an appropriate annealing process. Since then, most workers in this field have observed substantial decrease in apparent tunnel current simply by putting the films in dry nitrogen at room temperature.

The recent studies on conduction by Tredgold et. al. [95] have shown that the current-voltage curves always have the same shape, i.e. $J=Aexp(F)^{(1/4)}$ regardless of aging or baking (Figure 21).

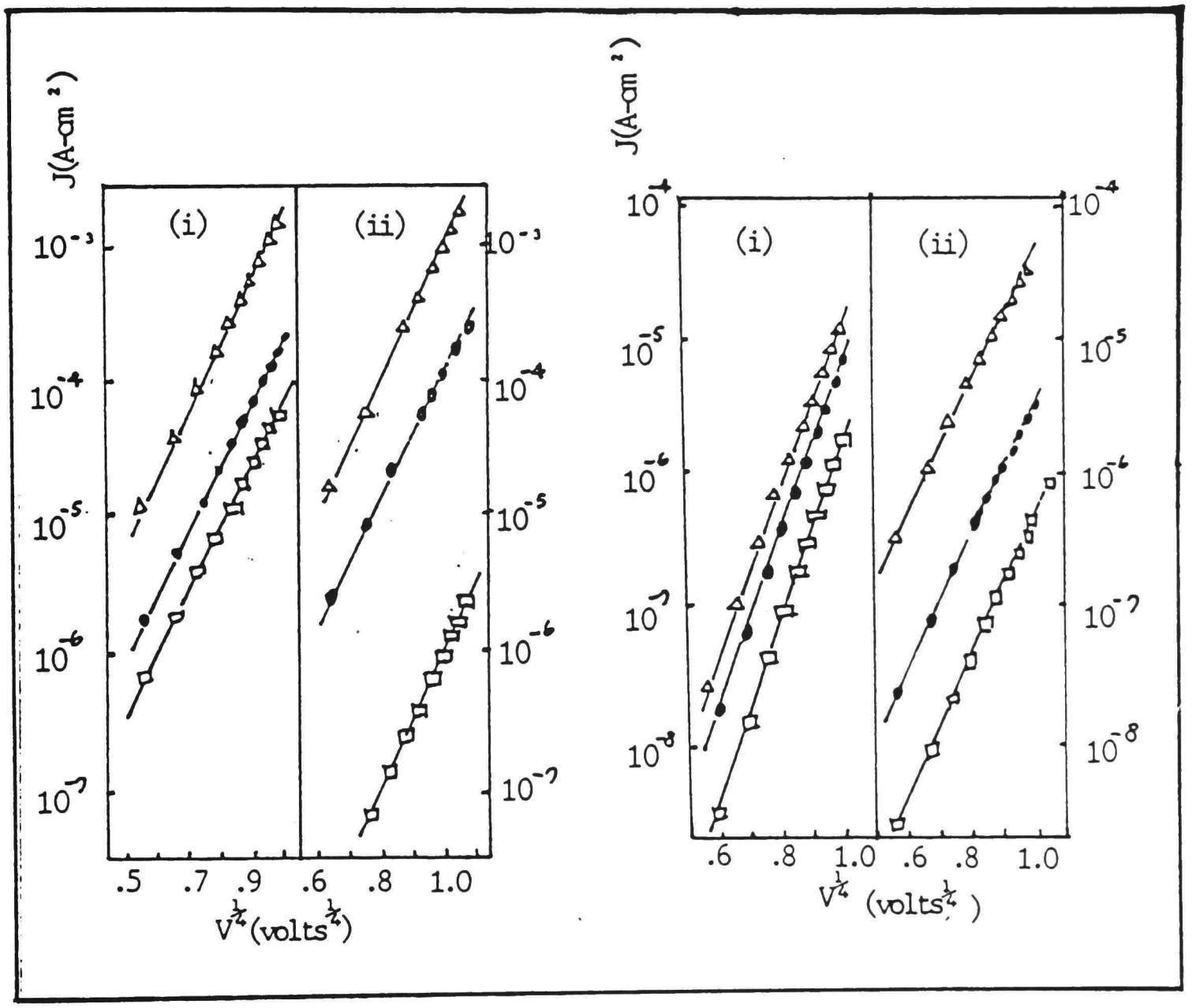

Figure 21: Current density versus voltage of stearic acid films [28].

The interpretation of these results was that the currents measured (largely due to tunnelling) are not

through the organic layer but rather via defects in it. It is suggested that as the film is annealed the density of defects decreases and hence the resulting current decreases. The n=.25 field dependence indicates that the Poole-Fenkel mechanism, which is defect controlled conduction, dominates in temperature ranges used in their work.

Annealing and Irreversible Defect Density

Since defects play an important, and maybe decisive, role in the conduction, the information of defect density in the system is desirable. Defect density in fatty acid film has been estimated by Sugi [96] and Agarwal [97] et al. Based on the variable range hopping mechanism, Sugi found that the density of the surface states is about 2.25 x 10^{15}/eV/cm^2. On the other hand based on the Poole-Frenkel mechanism, Agarwal et al obtained about 1.2 x 10^{16}/eV/cm^2 for the density of trapping states inside the film. In section 3.5 we have proposed an annealing formalism to estimate the irreversible defect densities and their corresponding activation energies via resistivity, R, verses temperature, T, measurements. Applying this formalism we obtain the density of the defect states about 2.0 x 10^{16}/eV/cm^2 and the activation energy about 0.56eV. The resistance versus temperature data in stearic acid films are

taken from Polymeropoulos [98], and are listed in Table 8. The computer code for this calculation is shown in Appendix. The results are shown in Table 9 and Figure 22.

TABLE 8

The resistivity versus temperature data in stearic-acid films.

R ($x10^{15}$ mho-cm)	T (K)
1.00	300
1.36	253
1.82	220
2.5	180
3.12	150
5.00	130
6.66	100
14.28	77

TABLE 9

Defect density and its corresponding activation energy.

Activation energy (eV)	Defect density ($x10^{16}/cm^2/eV$)
.56	2.06
.58	0.84
.64	.75
.69	.71
.74	.70
.80	.63
.85	.68

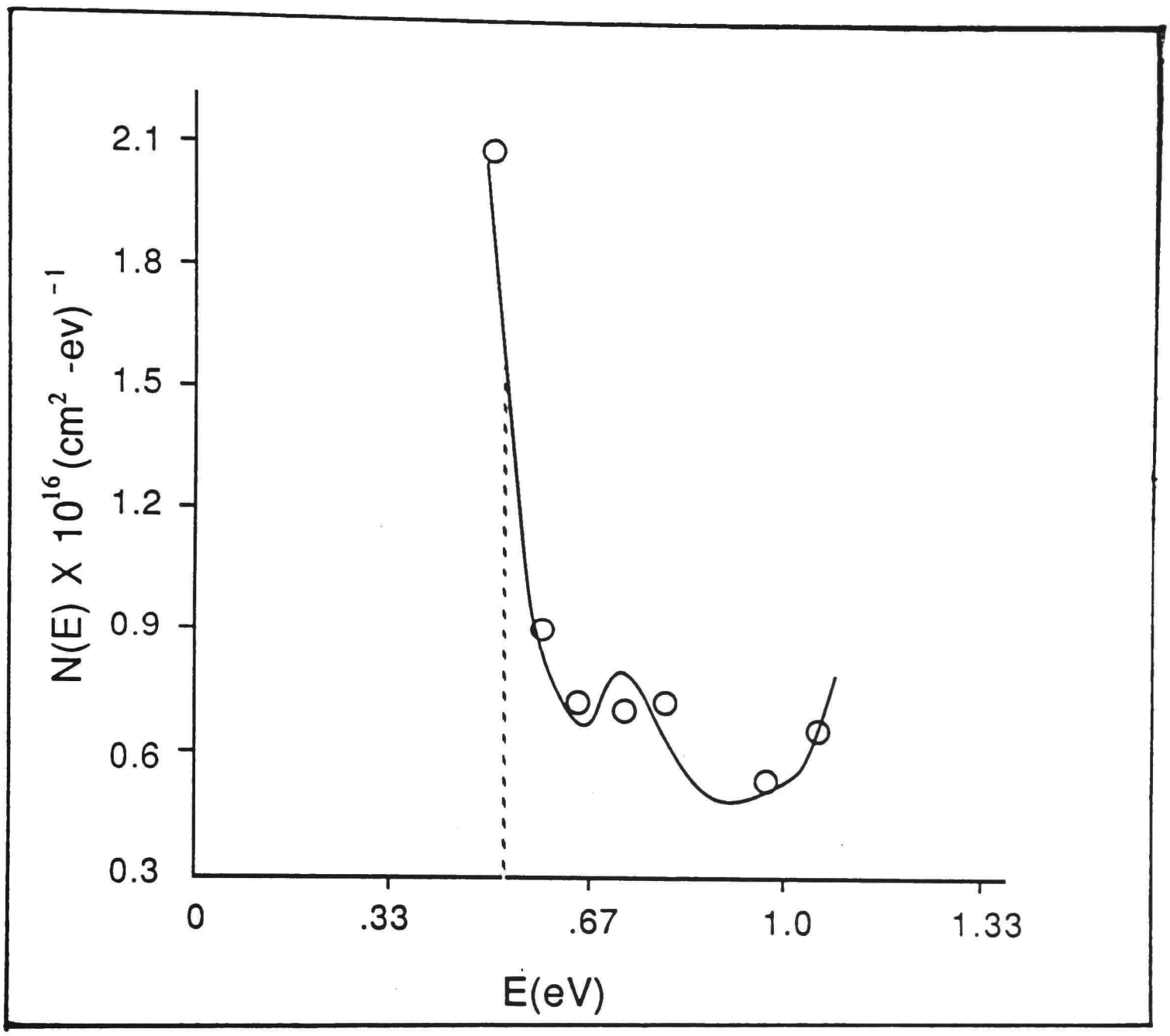

Figure 22: Defect density and its corresponding activation energy.

The defect density obtained in this way is consistent with the previous finding, and the activation energy is comparable with Lundstrom's report [99]. His capacitance verses voltage measurement suggests an about 0.7eV thermal-activation energy. We have applied the same

formalism to determine the defect density in evaporated SiO film, and obtain $3.86 \times 10^{19}/cm^3$ which is comparable to $1.25 \times 10^{20}/cm^3$ determined earlier by Hill [100] based on Poole-Frenkel mechanism.

Temperature Dependence of Conductance

The temperature dependence of conductivity in fatty-acid was studied by Sugi [101], who showed experimentally that $G=Goexp(-To/T)^{(1/2)}$. The same temperature dependence is also observed at the low fields photocurrent measurement [102]. Sugi applied variable-range hopping model to explain his experimental data. By assuming the defect density at Fermi-level is constant, his two dimensional optimization of the transition probability leads to a n=.5 temperature dependence.

In section 4.3 we have shown that an alternative explanation of the n=.5 fractional exponential temperature dependence is to include the nonlinear electron-electron interaction between defects or defect dipoles. If this is the case, according to RD model, there should exist a Coulomb's gap at the Fermi-level. This was in fact observed in Gundlach's experiment [103], which shows a 80meV gap across the Fermi-level, as shown in Figure 23.

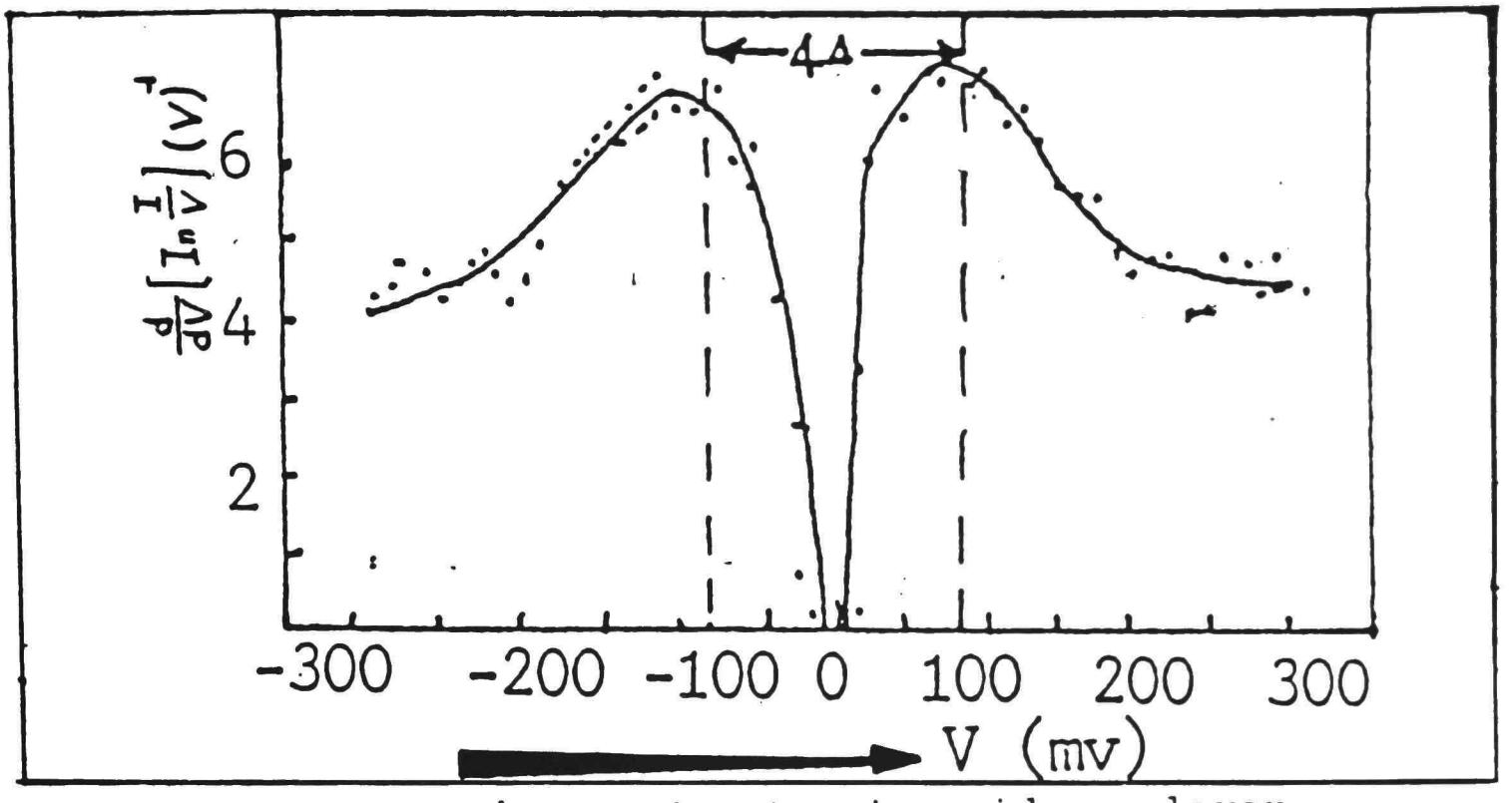

Figure 23: Coulomb's gap in stearic scid monolayer sandwich.

A computer simulation of the hopping path with a stable distribution in the position of defects, as proposed by RD model, is shown in Figure 24(a). This has been compared schematically with Sugi's diagram involving hopping process (Figure 24(b)). Sugi's interpretation of the variable-range hopping is somewhat different from the percolation theory (although he also assume, implicitly, the defect density at Fermi-level is constant), his optimization in two dimensional space, leads to a n=0.5 temperature dependence.

Table 10 lists experimental data in fatty-acid films. From our discussion in chapter four and five all these data can be explained by the RD model.

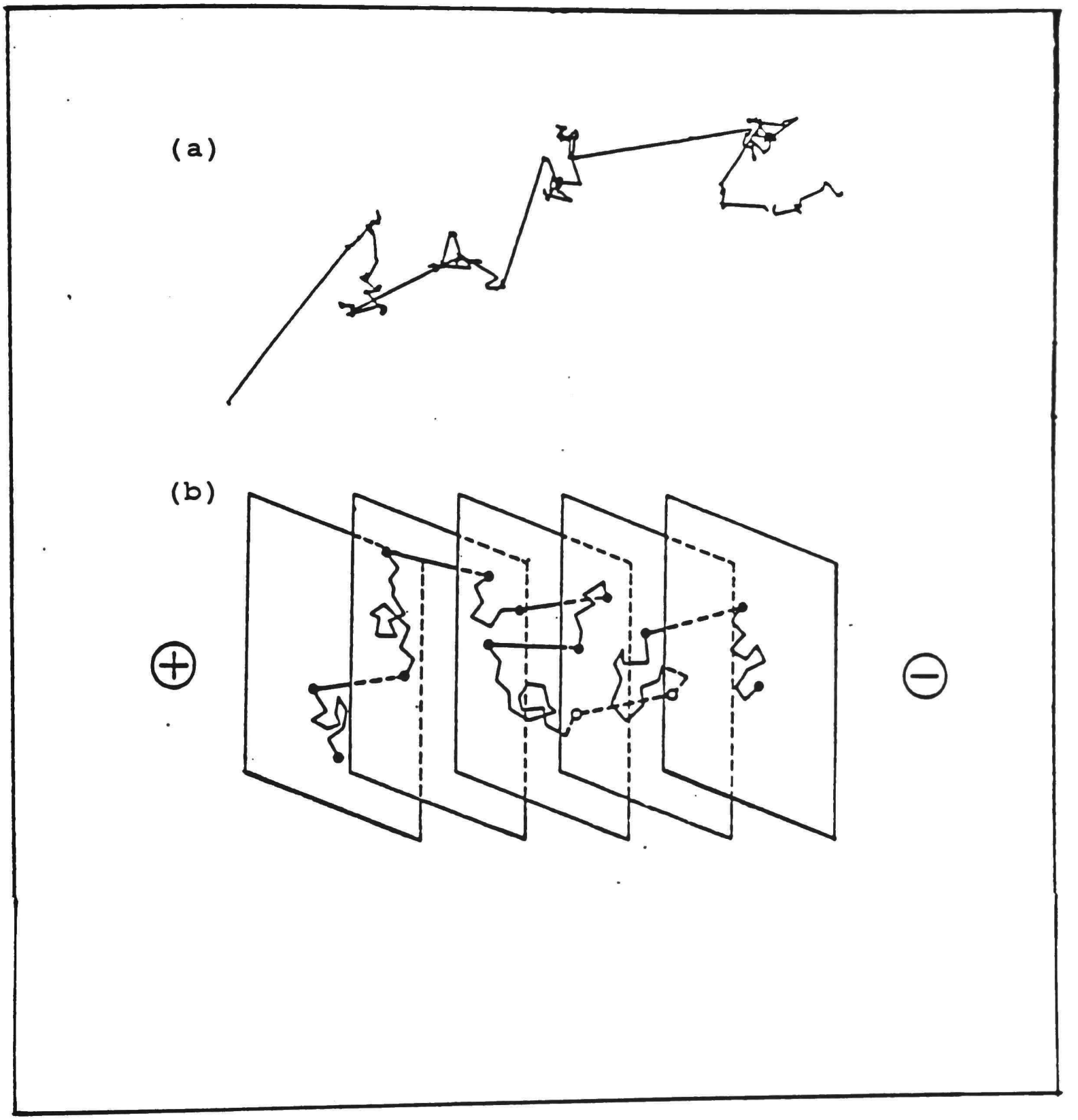

Figure 24: (a) Random hopping with the hopping distances determined by the stable distribution, n=1. (b) Schematic hopping path.

TABLE 10

Experimental data in fatty-acid films.

Conductivity

$$G = G_o e^{\left(\frac{X_o}{X}\right)^{\pm n}}$$

X	n	comment	reference
Temperature dependence	.5	77K to 300K.	[97, 105]
	1.0	above 300K.	
Field dependence	.25	low field $V=10^5$ volts/cm	[105,106]
	.5	intermediate thickness, high fields.	[107]
	1.0	high field $V>10^6$ volts/cm	[108,109]
thickness dependence	.5-.8		[110]
frequency dependence	.5	low frequency, low field, high temperature	
	1.0	low to room temps, low field, low frequency.	[60]
	.87-.9	high frequency,	[97, 106]

Breakdown strength

$$F_b \propto d^n.$$

thickness dependence	1.01	< 250A	[111, 103]
	.59	> 250A	

Conclusion and Discussion

In this chapter we have shown how the RD model can be applied to explain the experimental data in the fatty-acid films. The defects have been suggested to play an important role in the electric conduction and breakdown processes. A formalism and computer code has been provided to estimate the total defect density and its corresponding activation energy. Using the available experimental data it is found that the total irreversible defect density is about $2x10^{16}/eV/cm^2$ with defect levels 0.56ev below the mobility edge. This reasonably agrees with the published data. The parameteric dependence has been explained by the assumption that the size and position of defects have stable distributions. A result of computer simulation of the charged particles' hopping paths with correlation index n=1.0 is shown in Figure 24(a). The n=0.5 temperature dependence has been interpreted as a result of the nonlinear electron-electron interaction rather than variable-range hopping. This nonlinear interaction suggests an 80meV Coulomb's gap at the Fermi-level.

In the following chapter we are going to outline the main conclusions of our work, and discuss the unavoidable theoretical difficulties of the model. The soliton solutions of RD equation will be used to discuss the common features of growth, aging and annealing mechanism.

CHAPTER VII

SUMMARY AND CONCLUSION

In the conventional approaches for the understanding of electronic properties in dielectric thin film systems the role of defects is either neglected or is not explicitly considered. There are at least two basic reasons for these: (1) the structural defects are not easy to determine or distinguish experimentally, and (2) the concept of defects known in crystalline materials has only limited application to dielectric thin films. In this dissertation the definition of defects has been extended to include all the states inside the band gap. Subsequently, we show the significant role that the defects can play in the electronic conduction and breakdown processes. After analyzing the conventional theoretical approaches (Table 2) we propose a defects reaction-diffusion (RD) model. Instead of the conventional approaches, which are based on the phenomenological equations (equation (1.1-1.3)) and (quasi-)equilibrium thermodynamic theory (which assume that the equilibrium can be reached at any instant), the RD model is a stochastic model which emphasizes the effects of nonlinearity and nonequilibrium. Consequently, one finds

that if the defect related parameters (e.g., size, position, activation energy), which are random variables, have stable distributions then the general experimental observations in Figure 2 to Figure 8 can be explained. Besides these phenomenological (macroscopic) and stochastic (mazoscopic) descriptions (chapter one and four respectively), this RD model also provides a microscopic picture of conduction to breakdown processes (chapter five).

Variable-range-hopping and percolation theory, which are not yet applied in dielectric thin films, have been discussed briefly. From our understanding about these two theories we find that they can explain part of the experimental data in electronic conduction and possibly long range correlation, however, they can not explain the general fractional parameteric dependence and the complex nonlinear interactions which likely occur during the transport processes (section 5.3). In some respect, the RD model is similar to these two theories, however, the important differences are that the RD model include reaction term and the coupling between reaction and diffusion. This makes the model more flexible and thus capable to include, for example, the cooperative effects (different from the scaling theory), strong nonlinearities, NDR, memory effects (different from the percolation theory) feedback mechanisms and breakdown phenomena.

From a quantitative point of view, the RD model faces a fundamental difficulty, i.e., the solutions of the equation are not unique and sometimes unpredictable. This is so even the initial and boundary conditions are precisely known. Although we have suggested that the asymptotic solutions are of interest to us, however, the analytic solutions are sometimes desirable. This is because the analytic solutions enable us to predict the final states that the system may go beyond bifurcation.

The uncertainty beyond bifurcation suggests that both deterministic and probabilistic have to be accepted as the natures of this RD model (Fig. 11). At or near thermal equilibrium the defects distribution function is Poissonian, hence the defect density at Fermi-level is approximately constant. Based on this assumption the Mott's variable range hopping model predicts n=0.25 temperature dependence, and the percolation theory extends it to $\frac{1}{(d+1)}$, where d is the dimensionality. However, n=.25 temperature dependence has not been observed in dielectric thin film systems. If we assume that the thin film systems may be two dimensional, then, according to percolation theory n shall be equal to (1/3), which is not seen in dielectric thin film systems either. This may imply that the equilibrium and

quasi-equilibrium physics may not be applicable to the dielectric thin film systems, and thus theory of far from thermal equilibrium should be used. One of the possible significance of this finding is that when we analyze the microelectronic systems, devices and circuits, etc., the mechanisms of open system should replace the conventional theories.

At a distance far from equilibrium the defects distribution functions are not Poissonian. Usually, they have multiple humps instead of one hump. A special case has been shown in section 3.2, where the distribution function has two humps with minimum at the Fermi-energy level. In the extreme case (e.g., increase the depth of the defect potentials), this minimum density approaches to zero. The zero density gap between defect states was referred to as Coulomb's gap, which is due to the electron-electron interaction (or correlation [112]) and was suggested to be responsible for the n=.5 temperature dependence of conductivity. No matter this gap comes from electron-electron interaction or other nonlinear interactions, the n=.5 temperature dependence has indeed been observed in many thin film systems, e.g., stearic-acid molecular films, Fermi glass systems, granular metallic films (Table 5).

The n=.5 temperature dependence observed in these thin film systems indicates again that the mechanism of open system should be used. A direct extension of the above n=.5 dependence to other fractional parametric dependence may be obtained by considering that the defect density at the Fermi-level has the following form (e.g., [112])

$$N(E)=C(E-E_f)^m , \qquad (7.1)$$

where C is some constant, which represents the defect density at equilibrium, E is the defect energy level, E_f is the Fermi energy level and m is constant. At $E=E_f$ equation (7.1) diverges, this suggests that the defect density at fermi-level is zero. Under this consideration the correlation index become $n=\frac{(m+1)}{(m+4)}$. For the special case when m=0, N(E)=constant, and n=.25, which is the Mott's prediction.

Several problems faced by this generalization are that (1) m does not have either upper bound or lower bound, i.e., m is arbitrary, and (2) There is no clear physical evidence for the assumption of Equation (7.1). According to percolation theory the relation between conductivity and the position of fermi-level is

$$\langle G\rangle=\langle Go\rangle(E-Ec)^{(-a)} , \qquad (7.2)$$

where "a" is called universal exponent, which has value from 1.4 to 1.8 for three dimensional system and 1.0 to 1.4 for two dimensional systems [113]. Compare equation (7.1) and (7.2) we find

$$<G>=N(E-Ef)^{(a-m)} . \qquad (7.3)$$

This suggests that the conductivity of the dielectric thin film systems only depends on (a) defect density, (b) the position of the Fermi level, and (c) the kinetic energy of electron. These agree with the conclusions of chapter two (Fig. 11).

Another possible generalization of non-Poissonian distribution is the stable distribution function. One immediate advantage of this distribution is that it has both upper and lower bound, i.e., $0 \le n \le 2$, which exhaust all the correlation indexes observed in dielectric thin film systems so far (Table 5). Another advantage is that it has direct physical meaning, i.e., it is one of the asymptotic solutions of the reaction-diffusion equations.

Before we leave this discussion, we have to point out that although n=.25 dependence is predicted at equilibrium or quasi-equilibrium conditions, this does not mean that n=.25 dependence guarantees the applicablity of Poissonian distribution. On the other hand, n=.5 dependence does not promise the applicability of the non-Poissonian distribution

either. Our understanding is that both n=.25 and n=.5 dependence can occur in either equilibrium or nonequilibrium situation (i.e., closed or open system). The main difference is that in the former the constant parameter in the exponent (e.g., the T_o, F_o, and d_o in equation 4.6, 4.9 and 4.10 respectively) does not depend on the order parameter, whereas in the latter they depend nonlinearly on the order parameter.

Another problem we want to discuss below is the application of RD model to annealing (section 3.5), aging, and growth processes (section 2.2). Here by aging we mean the changes in the microscopic structure (or equivalently the density of defect states) of the film by all external parameters. The solitary wave solution of equation (3.4a) is shown schematically in Figure 25. In this Figure v represents the velocity of the solitary wave, and n represents the correlation index. In the case of annealing the defect density decrease, v is v_1 ; for the growth processes, $v=v_3$, the defect density decrease to some saturated value; and in the case of aging $v=v_2$, the net effect is to increase the total density of defect states. Different correlation index, n's, in Figure 25 represent different defects correlated states, or different growth

stages (section 2.2), or different conduction regimes (e.g., Fig. 13). Since n is inversely proportional to the defect density, and proportional to the strength of the nonlinear interactions and correlations, n_1 is therefore less than n_2, n_3, etc.

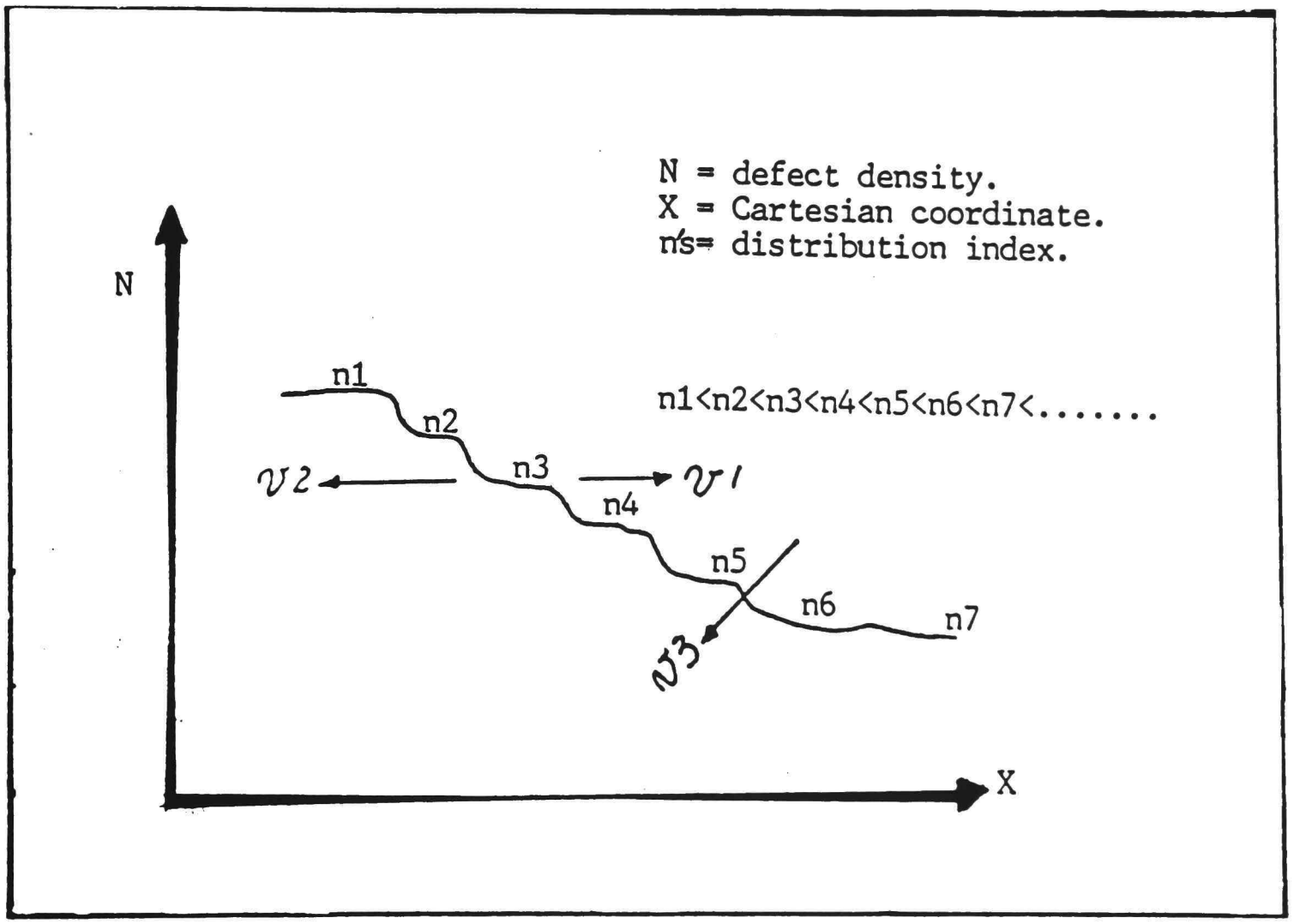

Figure 25: Soliton solution of reaction-diffusion equation.

Finally, we point out the possible future directions of this work. They are (1) to find out what new information can be gained by applying RD model to numbers of experimental

techniques, e.g., thermal emission, thermal stimulated current (conductivity), and thermal stimulated electrons emission. The theoretical basis for these techniques are so far the conventional electronic kinetics, (2) to see what the RD equation can do in nucleation and growth processes.

REFERENCES

1. K.L. Chopra, Thin Film Device Application (Plenum Press, New-York, 1983).

2. K.L. Chopra, Thin Film Phenomenon (McGraw-Hill Inc., New York, 1969).

3. H.R. Zeller, IEEE Trans. EI-22 (1987) 113.

4. J.J. O'Dywer, The Theory of Electrical Conduction and Breakdown in Solid Dielectrics (Clarendon Press, Oxford, 1973).

5. J.J. O'Dywer, IEEE Trans. EI-19 (1984) 1.

6. N. Klein, Thin Solid Films, V100 (1985) 335.

7. M. Sze, Semiconductor Device (Wiley Press, New-York, 1981)

8. M. Ieda, IEEE Trans. EI-15 (1980) 206.

9. H. Frohlich, Proc. R. Soc. London, A160 (1937) 230.

10. H. Haken, An Introduction to Synergetics (Springer-Verlag, New York, 1983).

11. H. Haken, ed. Synergetics Workshop (Springer-Verlag, New York, 1978).

12. A. Pacault, ed. Synergetics at Far From Equilibrium (Springer-Verlag, New York, 1978).

13. L.I. Maissel and R. Glang, eds. Handbook of Thin Film Technology (McGraw-Hill Press, New York, 1970).

14. G.A. Bassett, Proc. European Conf. Electron Microscopy, (1960) 270.

15. P.W. Anderson, Phys. Rev. V109 (1958) 1492.

16. N.F. Mott and E.A. Davis, Electronic Processes in Non-Crystalline Materials (Oxford Press, London, 1970 and 1979)

17. A. Miller and E. Abrahams, Phys. Rev. V120 (1960) 745.

18. S. Kirkpatrick, Rev. Mod. Phys. V45 (1973) 574.

19. J.W. Diggle, Oxides and Oxide Films V1, V2, and V4 (Marcel Dekker Press, New York, 1973 and 1976).

20. J.M. Ziman, Models of Disorder (Combridge Univ. Press, London, 1979).

21. T.J. Tuner, Self-Organization (Addison-Wesley, New York, 1982).

22. G. Gilmore, Catastrophe Theory (McGraw-Hill Press, New York, 1981).

23. M.D. Mikhailov, Unified Analyses of Heat and Mass Diffusion (John Wiley Press, New York, 1984).

24. E.C. Zeeman, Catastrophe Theory (Addison-Wesley, New York, 1977).

25. V.I. Arnold, Catastrophe Theory (Springer-Verlag Press, New York, 1985).

26. K. Nakamura, J. Phys. Soc. Jpn. V38 (1975) 46.

27. R.H. Tredgold and C.S. Winter, J. Phys. D14 (1981) L185.

28. R.H. Tredgold and C.S. Winter, J. Phys. D17 (1984) L5.

29. F.W. Schulter, J. Appl. Phys. V37 (1966) 2823.

30. N.F. Mott, Phil. Mag. V19 (1969) 835.

31. V. Ambegaokar, B.I. Halperin and J.S. Langer, Phys. Rev. B4 (1971) 2612.

32. A.L. Efros and B.I. Shklovskii, J. Phys. C8 (1975) L49.

33. A.L. Efors, V.L. Nguyen and B.I. Shklovskii, J. Phys. C12 (1976) 1869.

34. H. Fritzsche and D. Adler, eds. Localization and Metal-Insulator Transitions (Plenum Press, London, 1985).

35. M. Pollak, Phil. Mag. B42 (1980) 781.

36. J.D. Davies, P.A. Lee and T.M. Rice, Phys. Rev. B29 (1984) 4260.

37. W. Brenig, Phil. Mag. V27 (1973) 1093.

38. K.J. Hayden, Phil. Mag. B41 (1980) 619.

39. G. Nicolis and J. Turner, J. Ann. N.Y. Acad. V316 (1979) 251.

40. P. Sheng and J. Klafter, Phys. Rev. B27 (1983) 2583.

41. L. R. Melby, Can. J. Chem. V43 (1965) 1448.

42. E.K. Sichel et al., Phys. Rev. B25 (1982) 5574.

43. V.M. Zolotarev, One-Dimensional Stable Distribution (AMS, Rhodelsland, 1986).

44. E.W. Montroll, J. Stat. Phys. V34 (1984) 129.

45. P. Levy, Theory of l'addition des Variables aleatoires (Gauthic-Villars, Pairs, 1937).

46. R.M. Hill, Physics of Nonmetallic Thin film, C.H.S. Dupuy and A. Cachard, eds. (Plenum Press, New York, 1974).

47. B.I. Shklovskii, Sov. Phys. Solid-State, V6 (1973) 1964.

48. M. Van der Meer, Phys. Status Solidi, B110 (1982) 571.

49. J. Frenkel, J. Phys. (USSR) V9 (1945) 487.

50. N. Klein, Pro. IEEE Trans. V54 (1966) 979.

51. S.M. Sze, J. Appl. Phys. V38 (1967) 951.

52. N. Klein, Adv. Elec. Elec. V26 (1969) 309.

53. P.P. Budenstein and P.J. Hayes, J. Appl. Phys. V38 (1967) 2837.

54. P.P. Budenstein, P.J. Hayes and W.B. Smith et. al., J. Vac. Sci. Technol. V6 (1969) 289.

55. P.P. Budenstein and P.J. Hayes, J. Appl. Phys. V40 (1969) 3491.

56. M. Ieda, IEEE Trans. EI-19 (1984) 162.

57. C.M. Osburn and D.W. Ormond, J. Electrochem. Soc. V119 (1972) 597.

58. V.F. Karzo, Sov. Phys. Solid-State, V8 (1966) 494.

59. V.K. Agarwal and V.K. Srivastava, J. Appl. Phys. V44 (1973) 2900.

60. V.K. Agarwal and V.K. Srivastava, Solid State Com. V12 (1973) 329.

61. A.R Kadilingam, C. Balasubramanian and M. Radhakrishnan, J. Appl. Phys. V13 (1980) 853.

62. C.H. Huang and V.K. Agarwal, J. Vac. Sci. Technol. A3 (1985) 2000.

63. T.N. Agarwal, India J. Pure Appl. Phys. V20 (1982) 780.

64. D.K. Thakur and J.G. Gary, Indian J. Pure and Appl. Phys. V13 (1975) 437.

65. A. Singh, Thin Solid Films, V105 (1983) 163.

66. A. Goswani and A.P. Goswani, Thin Solid Films, V16 (1973) 175.

67. K.L. Chopra, J. Appl. Phys. V38 (1965) 655.

68. S.M. Sze, J. Appl. Phys. V38 (1967) 2951.

69. V.F. Korzo, Sov. Phys. Solid-State, V10 (1969) 2665.

70. V.F. Korzo, Sov. Phys. Solid-State, V9 (1968) 2167.

71. R.G. Greenler and R.M. Kay, J. Appl. Phys. V32 (1961) 1252.

72. P.D. Lomer, Nature, V166 (1950) 191.

73. A. Goswani and A.P. Goswani, Indian J. Phys. V49 (1975) 318.

74. T.N. Agarwal and R.N. Saxena, Indian J. Pure and Appl. Phys. V20 (1982) 780.

75. R.N. Saxena, Indian J. Phys. A53 (1979) 257.

76. S. Sinch, Phys. Sot. Sol. A54 (1979) K91.

77. A.P. Goswami and A. Goswami, Indian J. Pure and Appl. Phys. V12 (1974) 26.

78. T.J. Levis, IEEE Trans. EI-19 (1984) 210.

79. K.C. Kao, J. Appl. Phys. V55 (1984) 752.

80. A Von Hippel, Naturwissenschafter, (1935) 79.

81. F. Seitz, Noncrystalline Solid (Academic Press, London, 1960).

82. F. Forlani and N. Minnaja, Phys. Stat. Sol. V4 (1964) 311.

83. A.K. Jonscher and R. Locoste, IEEE Trans. EI-19 (1984) 6.

84. Y. Toyozawa, J. Phys. Soc. Jpn. V50 (1981) 1861.

85. D.L. Dexter, Phys. Rev. V100 (1956) 603.

86. F. Luty, Semiconding Insulators, V5 (1983) 245.

87. A. Forker, Linear Stability Criteria Theory (Academic Press, London, 1980).

88. L.A. Dissado and R.M. Hill, IEEE Trans. EI-19 (1984) 227.

89. R.M. Hill and L.A. Dissado, Proc. R. Soc. London, V100 (1983) 2249.

90. H. Kuhn, D. Mobius and H. Bucher, Physical Methods of Chemistry, Vol. 1. Part IIIB, A. Weissberger, eds. (Wiley Press, New York, 1972).

91. V.K. Agarwal, Electrocomp. Sci. Technol. V2 (1975) 1 and 75.

92. G. Sichel, Phys. Rev. B27 (1982) 1132.

93. B. Mann and H. Kuhn, J Appl. Phys. V42 (1970) 4398.

94. W.L. Procarione and J.W. Kauffman, Chem. Phys. Lipids, V12 (1974) 251.

95. R.H. Tredgold and C.S. Winter, J. Appl. Phys. D16 (1983) 230.

96. M. Sugi, T. Fukui and S. Iizima, Chem. Phys. Lett. V45 (1977) 163.

97. V.K. Agarwal, Thin Solid Films, V41 (1977) 271.

98. E.E. Polymeropoulos, J. Appl. Phys. V48 (1977) 2404.

99. I. Lundstrom, Chem. Phys. Lipids, V12 (1974) 287.

100. R.M. Hill, Thin Solid Films, V9 (1971) 88.

101. M. Sugi, K. Nembach, D. Mobius and H. Kuhn, Solid State Com. V13 (1973) 603.

102. M.A. Careem and A. K. Jonscher, Philos. Mag. V35 (1977) 1503.

103. K.H. Gaudlach and J. Kadlec, Chem. Phys. Lett. V24 (1974) 293.

104. M. Sugi, Molecular Electronics, V2 (1985) 1.

105. G.G. Roberts, J. Phys. C11 (1978) 2077.

106. M.H. Nathoo, Thin Solid Films, V16 (1973) 215.

107. L.L. Chang, Appl. Phys. Lett. V24 (1974) 593.

108. M.H. Nathoo and A.K. Jonscher, J. Phys. C4 (1971) L301.

109. M. Sugi, T. Fukui and S. Iizima, Appl. Phys. Lett. V27 (1975) 559; V28 (1976) 240.

110. A.K. Jonscher and M.H. Nathoo, Thin Solid Films, V12 (1972) S15.

111. V.K. Agarwal, Thin Solid Films, V23 (1974) S3; V23 (1974) S9; V33 (1976) L27.

112. M. Pollak, Phil. Mag. B42 (1980) 781.

113. D. Stauffer, Phys. Rep. V54 (1979) 1.

APPENDIX

THE COMPUTER CODE OF ANNEALING

```
**********************************************************
*   Estimating the initial defect density which has been   *
*   eliminated during annealing process via Resistance     *
*   verse Temperature measurements.                        *
**********************************************************
      PARAMETER (M=7)   ! # of data points
      dimension R(M),T(M),GRA(M),A(M),E(M),DD(M),Tem1(M)
      Bk=8.62   ! *10^(-5)   ! eV/K  BOLTZMAN CONSTANT
      f1=10.    ! 10^12-13 CHARACTERISTIC (phonon)
                ! FREQUENCY OF HOST MATERIAL
      N1=10     ! # OF DEFECTS IN THE CLUSTER.
      TIME=200. ! sec. TIME INTERNAL OF TWO SEQUENCE
                ! TEMPERATURE MEASUREMENTS.
      TEM=4*f1*N1*(TIME)    ! 10^12 unitless

C  READ DATA. resistivity R VS temperature T

      T(1)=77.    ! INITIAL TEMPERATURE
      R(1)=14.28   ! mho/cm  INITIAL RESISTIVITY
      DO I=1,M
      PRINT*,'T(',I+1,')=','     R(',I+1,')='
      READ(5,*) T(I+1), R(I+1)
C  SUCCESSIVE APPROXIMATION TO SOLVE
C  U+ln(U)=ln(4fnt)+ln(T/T-T0)
      TEM1(I)=T(I+1)/(T(I+1)-T(1))
      A(I)= Log(TEM1(I)) + Log(TEM) + 27.62
C  27.62=12*ln(10). if N1 increase 10
c  times and time increase 10 times the last constant of
c  above equation increase 4.6.  i.e ln(100)=4.6

      PRINT*, 'initial U= ,U should make E has the
                ! order of eV'
      READ (5,*) U
90  B=log(U)
      C=U+B
      print*,'A(',I,')=',A(I),'    C=',C
      IF(abs(C-A(I)).LE.0.2) GO TO 100
      U=U+0.1  ! step of increase
      GO TO 90
100  print*,'u=',u
      TEM2=U*(U+2)/(U+1)  ! DEFINITION
      E(I)=U*Bk*T(I+1)
! DECAY ENERGY OF DEFECT CLUSTERS
      GRA(I)=(R(I+1)-R(I))/(T(I+1)-T(I))
! 10^(15) DEFINITION
      DD(I)=-GRA(I)/(Bk*TEM2)
! 10^(20)  DD=DEFECT DENSITY
```

```
        E(I)=E(I)/100000   !*10^(-5)
! eV. real scale
        DD(I)=DD(I)*10**4
! constant scale *10^16
        print*,'DD(I)=',DD(I),'    E(I)=',E(I)
        END DO
        CALL PLOT(E,DD,M)
        END

        subroutine plot(x,y,mm)
!IMSL library: UGETIO, USPLO
        real    x(mm),y(mm,1), range(4)
        data    range/0,2,0,11/  ! range of the plot
        n=mm
        m=1
        iy=mm
        inc=1
        iopt=0   ! screen width  0=80col, 1=129 col.
        call ugetio(3,5,6)
        call usplo(x,y,iy,n,m,inc,
        1 'DEFECT DENSITY VS ACT. ENERGY'
        2  ,50,'E(eV)',6,'N(10**17mho/cm)',
        3  20,range,1h1,iopt,ier)
        do i=1,n
        print*,'activation energy=',x(I),
        1 ' defect density=',y(I,1)
        end do
        return
        end
```